Schweizerische Eidgenossenschaft
Confédération suisse
Confederazione Svizzera
Confederaziun svizra

Federal Institute of Metrology METAS

METAS VNA Tools - Math Reference V2.8.1

Michael Wollensack & Johannes Hoffmann

September 2023

Contents

1 Introduction

This document describes the computation of the uncertainties of coaxial S-parameter measurements, see [1]. This is a rather complicated task as all treated quantities are complex and the required operations are numerous.

Up to now a common way to handle uncertainties of vector network analyzer (VNA) measurements is the ripple technique described in [2]. The ripple technique uses precision airlines and other physical standards to extract the residual errors of a calibrated VNA system. It is based on the assumption that the precision transmission line has zero reflection. However, the systematic reflection coefficients of connectors make this assumption invalid, see [3]. This makes that the ripple method is unsuitable for computing the uncertainty of very accurate measurements. A more sophisticated computation of uncertainties has been implemented in StatistiCAL [4]. It relies on predefined uncertainties in standards and raw data. Thus it can capture certain imperfections of the VNA and the used standards. On the other hand it has neither a clear Bayesian nor frequentist concept for the imperfections of the VNA and does not provide means for producing a detailed uncertainty budget.

The present document describes in a first part the measurement model. A very well known measurement model for VNAs is described in [5]. However the model used here is slightly different. It is a N-port model and it has a more detailed uncertainty mechanism than [5]. The second part is the propagation of uncertainties through this measurement model. This methodology is described in the Guide to the Expression of Uncertainty in Measurement (GUM) [6], [7]. METAS UncLib [8], [9] is used for the linear propagation of uncertainties. The result is not only an uncertainty region but a list of uncertainty contributions with correlations. Thus the uncertainties can be propagated into eventual post-processing steps. A short description of METAS VNA Tools can be found in [10].

2 VNA Measurement Model
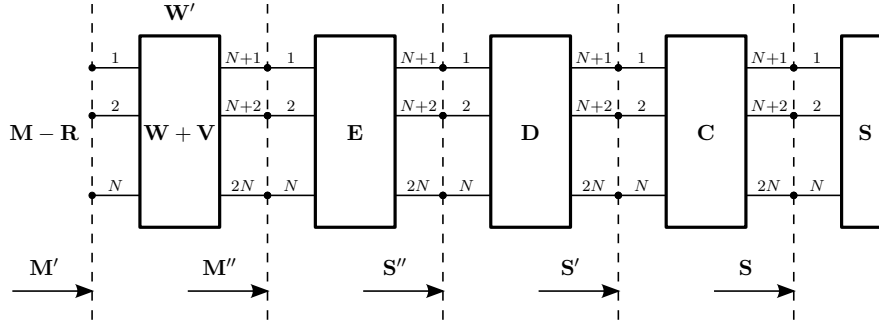
Figure 1: VNA Measurement Model

The following equation describes the in METAS VNA Tools used N-port VNA measurement model.

$$\mathbf{M}^{(i)} = \mathbf{R}^{(i)} + \left[\left(\mathbf{W} + \mathbf{V}^{(i)} \right) \oplus \left[\mathbf{E} \oplus \left[\mathbf{D}^{(i)} \oplus \left[\mathbf{C}^{(i)} \oplus \mathbf{S}^{(i)} \right] \right] \right] \right] \tag{1}$$

All bold variables are S-parameter matrices. $\mathbf{M}$, $\mathbf{R}$ and $\mathbf{S}$ are N-ports, the other bold variables are $2N$-ports and i is the measurement index.

$\mathbf{M}$ denotes the raw data measured by the VNA.

$\mathbf{R}$ denotes the noise and linearity influences.

$\mathbf{W}$ denotes the switch terms.

$\mathbf{V}$ denotes the drift of the switch terms.

$\mathbf{E}$ denotes the calibration error terms.

$\mathbf{D}$ denotes the drift of the calibration error terms.

$\mathbf{C}$ denotes the cable stability, connector repeatability and DUT uncertainty influences.

$\mathbf{S}$ denotes the error corrected data or the calibration kit standard definitions.

$\mathbf{M}$, $\mathbf{R}$, $\mathbf{V}$ and $\mathbf{D}$ change from measurement to measurement. $\mathbf{W}$ and $\mathbf{E}$ are constant during an entire calibration. $\mathbf{C}$ changes for every new connection or cable movement. $\mathbf{S}$ changes if a new device is connected.
The operator $\oplus$ denotes the cascading of two S-parameter sets, as described in appendix A.1.1.

The inverse function of equation 1 can be used for error correction.

$$\mathbf{S}^{(i)} = \left[\left[\left[\left(\mathbf{M}^{(i)} - \mathbf{R}^{(i)} \right) \ominus \left(\mathbf{W} + \mathbf{V}^{(i)} \right) \right] \ominus \mathbf{E} \right] \ominus \mathbf{D}^{(i)} \right] \ominus \mathbf{C}^{(i)} \tag{2}$$

The operator $\ominus$ denotes the decascading of two S-parameter sets, as described in appendix A.1.1.

One can introduce two new auxiliary variables.

$$\mathbf{M}'^{(i)} = \mathbf{M}^{(i)} - \mathbf{R}^{(i)} \tag{3}$$

$$\mathbf{S}'^{(i)} = \mathbf{C}^{(i)} \oplus \mathbf{S}^{(i)} \tag{4}$$

where $\mathbf{M}'$ designates the measured data including the noise and linearity influences and $\mathbf{S}'$ designates the actual data including the cable stability and connector repeatability. Now equation 1 can be rewritten as

$$\mathbf{M}'^{(i)} = \left(\mathbf{W} + \mathbf{V}^{(i)} \right) \oplus \left[\mathbf{E} \oplus \left[\mathbf{D}^{(i)} \oplus \mathbf{S}'^{(i)} \right] \right]. \tag{5}$$

One can introduce two further auxiliary variables.

$$\mathbf{W}'^{(i)} = \mathbf{W} + \mathbf{V}^{(i)} \tag{6}$$

$$\mathbf{S}''^{(i)} = \mathbf{D}^{(i)} \oplus \mathbf{S}'^{(i)} \tag{7}$$

where $\mathbf{W}'^{(i)}$ denotes the switch terms including the drift and $\mathbf{S}''^{(i)}$ the actual data including the cable stability, connector repeatability and the drift of the calibration error terms. Now equation 5 can be rewritten as

$$\mathbf{M}'^{(i)} = \mathbf{W}'^{(i)} \oplus \left[\mathbf{E} \oplus \mathbf{S}''^{(i)} \right]. \tag{8}$$

Introducing one further auxiliary variable leads to

$$\mathbf{M}''^{(i)} = \mathbf{M}'^{(i)} \ominus \mathbf{W}'^{(i)}. \tag{9}$$

Here $\mathbf{M}''^{(i)}$ denotes the switch corrected measured data including noise, linearity influences and the drift of the switch terms. Equation 8 can be rewritten as

$$\mathbf{M}''^{(i)} = \mathbf{E} \oplus \mathbf{S}''^{(i)}. \tag{10}$$

2.1 Calibration Error Terms

The following S-parameter matrix describes the error terms of a N-port VNA.

$$\mathbf{E} = \begin{pmatrix} D_1 & X_{1,2} & & X_{1,N} & T_{1,} & & & \\ X_{2,1} & D_2 & & X_{2,N} & & T_{2,} & & \\ & & \ddots & & & & \ddots & \\ X_{N,1} & X_{N,2} & & D_N & & & & T_{N,} \\ T_{,1} & & & & M_1 & & & \\ & T_{,2} & & & & M_2 & & \\ & & \ddots & & & & \ddots & \\ & & & T_{,N} & & & & M_N \end{pmatrix} \tag{11}$$

D_x denotes the directivity of port x.

$X_{y,x}$ denotes the crosstalk from port x to port y.

$T_{x,x} = T_{x,}T_{,x}$ denotes the reflection tracking of port x.

$T_{y,x} = T_{y,}T_{,x}$ denotes the transmission tracking from port x to port y.

M_x denotes the match of port x.

And all other terms are additional crosstalk terms.

3 VNA Generic Calibration Model

The Generic VNA Model is used for the following calibration types: One Port, GSOLT, QSOLT [11], Unknown Thru [12], TRL [13], LRRM [14], Juroshek [15] and LHKM [16], [17]. If an N-port VNA has $2N$ receivers instead of $N+1$ receivers then the switch terms can be measured directly, see [18]. For one-port measurements the switch terms and the associated drift can be set to zero.

3.1 One Port Calibration

3.1.1 Reflection Error Terms
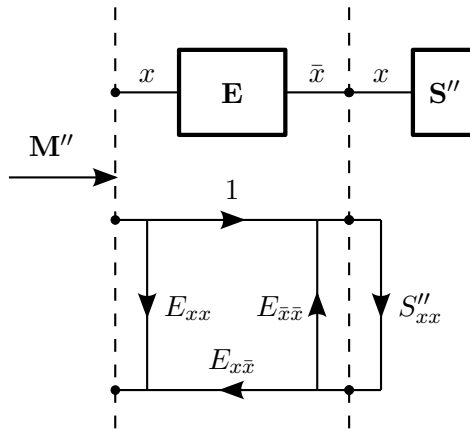
Figure 2: One Port Calibration

The following equation describes the cascading of the reflection error terms and the definition of the calibration standard

$$M_{xx}''^{(i)} = E_{xx} + \frac{E_{x\bar{x}}S_{xx}''^{(i)}}{1 - E_{\bar{x}\bar{x}}S_{xx}''^{(i)}} \tag{12}$$

with

$$\bar{x} = N + x. \tag{13}$$

N is the number of ports and x is the actual port where the reflection calibration is performed. Equation 12 can be rearranged as

$$\underbrace{M_{xx}''^{(i)}}_{y_i} = \underbrace{E_{xx}}_{p_1} + \underbrace{E_{\bar{x}\bar{x}}}_{p_2}M_{xx}''^{(i)}S_{xx}''^{(i)} + \underbrace{(E_{x\bar{x}} - E_{xx}E_{\bar{x}\bar{x}})}_{p_3}S_{xx}''^{(i)}. \tag{14}$$

Equation 14 can be written as a system of linear equations

$$\mathbf{p} = \mathbf{A}^{-1}\mathbf{y} \tag{15}$$

with

$$\mathbf{A} = \begin{pmatrix} 1 & M_{xx}''^{(1)}S_{xx}''^{(1)} & S_{xx}''^{(1)} \\ 1 & M_{xx}''^{(2)}S_{xx}''^{(2)} & S_{xx}''^{(2)} \\ 1 & M_{xx}''^{(3)}S_{xx}''^{(3)} & S_{xx}''^{(3)} \end{pmatrix} \tag{16}$$

and

$$\mathbf{y} = \begin{pmatrix} M_{xx}''^{(1)} \\ M_{xx}''^{(2)} \\ M_{xx}''^{(3)} \end{pmatrix}. \tag{17}$$

For example the first measurement could be a short, the second an open and the third a load. The vector $\mathbf{p}$ contains the solution for the error terms.

$$E_{xx} = p_1 \tag{18}$$
$$E_{\bar{x}x} = 1 \tag{19}$$
$$E_{x\bar{x}} = p_3 + p_1 p_2 \tag{20}$$
$$E_{\bar{x}\bar{x}} = p_2 \tag{21}$$

E_{xx} stands for the directivity, $E_{x\bar{x}}E_{\bar{x}x}$ denotes the reflection tracking and $E_{\bar{x}\bar{x}}$ designates the source match term.

3.1.2 Power

For a power calibration the scaling factor of the tracking terms have to be determined.
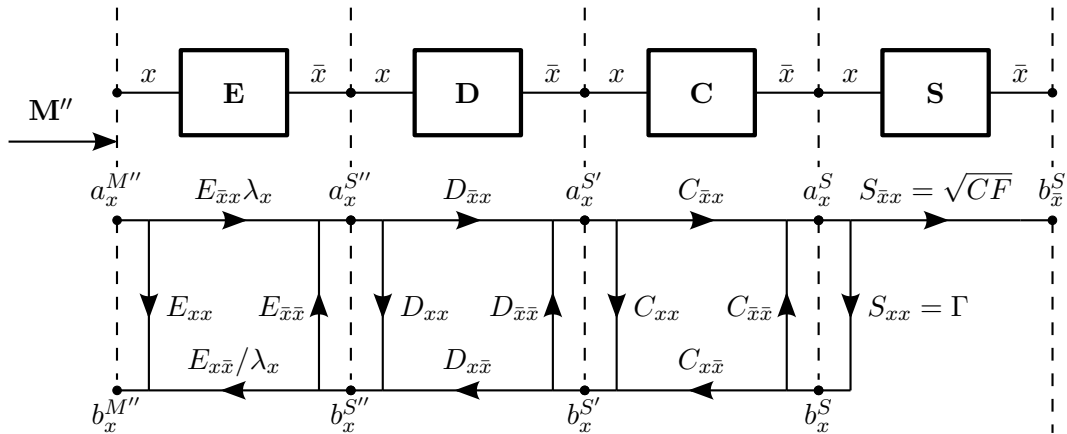
Figure 3: Power Calibration

In a first step the reflection coefficient Γ of the power sensor is computed using error correction, see section 2.

In a second step the scaling factor λ is computed using the receiver values from the VNA, the indicated power of the power sensor, the calibration factor CF of the power sensor, the error terms and all uncertainty influences. The following set of equations holds

$$b_x^{M''} = a_x^{M''} E_{xx} + b_x^{S''} E_{x\bar{x}}/\lambda \tag{22}$$
$$a_x^{S''} = a_x^{M''} E_{\bar{x}x}\lambda + b_x^{S''} E_{\bar{x}\bar{x}} \tag{23}$$

where

$a_x^{M''}$ denotes the reference receiver value of port x including noise and linearity uncertainties,

$b_x^{M''}$ denotes the test receiver value of port x including noise and linearity uncertainties,

$a_x^{S''}$ denotes the incident wave of the power sensor connected to port x in $\sqrt{\text{mW}}$ including drift, cable stability, connector repeatability and standard definition uncertainties,

$b_x^{S''}$ denotes the reflected wave of the power sensor connected to port x in $\sqrt{\text{mW}}$ including drift, cable stability, connector repeatability and standard definition uncertainties,

$b_{\bar{x}}^{S}$ denotes the indicated power of the power sensor in mW including all absolute and relative uncertainties of the power sensor,

E_{xx} denotes the directivity of port x,

$E_{x\bar{x}}E_{\bar{x}x}$ denotes the reflection tracking of port x,

$E_{\bar{x}\bar{x}}$ denotes the source match term of port x,

λ denotes the scaling factor of the tracking terms,

D_{xx}, $D_{\bar{x}x}$, $D_{x\bar{x}}$, $D_{\bar{x}\bar{x}}$ denote the drift influences of the power sensor measurement at port x,

C_{xx}, $C_{\bar{x}x}$, $C_{x\bar{x}}$, $C_{\bar{x}\bar{x}}$ denote the cable stability and the connector repeatability influences of the power sensor measurement at port x,

S_{xx} denotes the reflection coefficient Γ of the power sensor and

$S_{\bar{x}x}$ denotes the square root of the calibration factor $\sqrt{CF}$ of the power sensor, see section 6.18.

One can solve equation 22 for $b_x^{S''}$

$$b_x^{S''} = \frac{b_x^{M''} - a_x^{M''} E_{xx}}{E_{x\bar{x}}} \lambda \tag{24}$$

and plug the result into 23

$$a_x^{S''} = a_x^{M''} E_{\bar{x}x} \lambda + \frac{b_x^{M''} - a_x^{M''} E_{xx}}{E_{x\bar{x}}} E_{\bar{x}\bar{x}} \lambda. \tag{25}$$

One can solve the above equation for the scaling factor λ of the tracking terms

$$\lambda = \frac{a_x^{S''}}{a_x^{M''} E_{\bar{x}x} + \frac{b_x^{M''} - a_x^{M''} E_{xx}}{E_{x\bar{x}}} E_{\bar{x}\bar{x}}}. \tag{26}$$

The phase of λ is unknown because the phase of the incident wave of the power sensor $a_x^{S''}$ is unknown. For further data processing the absolute value of λ is used, e.g.: average of multiple power calibrations which finally yields to

$$|\lambda| = \sum_{i=1}^{n} \left| \frac{a_x^{S''(i)}}{a_x^{M''(i)} E_{\bar{x}x} + \frac{b_x^{M''(i)} - a_x^{M''(i)} E_{xx}}{E_{x\bar{x}}} E_{\bar{x}\bar{x}}} \right| / n. \tag{27}$$

3.2 GSOLT Calibration

For a GSOLT calibration the switch terms have to be determined.
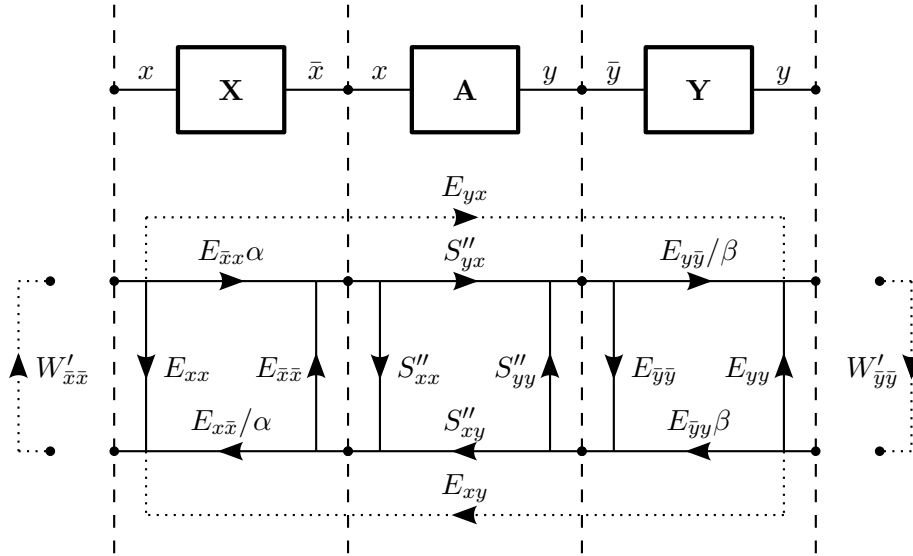
Figure 4: GSOLT Calibration

The following S-parameter matrix describes the transmission standard

$$\mathbf{A}^{(i)} = \begin{pmatrix} S_{xx}''^{(i)} & S_{xy}''^{(i)} \\ S_{yx}''^{(i)} & S_{yy}''^{(i)} \end{pmatrix}. \tag{28}$$

The error box of port x is denoted as

$$\mathbf{X} = \begin{pmatrix} E_{xx} & E_{x\bar{x}} \\ E_{\bar{x}x} & E_{\bar{x}\bar{x}} \end{pmatrix} \tag{29}$$

with

$$\bar{x} = N + x \tag{30}$$

and the error box of port y is designated by

$$\mathbf{Y} = \begin{pmatrix} E_{\bar{y}\bar{y}} & E_{\bar{y}y} \\ E_{y\bar{y}} & E_{yy} \end{pmatrix} \tag{31}$$

with

$$\bar{y} = N + y. \tag{32}$$

Cascading the error box of port x, the transmission standard definition and the error box of port y yields a new S-parameter matrix.

$$\mathbf{T}^{(i)} = \mathbf{X} \otimes \mathbf{A}^{(i)} \otimes \mathbf{Y} \tag{33}$$

The operator $\otimes$ denotes the cascading of two 2-ports, as described in appendix A.1.3.
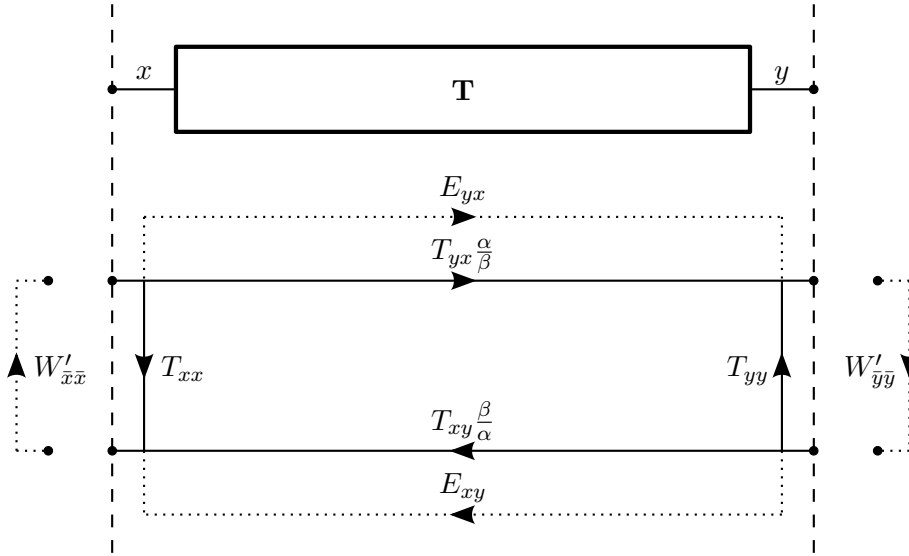
Figure 5: GSOLT Calibration (simplified)

The reflection measurement at port x is described by

$$M_{xx}^{\prime(i)} = T_{xx}^{(i)} + \frac{\left(\frac{\alpha^{(i)}}{\beta^{(i)}}T_{yx}^{(i)} + E_{yx}\right)\left(\frac{\beta^{(i)}}{\alpha^{(i)}}T_{xy}^{(i)} + E_{xy}\right)W_{\bar{y}\bar{y}}^{\prime(i)}}{1 - T_{yy}^{(i)}W_{\bar{y}\bar{y}}^{\prime(i)}}, \tag{34}$$

the transmission measurement from port x to y is described by

$$M_{yx}^{\prime(i)} = \frac{\left(\frac{\alpha^{(i)}}{\beta^{(i)}}T_{yx}^{(i)} + E_{yx}\right)}{1 - T_{yy}^{(i)}W_{\bar{y}\bar{y}}^{\prime(i)}}, \tag{35}$$

the transmission measurement from port y to x is described by

$$M_{xy}^{\prime(i)} = \frac{\left(\frac{\beta^{(i)}}{\alpha^{(i)}}T_{xy}^{(i)} + E_{xy}\right)}{1 - T_{xx}^{(i)}W_{\bar{x}\bar{x}}^{\prime(i)}}, \tag{36}$$

and the reflection measurement at port y is described by

$$M_{yy}^{\prime(i)} = T_{yy}^{(i)} + \frac{\left(\frac{\alpha^{(i)}}{\beta^{(i)}}T_{yx}^{(i)} + E_{yx}\right)\left(\frac{\beta^{(i)}}{\alpha^{(i)}}T_{xy}^{(i)} + E_{xy}\right)W_{\bar{x}\bar{x}}^{\prime(i)}}{1 - T_{xx}^{(i)}W_{\bar{x}\bar{x}}^{\prime(i)}}. \tag{37}$$

3.2.1 Switch Terms without Crosstalk

If the crosstalk E_{yx} and E_{xy} are assumed as zero, equations 34 and 37 can be simplified as

$$M_{xx}^{\prime(thru)} = T_{xx}^{(thru)} + \frac{T_{yx}^{(thru)}T_{xy}^{(thru)}W_{\bar{y}\bar{y}}^{\prime(thru)}}{1 - T_{yy}^{(thru)}W_{\bar{y}\bar{y}}^{\prime(thru)}} \tag{38}$$

and

$$M'^{(thru)}_{yy} = T^{(thru)}_{yy} + \frac{T^{(thru)}_{yx} T^{(thru)}_{xy} W'^{(thru)}_{\bar{x}\bar{x}}}{1 - T^{(thru)}_{xx} W'^{(thru)}_{\bar{x}\bar{x}}}. \tag{39}$$

Equation 39 can be rearranged as

$$\left(M'^{(thru)}_{yy} - T^{(thru)}_{yy} \right) \left(1 - T^{(thru)}_{xx} W'^{(thru)}_{\bar{x}\bar{x}} \right) = T^{(thru)}_{yx} T^{(thru)}_{xy} W'^{(thru)}_{\bar{x}\bar{x}} \tag{40}$$

and one can solve for the switch term of port x

$$W'^{(thru)}_{\bar{x}\bar{x}} = \frac{M'^{(thru)}_{yy} - T^{(thru)}_{yy}}{\left(M'^{(thru)}_{yy} - T^{(thru)}_{yy} \right) T^{(thru)}_{xx} + T^{(thru)}_{yx} T^{(thru)}_{xy}}. \tag{41}$$

The other switch term of port y can be calculated with the following equation

$$W'^{(thru)}_{\bar{y}\bar{y}} = \frac{M'^{(thru)}_{xx} - T^{(thru)}_{xx}}{\left(M'^{(thru)}_{xx} - T^{(thru)}_{xx} \right) T^{(thru)}_{yy} + T^{(thru)}_{yx} T^{(thru)}_{xy}}. \tag{42}$$

Finally one can remove the drift effects from the switch terms.

$$W_{\bar{x}\bar{x}} = W'^{(thru)}_{\bar{x}\bar{x}} - V^{(thru)}_{\bar{x}\bar{x}} \tag{43}$$

$$W_{\bar{y}\bar{y}} = W'^{(thru)}_{\bar{y}\bar{y}} - V^{(thru)}_{\bar{y}\bar{y}} \tag{44}$$

3.2.2 Switch Terms with Crosstalk

A new auxiliary variable m_x is introduced by combining equations 34, 35 and 36

$$m_x = \frac{M'^{(thru)}_{xx} - T^{(thru)}_{xx}}{M'^{(thru)}_{yx} M'^{(thru)}_{xy}} = \left(1 - T^{(thru)}_{xx} W'^{(thru)}_{\bar{x}\bar{x}} \right) W'^{(thru)}_{\bar{y}\bar{y}} \tag{45}$$

and m_y by combining equations 35, 36 and 37

$$m_y = \frac{M'^{(thru)}_{yy} - T^{(thru)}_{yy}}{M'^{(thru)}_{yx} M'^{(thru)}_{xy}} = \left(1 - T^{(thru)}_{yy} W'^{(thru)}_{\bar{y}\bar{y}} \right) W'^{(thru)}_{\bar{x}\bar{x}}. \tag{46}$$

Now one has a system with two equations and two unknown variables, which are both switch terms. Equation 45 can be rewritten as

$$W'^{(thru)}_{\bar{y}\bar{y}} = \frac{m_x}{1 - T^{(thru)}_{xx} W'^{(thru)}_{\bar{x}\bar{x}}} \tag{47}$$

and one can put equation 47 into equation 46

$$m_y = \left(1 - T^{(thru)}_{yy} \frac{m_x}{1 - T^{(thru)}_{xx} W'^{(thru)}_{\bar{x}\bar{x}}} \right) W'^{(thru)}_{\bar{x}\bar{x}}. \tag{48}$$

One can find the root of equation 48

$$\underbrace{T^{(thru)}_{xx}}_{a} \left(W'^{(thru)}_{\bar{x}\bar{x}} \right)^2 + \underbrace{\left(m_x T^{(thru)}_{yy} - m_y T^{(thru)}_{xx} - 1 \right)}_{b} W'^{(thru)}_{\bar{x}\bar{x}} + \underbrace{m_y}_{c} = 0 \tag{49}$$

and solving the quadratic equation yields the switch term of port x. The other switch term of port y can be calculated with equation 47.

$$W_{\bar{x}\bar{x}}^{\prime(thru)} = \frac{-b \pm \sqrt{b^2 - 4ac}}{2a} \tag{50}$$

Finally one can remove the drift effects from the switch terms.

$$W_{\bar{x}\bar{x}} = W_{\bar{x}\bar{x}}^{\prime(thru)} - V_{\bar{x}\bar{x}}^{(thru)} \tag{51}$$

$$W_{\bar{y}\bar{y}} = W_{\bar{y}\bar{y}}^{\prime(thru)} - V_{\bar{y}\bar{y}}^{(thru)} \tag{52}$$

3.2.3 Crosstalk

If the switch terms are known, the crosstalk between two ports can be measured directly. Note that is is assumed that there is no drift of the isolation.

$$E_{yx} = M_{yx}^{\prime\prime(isol)} \tag{53}$$

$$E_{xy} = M_{xy}^{\prime\prime(isol)} \tag{54}$$

3.2.4 Symmetry

The following equation defines α.

$$\alpha = E_{\bar{x}x} \tag{55}$$

To find a solution for β, equation 35 can be rewritten as

$$\beta_1 = \alpha \frac{T_{yx}^{(thru)}}{M_{yx}^{\prime(thru)} \left(1 - T_{yy}^{(thru)} W_{\bar{y}\bar{y}}^{\prime(thru)}\right) - E_{yx}} \tag{56}$$

and equation 36 can be rewritten as

$$\beta_2 = \alpha \frac{M_{xy}^{\prime(thru)} \left(1 - T_{xx}^{(thru)} W_{\bar{x}\bar{x}}^{\prime(thru)}\right) - E_{xy}}{T_{xy}^{(thru)}}. \tag{57}$$

The GSOLT calibration algorithm assumes β as the mean of the forward β_1 and the reverse β_2

$$\beta = \frac{\beta_1 + \beta_2}{2} \tag{58}$$

then one can update the reflection and transmission tracking error terms of port x and y.

$$E_{x\bar{x}} := \frac{E_{x\bar{x}} E_{\bar{x}x}}{\alpha} \tag{59}$$

$$E_{\bar{x}x} := \alpha \tag{60}$$

$$E_{y\bar{y}} := \frac{E_{y\bar{y}} E_{\bar{y}y}}{\beta} \tag{61}$$

$$E_{\bar{y}y} := \beta \tag{62}$$

$E_{x\bar{x}} E_{\bar{x}x}$ stands for the reflection tracking of port x,

$E_{y\bar{y}} E_{\bar{x}x}$ stands for the transmission tracking from port x to port y,

$E_{x\bar{x}} E_{\bar{y}y}$ stands for the transmission tracking from port y to port x and

$E_{y\bar{y}} E_{\bar{y}y}$ stands for the reflection tracking of port y.

3.3 QSOLT Calibration

The QSOLT calibration is described in [11].

3.3.1 Crosstalk

The crosstalk between two ports can be measured directly. Note that is is assumed that there is no drift of the isolation.

$$E_{yx} = M_{yx}^{\prime\prime(isol)} \tag{63}$$

$$E_{xy} = M_{xy}^{\prime\prime(isol)} \tag{64}$$

3.3.2 Copy Calibration
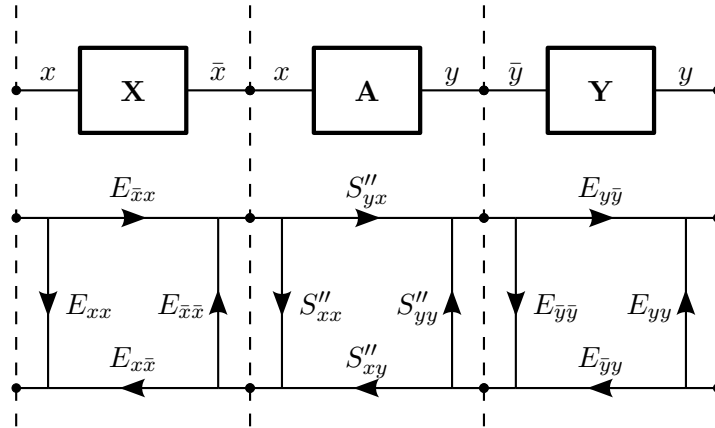
Figure 6: QSOLT Calibration

The following S-parameter matrix describes the switch term and crosstalk corrected measured data of the transmission standard

$$\mathbf{T}^{(i)} = \begin{pmatrix} M_{xx}^{\prime\prime(i)} & M_{xy}^{\prime\prime(i)} - E_{xy} \\ M_{yx}^{\prime\prime(i)} - E_{yx} & M_{yy}^{\prime\prime(i)} \end{pmatrix}. \tag{65}$$

Again the transmission standard is defined as

$$\mathbf{A}^{(i)} = \begin{pmatrix} S_{xx}^{\prime\prime(i)} & S_{xy}^{\prime\prime(i)} \\ S_{yx}^{\prime\prime(i)} & S_{yy}^{\prime\prime(i)} \end{pmatrix}. \tag{66}$$

The error box of port x is defined as

$$\mathbf{X} = \begin{pmatrix} E_{xx} & E_{x\bar{x}} \\ E_{\bar{x}x} & E_{\bar{x}\bar{x}} \end{pmatrix} \tag{67}$$

with

$$\bar{x} = N + x \tag{68}$$

and the error box of port y id defined as

$$\mathbf{Y} = \left(\begin{array}{cc} E_{\bar{y}\bar{y}} & E_{\bar{y}y} \\ E_{y\bar{y}} & E_{yy} \end{array} \right) \tag{69}$$

with

$$\bar{y} = N + y. \tag{70}$$

To copy the error terms of port x to port y one decascades $\mathbf{X}$ and $\mathbf{A}$ from $\mathbf{T}$.

$$\mathbf{Y} = \left(\mathbf{X} \otimes \mathbf{A}^{(thru)} \right)^{\ominus 1} \otimes \mathbf{T}^{(thru)} \tag{71}$$

The operator $\otimes$ denotes the cascading of two 2-ports, as described in appendix A.1.3.

3.4 Unknown Thru Calibration

The Unknown Thru calibration is described in [12].

3.4.1 Crosstalk

The crosstalk between two ports can be measured directly. Note that is is assumed that there is no drift of the isolation.

$$E_{yx} = M_{yx}''^{(isol)} \tag{72}$$
$$E_{xy} = M_{xy}''^{(isol)} \tag{73}$$

3.4.2 Symmetry

The following S-parameter matrix describes the error box of port x and y.

$$\mathbf{E}' = \left(\begin{array}{cccc} E_{xx} & E_{xy} & E_{x\bar{x}} & E_{x\bar{y}} \\ E_{yx} & E_{yy} & E_{y\bar{x}} & E_{y\bar{y}} \\ E_{\bar{x}x} & E_{\bar{x}y} & E_{\bar{x}\bar{x}} & E_{\bar{x}\bar{y}} \\ E_{\bar{y}x} & E_{\bar{y}y} & E_{\bar{y}\bar{x}} & E_{\bar{y}\bar{y}} \end{array} \right) \tag{74}$$

One can error correct the unknown thru measurement data without knowing the symmetry error terms.

$$\mathbf{S}''^{(thru)} = \mathbf{M}''^{(thru)} \ominus \mathbf{E}' \tag{75}$$

The operator $\ominus$ denotes the decascading of two S-parameter sets, as described in appendix A.1.1.

The forward and reverse transmission S-parameter of an unknown thru have to be the same, because the unknown thru assumed to be a reciprocal device. The nominal magnitude of the transmission of the unknown thru is described by

$$|s_{yx}| = \sqrt{\left| S_{yx}''^{(thru)} S_{xy}''^{(thru)} \right|} \tag{76}$$

and the nominal phase is described by

$$\arg\left(s_{yx}\right) = \frac{\arg\left(S_{yx}''^{(thru)} S_{xy}''^{(thru)}\right)}{2}. \tag{77}$$

The following equation defines α.

$$\alpha = E_{\bar{x}x} \tag{78}$$

One can compute β with the nominal transmission and the error corrected unknown thru measurement.

$$\beta = \alpha \frac{s_{yx}}{S_{yx}''^{(thru)}} \tag{79}$$

Then one can update the reflection and transmission tracking error terms of port x and y.

$$E_{x\bar{x}} := \frac{E_{x\bar{x}} E_{\bar{x}x}}{\alpha} \tag{80}$$

$$E_{\bar{x}x} := \alpha \tag{81}$$

$$E_{y\bar{y}} := \frac{E_{y\bar{y}} E_{\bar{y}y}}{\beta} \tag{82}$$

$$E_{\bar{y}y} := \beta \tag{83}$$

$E_{x\bar{x}} E_{\bar{x}x}$ is the reflection tracking of port x,

$E_{y\bar{y}} E_{\bar{x}x}$ is the transmission tracking from port x to port y,

$E_{x\bar{x}} E_{\bar{y}y}$ is the transmission tracking from port y to port x and

$E_{y\bar{y}} E_{\bar{y}y}$ is the reflection tracking of port y.

3.5 TRL Calibration

The TRL calibration is described in [13] works only with two ports.

3.5.1 Crosstalk

The crosstalk between two ports can be measured directly. Note that is is assumed that there is no drift of the isolation.

$$E_{yx} = M_{yx}''^{(isol)} \tag{84}$$

$$E_{xy} = M_{xy}''^{(isol)} \tag{85}$$

3.5.2 Thru Reflect Line

The following T-parameter matrix describes the measurement of the thru which is corrected for switch terms and crosstalk.

$$\mathbf{T}_{thru} = \text{StoTParam}\begin{pmatrix} M_{xx}''^{(thru)} & M_{xy}''^{(thru)} - E_{xy} \\ M_{yx}''^{(thru)} - E_{yx} & M_{yy}''^{(thru)} \end{pmatrix} \tag{86}$$

The next matrix describes the measurement of the line which is corrected for switch terms and crosstalk.

$$\mathbf{T}_{line} = \text{StoTParam} \begin{pmatrix} M_{xx}^{\prime\prime(line)} & M_{xy}^{\prime\prime(line)} - E_{xy} \\ M_{yx}^{\prime\prime(line)} - E_{yx} & M_{yy}^{\prime\prime(line)} \end{pmatrix} \tag{87}$$

One can cascade the line and the inverted thru.

$$\mathbf{m} = \mathbf{T}_{line} \times \mathbf{T}_{thru}^{-1} \tag{88}$$

With the elements of the matrix $\mathbf{m}$ one forms

$$a_m = m_{21} \tag{89}$$
$$b_m = m_{22} - m_{11} \tag{90}$$
$$c_m = -m_{12}. \tag{91}$$

$$x_1 = \frac{-b_m + \sqrt{b_m^2 - 4a_m c_m}}{2a_m} \tag{92}$$

$$x_2 = \frac{-b_m - \sqrt{b_m^2 - 4a_m c_m}}{2a_m} \tag{93}$$

If $|x_1| > |x_2|$ then one sets

$$\alpha = x_1 \tag{94}$$
$$\beta = x_2 \tag{95}$$

else one makes the inverse assignment

$$\alpha = x_2 \tag{96}$$
$$\beta = x_1. \tag{97}$$

One can cascade the inverted thru and the line.

$$\mathbf{n} = \mathbf{T}_{thru}^{-1} \times \mathbf{T}_{line} \tag{98}$$

With the elements of the matrix $\mathbf{n}$ one forms

$$a_n = n_{12} \tag{99}$$
$$b_n = n_{22} - n_{11} \tag{100}$$
$$c_n = -n_{21}. \tag{101}$$

$$y_1 = \frac{-b_n + \sqrt{b_n^2 - 4a_n c_n}}{2a_n} \tag{102}$$

$$y_2 = \frac{-b_n - \sqrt{b_n^2 - 4a_n c_n}}{2a_n} \tag{103}$$

If $|y_1| > |y_2|$ then one sets

$$\gamma = y_1 \tag{104}$$
$$\delta = y_2 \tag{105}$$

else one makes the inverse assignment

$$\gamma = y_2 \tag{106}$$
$$\delta = y_1. \tag{107}$$

The TRL algorithm additionally uses the following intermediate quantities.

$$f_1 = \frac{\beta - M_{xx}''^{(reflect)}}{\alpha - M_{xx}''^{(reflect)}} \tag{108}$$

$$f_2 = \frac{\gamma + M_{yy}''^{(reflect)}}{\delta + M_{yy}''^{(reflect)}} \tag{109}$$

$$f_3 = \frac{\beta - M_{xx}''^{(thru)}}{\alpha - M_{xx}''^{(thru)}} \tag{110}$$

Now one can determine the parameters of the cascaded error boxes. The sign of e_{11} is chosen by the approximate definition of the reflection standard.

$$e_{00} = \beta \tag{111}$$
$$e_{33} = -\delta \tag{112}$$
$$e_{11} = \pm\sqrt{f_1 f_2 f_3} \tag{113}$$
$$e_{22} = \frac{f_3}{e_{11}} \tag{114}$$
$$e_{1001} = (\beta - a)\, e_{11} \tag{115}$$
$$e_{2332} = (\gamma - d)\, e_{22} \tag{116}$$
$$e_{1032} = \left(M_{yx}''^{(thru)} - E_{yx}\right)(1 - e_{11}e_{22}) \tag{117}$$
$$e_{2301} = \left(M_{xy}''^{(thru)} - E_{xy}\right)(1 - e_{11}e_{22}) \tag{118}$$

Now the offset delay $d = e^{-\gamma l}$ of the thru definition is removed from the error boxes.

$$e_{11} := e_{11}/d \tag{119}$$
$$e_{22} := e_{22}/d \tag{120}$$
$$e_{1001} := e_{1001}/d \tag{121}$$
$$e_{2332} := e_{2332}/d \tag{122}$$
$$e_{1032} := e_{1032}/d \tag{123}$$
$$e_{2301} := e_{2301}/d \tag{124}$$

Setting one transmission term to 1 defines the remaining terms.

$$
\begin{align}
e_{10} &= 1 \tag{125} \\
e_{01} &= \frac{e_{1001}}{e_{10}} \tag{126} \\
e_{32} &= \frac{e_{1032}}{e_{10}} \tag{127} \\
e_{23} &= \frac{e_{2301}}{e_{01}} \tag{128}
\end{align}
$$

Finally one can update the error terms of the VNA measurement model.

$$
\begin{align}
E_{xx} &= e_{00} \tag{129} \\
E_{\bar{x}x} &= e_{10} \tag{130} \\
E_{x\bar{x}} &= e_{01} \tag{131} \\
E_{\bar{x}\bar{x}} &= e_{11} \tag{132} \\
E_{\bar{y}\bar{y}} &= e_{22} \tag{133} \\
E_{y\bar{y}} &= e_{32} \tag{134} \\
E_{\bar{y}y} &= e_{23} \tag{135} \\
E_{yy} &= e_{33} \tag{136}
\end{align}
$$

E_{xx} is the directivity of port x,

$E_{\bar{x}\bar{x}}$ is the match of port x,

$E_{x\bar{x}}E_{\bar{x}x}$ is the reflection tracking of port x,

$E_{y\bar{y}}E_{\bar{x}x}$ is the transmission tracking from port x to port y,

$E_{x\bar{x}}E_{\bar{y}y}$ is the transmission tracking from port y to port x,

$E_{y\bar{y}}E_{\bar{y}y}$ is the reflection tracking of port y,

$E_{\bar{y}\bar{y}}$ is the match of port y and

E_{yy} is the directivity of port y.

3.6 LRRM Calibration

The in METAS VNA Tools implemented LRRM algorithm is a generalization of the LRRM calibration described in [14]. The generalization consists of implementing a reflective non-reciprocal line standard. The line standard has to be fully known. The two reflection standards are measured each at both ports and have to have different reflection angles or amplitudes. The match standard is only measured at one port. The DC resistance R of the match has to be known. The following table describes the used calibration standards in the LRRM calibration.

Table 1: LRRM Standards

Standard	S-parameter
Line	$\mathbf{S}^{(t)} = \begin{pmatrix} s_{xx}^{(t)} & s_{xy}^{(t)} \\ s_{yx}^{(t)} & s_{yy}^{(t)} \end{pmatrix}$
Reflect 1 (unknown capacitance)	$S^{(o)} = \frac{1-j\omega C Z_r}{1+j\omega C Z_r}$ with $C =?$ and $C \geq 0$
Reflect 2 (unknown reflection)	$S^{(r)} = r_{re} + j r_{im}$ with $r_{re} =?$, $r_{im} =?$ and $r_{re} \leq 0$
Match (unknown inductance)	$S^{(m)} = \frac{R+j\omega L - Z_r}{R+j\omega L + Z_r}$ with $L =?$

The LRRM calibration can be described by the following nine linear equations, see section 3.8.

$$
\left(
\begin{array}{cccccccc}
M_{xx}^{\prime\prime(t)} & 0 & 1 & 0 & M_{xx}^{\prime\prime(t)} S_{xx}^{\prime\prime(t)} & M_{xy}^{\prime\prime(t)} S_{yx}^{\prime\prime(t)} & S_{xx}^{\prime\prime(t)} & 0 \\
M_{yx}^{\prime\prime(t)} & 0 & 0 & 0 & M_{yx}^{\prime\prime(t)} S_{xx}^{\prime\prime(t)} & M_{yy}^{\prime\prime(t)} S_{yx}^{\prime\prime(t)} & 0 & S_{yx}^{\prime\prime(t)} \\
0 & M_{xy}^{\prime\prime(t)} & 0 & 0 & M_{xx}^{\prime\prime(t)} S_{xy}^{\prime\prime(t)} & M_{xy}^{\prime\prime(t)} S_{yy}^{\prime\prime(t)} & S_{xy}^{\prime\prime(t)} & 0 \\
0 & M_{yy}^{\prime\prime(t)} & 0 & 1 & M_{yx}^{\prime\prime(t)} S_{xy}^{\prime\prime(t)} & M_{yy}^{\prime\prime(t)} S_{yy}^{\prime\prime(t)} & 0 & S_{yy}^{\prime\prime(t)} \\
\hline
M_{xx}^{\prime\prime(o)} & 0 & 1 & 0 & M_{xx}^{\prime\prime(o)} S_{xx}^{\prime\prime(o)} & 0 & S_{xx}^{\prime\prime(o)} & 0 \\
0 & M_{yy}^{\prime\prime(o)} & 0 & 1 & 0 & M_{yy}^{\prime\prime(o)} S_{yy}^{\prime\prime(o)} & 0 & S_{yy}^{\prime\prime(o)} \\
\hline
M_{xx}^{\prime\prime(r)} & 0 & 1 & 0 & M_{xx}^{\prime\prime(r)} S_{xx}^{\prime\prime(r)} & 0 & S_{xx}^{\prime\prime(r)} & 0 \\
0 & M_{yy}^{\prime\prime(r)} & 0 & 1 & 0 & M_{yy}^{\prime\prime(r)} S_{yy}^{\prime\prime(r)} & 0 & S_{yy}^{\prime\prime(r)} \\
\hline
M_{xx}^{\prime\prime(m)} & 0 & 1 & 0 & M_{xx}^{\prime\prime(m)} S_{xx}^{\prime\prime(m)} & 0 & S_{xx}^{\prime\prime(m)} & 0
\end{array}
\right)
\left(
\begin{array}{c}
1 \\ x_2 \\ x_3 \\ x_4 \\ x_5 \\ x_6 \\ x_7 \\ x_8
\end{array}
\right) = 0 \quad (137)
$$

The LRRM calibration is solved with the following steps:

1. The seven unknowns x_2 to x_7 which represent the error terms can be eliminated. This yields two linear equations.

2. The numerators of these two equations have to be equal to zero:

$$
\begin{aligned}
M_{xx}''^{(o)}((M_{yy}''^{(o)} - M_{yy}''^{(t)})(M_{xx}''^{(r)}(S_{xx}''^{(o)} - S_{xx}''^{(r)})(S_{xy}''^{(t)}S_{yx}''^{(t)} - (S_{xx}''^{(m)} - S_{xx}''^{(t)})(S_{yy}''^{(o)} - S_{yy}''^{(t)})) \\
- M_{xx}''^{(t)}(S_{xx}''^{(m)} - S_{xx}''^{(r)})(S_{xy}''^{(t)}S_{yx}''^{(t)} - (S_{xx}''^{(o)} - S_{xx}''^{(t)})(S_{yy}''^{(o)} - S_{yy}''^{(t)})) + M_{xx}''^{(m)}(S_{xx}''^{(m)} \\
- S_{xx}''^{(o)})(S_{xy}''^{(t)}S_{yx}''^{(t)} - (S_{xx}''^{(r)} - S_{xx}''^{(t)})(S_{yy}''^{(o)} - S_{yy}''^{(t)}))) - M_{xy}''^{(t)}M_{yx}''^{(t)}(S_{xx}''^{(m)} \\
- S_{xx}''^{(r)})(S_{xy}''^{(t)}S_{yx}''^{(t)} - (S_{xx}''^{(o)} - S_{xx}''^{(t)})(S_{yy}''^{(o)} - S_{yy}''^{(t)}))) + M_{xx}''^{(r)}(-(M_{yy}''^{(o)} \\
- M_{yy}''^{(t)})(M_{xx}''^{(m)}(S_{xx}''^{(m)} - S_{xx}''^{(r)})(S_{xy}''^{(t)}S_{yx}''^{(t)} - (S_{xx}''^{(o)} - S_{xx}''^{(t)})(S_{yy}''^{(o)} - S_{yy}''^{(t)})) \\
- M_{xx}''^{(t)}(S_{xx}''^{(m)} - S_{xx}''^{(o)})(S_{xy}''^{(t)}S_{yx}''^{(t)} - (S_{xx}''^{(r)} - S_{xx}''^{(t)})(S_{yy}''^{(o)} - S_{yy}''^{(t)}))) \\
+ M_{xy}''^{(t)}M_{yx}''^{(t)}(S_{xx}''^{(m)} - S_{xx}''^{(o)})(S_{xy}''^{(t)}S_{yx}''^{(t)} - (S_{xx}''^{(r)} - S_{xx}''^{(t)})(S_{yy}''^{(o)} - S_{yy}''^{(t)}))) \\
+ M_{xx}''^{(m)}(M_{xy}''^{(t)}M_{yx}''^{(t)} + M_{xx}''^{(t)}(M_{yy}''^{(o)} - M_{yy}''^{(t)}))(S_{xx}''^{(o)} - S_{xx}''^{(r)})(S_{xy}''^{(t)}S_{yx}''^{(t)} - (S_{xx}''^{(m)} \\
- S_{xx}''^{(t)})(S_{yy}''^{(o)} - S_{yy}''^{(t)})) = 0
\end{aligned}
\tag{138}
$$

and

$$
\begin{aligned}
(M_{xy}''^{(t)}M_{yx}''^{(t)} + M_{xx}''^{(t)}(M_{yy}''^{(o)} - M_{yy}''^{(t)}))(M_{xy}''^{(t)}M_{yx}''^{(t)} + M_{xx}''^{(t)}(M_{yy}''^{(r)} - M_{yy}''^{(t)}))(S_{xx}''^{(m)} \\
- S_{xx}''^{(o)})S_{xy}''^{(t)}S_{yx}''^{(t)}(S_{yy}''^{(o)} - S_{yy}''^{(r)}) + M_{xx}''^{(o)}(M_{xx}''^{(t)}(M_{yy}''^{(o)} - M_{yy}''^{(t)})(-M_{yy}''^{(r)} \\
+ M_{yy}''^{(t)})(S_{xx}''^{(m)} - S_{xx}''^{(o)})S_{xy}''^{(t)}S_{yx}''^{(t)}(S_{yy}''^{(o)} - S_{yy}''^{(r)}) + M_{xy}''^{(t)}M_{yx}''^{(t)}(M_{yy}''^{(t)}(S_{xx}''^{(m)} \\
- S_{xx}''^{(o)})S_{xy}''^{(t)}S_{yx}''^{(t)}(S_{yy}''^{(o)} - S_{yy}''^{(r)}) - M_{yy}''^{(r)}(S_{xy}''^{(t)}S_{yx}''^{(t)} - (S_{xx}''^{(o)} - S_{xx}''^{(t)})(S_{yy}''^{(o)} \\
- S_{yy}''^{(t)}))(S_{xy}''^{(t)}S_{yx}''^{(t)} - (S_{xx}''^{(m)} - S_{xx}''^{(t)})(S_{yy}''^{(r)} - S_{yy}''^{(t)})) + M_{yy}''^{(o)}(S_{xy}''^{(t)}S_{yx}''^{(t)} - (S_{xx}''^{(m)} \\
- S_{xx}''^{(t)})(S_{yy}''^{(o)} - S_{yy}''^{(t)}))(S_{xy}''^{(t)}S_{yx}''^{(t)} - (S_{xx}''^{(o)} - S_{xx}''^{(t)})(S_{yy}''^{(r)} - S_{yy}''^{(t)})))) + M_{xx}''^{(m)}((M_{xx}''^{(o)} \\
- M_{xx}''^{(t)})(M_{yy}''^{(o)} - M_{yy}''^{(t)})(M_{yy}''^{(r)} - M_{yy}''^{(t)})(S_{xx}''^{(m)} - S_{xx}''^{(o)})S_{xy}''^{(t)}S_{yx}''^{(t)}(S_{yy}''^{(o)} - S_{yy}''^{(r)}) \\
+ M_{xy}''^{(t)}M_{yx}''^{(t)}(M_{yy}''^{(t)}(S_{xx}''^{(m)} - S_{xx}''^{(o)})S_{xy}''^{(t)}S_{yx}''^{(t)}(S_{yy}''^{(o)} - S_{yy}''^{(r)}) - M_{yy}''^{(o)}(S_{xy}''^{(t)}S_{yx}''^{(t)} \\
- (S_{xx}''^{(o)} - S_{xx}''^{(t)})(S_{yy}''^{(o)} - S_{yy}''^{(t)}))(S_{xy}''^{(t)}S_{yx}''^{(t)} - (S_{xx}''^{(m)} - S_{xx}''^{(t)})(S_{yy}''^{(r)} - S_{yy}''^{(t)})) \\
+ M_{yy}''^{(r)}(S_{xy}''^{(t)}S_{yx}''^{(t)} - (S_{xx}''^{(m)} - S_{xx}''^{(t)})(S_{yy}''^{(o)} - S_{yy}''^{(t)}))(S_{xy}''^{(t)}S_{yx}''^{(t)} - (S_{xx}''^{(o)} - S_{xx}''^{(t)})(S_{yy}''^{(r)} \\
- S_{yy}''^{(t)})))) = 0.
\end{aligned}
\tag{139}
$$

3. $S_{xx}''^{(o)}$ and $S_{yy}''^{(o)}$ can be replaced by the unknown capacitance C:

$$
S_{xx}''^{(o)} = D_{xx}^{(o)} + \frac{D_{\bar{x}x}^{(o)} S_{xx}'^{(o)} D_{x\bar{x}}^{(o)}}{1 - D_{\bar{x}\bar{x}}^{(o)} S_{xx}'^{(o)}} \text{ with } S_{xx}'^{(o)} = C_{xx}^{(o)} + \frac{C_{\bar{x}x}^{(o)} S^{(o)} C_{x\bar{x}}^{(o)}}{1 - C_{\bar{x}\bar{x}}^{(o)} S^{(o)}}
\tag{140}
$$

and

$$
S_{yy}''^{(o)} = D_{yy}^{(o)} + \frac{D_{\bar{y}y}^{(o)} S_{yy}'^{(o)} D_{y\bar{y}}^{(o)}}{1 - D_{\bar{y}\bar{y}}^{(o)} S_{yy}'^{(o)}} \text{ with } S_{yy}'^{(o)} = C_{yy}^{(o)} + \frac{C_{\bar{y}y}^{(o)} S^{(o)} C_{y\bar{y}}^{(o)}}{1 - C_{\bar{y}\bar{y}}^{(o)} S^{(o)}}
\tag{141}
$$

where

$$
S^{(o)} = \frac{1 - j\omega C Z_r}{1 + j\omega C Z_r}.
\tag{142}
$$

Here $C_{xx}^{(o)}$, $C_{\bar{x}x}^{(o)}$, $C_{x\bar{x}}^{(o)}$ and $C_{\bar{x}\bar{x}}^{(o)}$ are cable influences and $D_{xx}^{(o)}$, $D_{\bar{x}x}^{(o)}$, $D_{x\bar{x}}^{(o)}$ and $D_{\bar{x}\bar{x}}^{(o)}$ are drift influences of the reflection standard 1 (open) measurement at port x.

$C_{yy}^{(o)}$, $C_{\bar{y}y}^{(o)}$, $C_{y\bar{y}}^{(o)}$ and $C_{\bar{y}\bar{y}}^{(o)}$ are cable influences and $D_{yy}^{(o)}$, $D_{\bar{y}y}^{(o)}$, $D_{y\bar{y}}^{(o)}$ and $D_{\bar{y}\bar{y}}^{(o)}$ are drift influences of the reflection standard 1 (open) measurement at port y.

4. $S_{xx}''^{(r)}$ and $S_{yy}''^{(r)}$ can be replaced by the unknown reflection r_{re} and r_{im}:

$$S_{xx}''^{(r)} = D_{xx}^{(r)} + \frac{D_{\bar{x}x}^{(r)} S_{xx}'^{(r)} D_{x\bar{x}}^{(r)}}{1 - D_{\bar{x}\bar{x}}^{(r)} S_{xx}'^{(r)}} \text{ with } S_{xx}'^{(r)} = C_{xx}^{(r)} + \frac{C_{\bar{x}x}^{(r)} S^{(r)} C_{x\bar{x}}^{(r)}}{1 - C_{\bar{x}\bar{x}}^{(r)} S^{(r)}} \quad (143)$$

and

$$S_{yy}''^{(r)} = D_{yy}^{(r)} + \frac{D_{\bar{y}y}^{(r)} S_{yy}'^{(r)} D_{y\bar{y}}^{(r)}}{1 - D_{\bar{y}\bar{y}}^{(r)} S_{yy}'^{(r)}} \text{ with } S_{yy}'^{(r)} = C_{yy}^{(r)} + \frac{C_{\bar{y}y}^{(r)} S^{(r)} C_{y\bar{y}}^{(r)}}{1 - C_{\bar{y}\bar{y}}^{(r)} S^{(r)}} \quad (144)$$

where

$$S^{(r)} = r_{re} + j r_{im}. \quad (145)$$

Here $C_{xx}^{(r)}$, $C_{\bar{x}x}^{(r)}$, $C_{x\bar{x}}^{(r)}$ and $C_{\bar{x}\bar{x}}^{(r)}$ are cable influences and $D_{xx}^{(r)}$, $D_{\bar{x}x}^{(r)}$, $D_{x\bar{x}}^{(r)}$ and $D_{\bar{x}\bar{x}}^{(r)}$ are drift influences of the reflection standard 2 measurement at port x.

$C_{yy}^{(r)}$, $C_{\bar{y}y}^{(r)}$, $C_{y\bar{y}}^{(r)}$ and $C_{\bar{y}\bar{y}}^{(r)}$ are cable influences and $D_{yy}^{(r)}$, $D_{\bar{y}y}^{(r)}$, $D_{y\bar{y}}^{(r)}$ and $D_{\bar{y}\bar{y}}^{(r)}$ are drift influences of the reflection standard 2 measurement at port y.

5. $S_{xx}''^{(m)}$ can be replaced by the unknown series inductance L:

$$S_{xx}''^{(m)} = D_{xx}^{(m)} + \frac{D_{\bar{x}x}^{(m)} S_{xx}'^{(m)} D_{x\bar{x}}^{(m)}}{1 - D_{\bar{x}\bar{x}}^{(m)} S_{xx}'^{(m)}} \text{ with } S_{xx}'^{(m)} = C_{xx}^{(m)} + \frac{C_{\bar{x}x}^{(m)} S^{(m)} C_{x\bar{x}}^{(m)}}{1 - C_{\bar{x}\bar{x}}^{(m)} S^{(m)}} \quad (146)$$

and

$$S^{(m)} = \frac{R + j\omega L - Z_r}{R + j\omega L + Z_r}. \quad (147)$$

Here $C_{xx}^{(m)}$, $C_{\bar{x}x}^{(m)}$, $C_{x\bar{x}}^{(m)}$ and $C_{\bar{x}\bar{x}}^{(m)}$ are cable influences and $D_{xx}^{(m)}$, $D_{\bar{x}x}^{(m)}$, $D_{x\bar{x}}^{(m)}$ and $D_{\bar{x}\bar{x}}^{(m)}$ are drift influences of the match measurement at port x.

6. This finally yields two complex non-linear equations with four scalar unknowns.

7. Non-linear optimization yields C, r_{re}, r_{im} and L. This optimization is independent of the error terms. The starting values are $C = 0$, $r_{re} = -1$, $r_{im} = 0$ and $L = 0$.

8. Now all standards are fully known and the QSOLT calibration, see section 3.3, is used to compute the error terms.

3.7 Juroshek Calibration

The Juroshek calibration is described in [15]. The following assignment prepares the raw data measured by the VNA.

$$M_{xx}'^{(i)} := \frac{M_{xx}'^{(i)}}{M_{yx}'^{(i)}} \quad (148)$$

Finally one can compute a one port calibration, see section 3.1. Where

x is the VNA port where port 1 of the splitter is connected,

y is the VNA port where port 2 or 3 of the splitter is connected,

$E_{\bar{x}\bar{x}}$ is the equivalent source match of port 3 or 2 of the splitter.

3.8 LHKM Calibration

The LHKM calibration is described in [16], [17]. This calibration is not fully implemented in METAS VNA Tools and it's still under development. At the current state it only supports the non-leaky error model and not the full-leaky error model.

The following equation describes the in METAS VNA Tools used LHKM calibration model

$$\mathbf{M}''^{(i)}\mathbf{A} - \mathbf{B} - \mathbf{M}''^{(i)}\mathbf{C}\mathbf{S}''^{(i)} + \mathbf{D}\mathbf{S}''^{(i)} = 0 \tag{149}$$

with

$$\mathbf{A}_{00} = 1 \tag{150}$$

where $\mathbf{M}''$ denotes the switch corrected measured data including noise and linearity influences. And $\mathbf{S}''$ denotes the actual data including the cable stability, connector repeatability and the drift of the calibration error terms.

The ABCD terms of the LHKM calibration model can be converted to the generic calibration model. The result will be the error terms $\mathbf{E}$

$$\mathbf{E} = \left(\begin{array}{cc} \mathbf{E}_{00} & \mathbf{E}_{01} \\ \mathbf{E}_{10} & \mathbf{E}_{11} \end{array} \right) \tag{151}$$

with

$$\mathbf{E}_{10} = \mathbf{A}^{-1} \tag{152}$$
$$\mathbf{E}_{00} = \mathbf{B}\mathbf{A}^{-1} \tag{153}$$
$$\mathbf{E}_{11} = \mathbf{A}^{-1}\mathbf{C} \tag{154}$$
$$\mathbf{E}_{01} = \mathbf{B}\mathbf{A}^{-1}\mathbf{C} - \mathbf{D}. \tag{155}$$

3.8.1 TRL, LRL, TRM, LRM

The LHKM (TRL, LRL) and LHKM (TRM, LRM) calibrations are described in [17]. These calibration algorithms and the associated uncertainty propagation can lead to over-determined linear and quadratic eigenvalue problems. The over-determined non-linear eigenvalue problem is described in appendix I.

3.9 Frequency Conversion Calibrations

3.9.1 Scalar Mixer

The scalar mixer calibration is based on one port calibrations including power for each port, see section 3.1.

The directivity E_{xx}, the reflection tracking $E_{x\bar{x}}E_{\bar{x}x}$ and the source match term $E_{\bar{x}\bar{x}}$ are known for each port x after the one port calibrations. The magnitudes of the tracking terms $|E_{x\bar{x}}|$ and $|E_{\bar{x}x}|$ are known for each port x after the power calibrations.

The unknown phase of the symmetry term $\arg(E_{\bar{x}x})$ is assumed as normal distribution $(0° \pm 180°/\sqrt{2})$ for $k = 2$. This uncertainty is uncorrelated over frequency and uncorrelated for each port x.

The following equation describes the phase of the other tracking term

$$\arg(E_{x\bar{x}}) = \arg(E_{x\bar{x}}E_{\bar{x}x}) - \arg(E_{\bar{x}x}). \tag{156}$$

This yields in an expanded uncertainty for the unknown phase of $\pm 180°$ for a transmission measurement and $\pm 0°$ for a reflection measurement. This uncertainty is uncorrelated over frequency.

3.9.2 Unknown Mixer Phase

The unknown mixer phase calibration is based on the scalar mixer calibration except the phase of the symmetry term $\arg(E_{\bar{x}x})$, see section 3.9.1.

The absolute phase of the symmetry term is given by

$$\arg(E_{\bar{x}x}) = \arg(E_{\bar{x}x}^O) + \arg(E_{\bar{x}x}^R). \tag{157}$$

where

$\arg(E_{\bar{x}x}^O)$ is the offset phase which is constant for all frequency points and

$\arg(E_{\bar{x}x}^R)$ is the relative phase between different frequency points.

The unknown offset phase of the symmetry term $\arg(E_{\bar{x}x}^O)$ is assumed as normal distribution $(0° \pm 180°/\sqrt{2})$ for $k = 2$. This uncertainty is correlated over frequency and uncorrelated for each port x. The relative phase of the symmetry term $\arg(E_{\bar{x}x}^R)$ is computed using the unknown thru calibration, see section 3.4.

The following equation describes the phase of the other tracking term

$$\arg(E_{x\bar{x}}) = \arg(E_{x\bar{x}}E_{\bar{x}x}) - \arg(E_{\bar{x}x}). \tag{158}$$

This yields in an expanded uncertainty for the unknown offset phase of $\pm 180°$ for a transmission measurement and $\pm 0°$ for a reflection measurement. This uncertainty is correlated over frequency. Therefor it drops out when computing the group delay.

3.9.3   Unknown Mixer Mag Phase

The unknown mixer mag phase calibration is based on the unknown mixer phase calibration except the magnitude of the symmetry term $|E_{\bar{x}x}|$, see section 3.9.2. A power calibration at each port is not needed.

The magnitude of the symmetry term $|E_{\bar{x}x}|$ and the relative phase of the symmetry term $\arg(E_{\bar{x}x}^R)$ are computed using the unknown thru calibration, see section 3.4.

The following equation describes the magnitude and phase of the other tracking term

$$E_{x\bar{x}} = \frac{E_{x\bar{x}}E_{\bar{x}x}}{E_{\bar{x}x}}. \tag{159}$$

4 VNA Switched Calibration Model

The Switched VNA Model uses N error terms matrices $\overset{x}{\mathbf{E}}$ for an N-port VNA. One for each switch position x of the source. The switch terms matrix $\mathbf{W}$ and the associated drift $\mathbf{V}$ is set to zero. The Switched VNA Model supports the following calibration types: SOLT, Reflection Normalization, Transmission Normalization and One Path Two Ports.

4.1 SOLT Calibration

4.1.1 Reflection
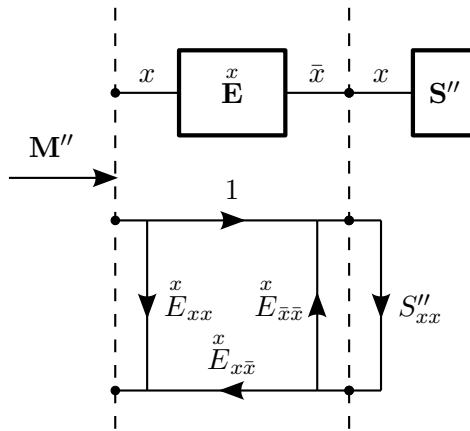
Figure 7: SOLT Reflection Calibration

The following equation describes the cascading of the reflection error terms and the definition of the calibration standard

$$M_{xx}^{\prime\prime(i)} = \overset{x}{E}_{xx} + \frac{\overset{x}{E}_{x\bar{x}} S_{xx}^{\prime\prime(i)}}{1 - \overset{x}{E}_{\bar{x}\bar{x}} S_{xx}^{\prime\prime(i)}} \tag{160}$$

with

$$\bar{x} = N + x. \tag{161}$$

N is the number of ports and x is the actual port where the reflection calibration is performed. Equation 160 can be rearranged as

$$\underbrace{M_{xx}^{\prime\prime(i)}}_{y_i} = \underbrace{\overset{x}{E}_{xx}}_{p_1} + \underbrace{\overset{x}{E}_{\bar{x}\bar{x}}}_{p_2} M_{xx}^{\prime\prime(i)} S_{xx}^{\prime\prime(i)} + \underbrace{\left(\overset{x}{E}_{x\bar{x}} - \overset{x}{E}_{xx} \overset{x}{E}_{\bar{x}\bar{x}} \right)}_{p_3} S_{xx}^{\prime\prime(i)}. \tag{162}$$

Equation 162 can be written as a system of linear equations

$$\mathbf{p} = \mathbf{A}^{-1}\mathbf{y} \tag{163}$$

with

$$\mathbf{A} = \begin{pmatrix} 1 & M_{xx}^{\prime\prime(1)} S_{xx}^{\prime\prime(1)} & S_{xx}^{\prime\prime(1)} \\ 1 & M_{xx}^{\prime\prime(2)} S_{xx}^{\prime\prime(2)} & S_{xx}^{\prime\prime(2)} \\ 1 & M_{xx}^{\prime\prime(3)} S_{xx}^{\prime\prime(3)} & S_{xx}^{\prime\prime(3)} \end{pmatrix} \tag{164}$$

and

$$\mathbf{y} = \begin{pmatrix} M_{xx}''^{(1)} \\ M_{xx}''^{(2)} \\ M_{xx}''^{(3)} \end{pmatrix}.$$ (165)

For example the first measurement could be a short, the second an open and the third a load. The vector $\mathbf{p}$ contains the solution for the error terms.

$$\overset{x}{E}_{xx} = p_1$$ (166)

$$\overset{x}{E}_{\bar{x}x} = 1$$ (167)

$$\overset{x}{E}_{x\bar{x}} = p_3 + p_1 p_2$$ (168)

$$\overset{x}{E}_{\bar{x}\bar{x}} = p_2$$ (169)

$\overset{x}{E}_{xx}$ stands for the directivity, $\overset{x}{E}_{x\bar{x}} \overset{x}{E}_{\bar{x}x}$ denotes the reflection tracking and $\overset{x}{E}_{\bar{x}\bar{x}}$ designates the source match term.

4.1.2 Power

For a power calibration the scaling factor of the tracking terms have to be determined.
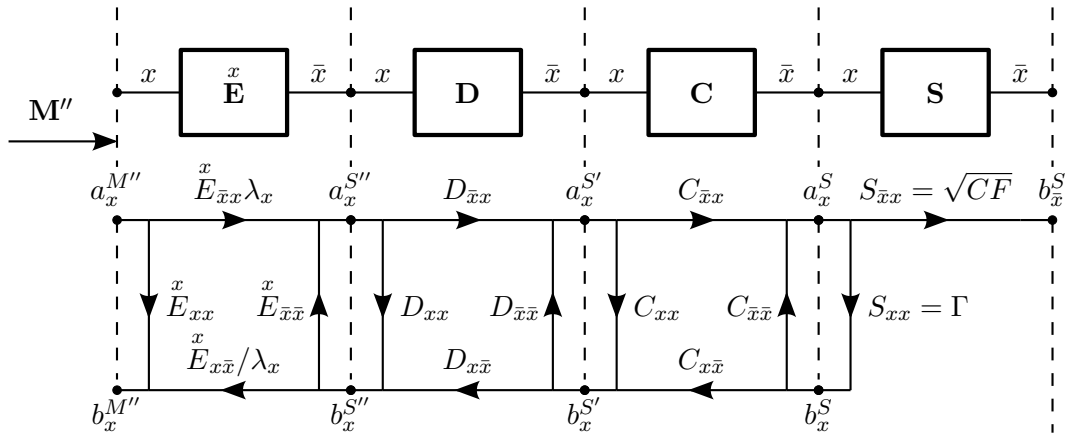
Figure 8: SOLT Power Calibration

In a first step the reflection coefficient Γ of the power sensor is computed using error correction, see section 2.

In a second step the scaling factor λ_x is computed using the receiver values from the VNA, the indicated power of the power sensor, the calibration factor CF of the power sensor, the error terms and all uncertainty influences. λ_x is computed for each switch position x of the source. The following set of equations holds

$$b_x^{M''} = a_x^{M''} \overset{x}{E}_{xx} + b_x^{S''} \overset{x}{E}_{x\bar{x}}/\lambda_x$$ (170)

$$a_x^{S''} = a_x^{M''} \overset{x}{E}_{\bar{x}x} \lambda_x + b_x^{S''} \overset{x}{E}_{\bar{x}\bar{x}}$$ (171)

where

$a_x^{M''}$ denotes the reference receiver value of port x including noise and linearity uncertainties,

$b_x^{M''}$ denotes the test receiver value of port x including noise and linearity uncertainties,

$a_x^{S''}$ denotes the incident wave of the power sensor connected to port x in $\sqrt{\text{mW}}$ including drift, cable stability, connector repeatability and standard definition uncertainties,

$b_x^{S''}$ denotes the reflected wave of the power sensor connected to port x in $\sqrt{\text{mW}}$ including drift, cable stability, connector repeatability and standard definition uncertainties,

$|b_{\bar{x}}^{S}|^2$ denotes the indicated power of the power sensor in mW including all absolute and relative uncertainties of the power sensor,

$\overset{x}{E}_{xx}$ denotes the directivity of port x,

$\overset{x}{E}_{x\bar{x}}\overset{x}{E}_{\bar{x}x}$ denotes the reflection tracking of port x,

$\overset{x}{E}_{\bar{x}\bar{x}}$ denotes the source match term of port x,

λ_x denotes the scaling factor of the tracking terms for the switch position x of the source,

D_{xx}, $D_{\bar{x}x}$, $D_{x\bar{x}}$, $D_{\bar{x}\bar{x}}$ denote the drift influences of the power sensor measurement at port x,

C_{xx}, $C_{\bar{x}x}$, $C_{x\bar{x}}$, $C_{\bar{x}\bar{x}}$ denote the cable stability and the connector repeatability influences of the power sensor measurement at port x,

S_{xx} denotes the reflection coefficient Γ of the power sensor and

$S_{\bar{x}x}$ denotes the square root of the calibration factor $\sqrt{CF}$ of the power sensor, see section 6.18.

One can solve equation 170 for $b_x^{S''}$

$$b_x^{S''} = \frac{b_x^{M''} - a_x^{M''}\overset{x}{E}_{xx}}{\overset{x}{E}_{x\bar{x}}}\lambda_x \tag{172}$$

and plug the result into 171

$$a_x^{S''} = a_x^{M''}\overset{x}{E}_{\bar{x}x}\lambda_x + \frac{b_x^{M''} - a_x^{M''}\overset{x}{E}_{xx}}{\overset{x}{E}_{x\bar{x}}}\overset{x}{E}_{\bar{x}\bar{x}}\lambda_x. \tag{173}$$

One can solve the above equation for the scaling factor λ_x of the tracking terms

$$\lambda_x = \frac{a_x^{S''}}{a_x^{M''}\overset{x}{E}_{\bar{x}x} + \frac{b_x^{M''} - a_x^{M''}\overset{x}{E}_{xx}}{\overset{x}{E}_{x\bar{x}}}\overset{x}{E}_{\bar{x}\bar{x}}}. \tag{174}$$

The phase of λ_x is unknown because the phase of the incident wave of the power sensor $a_x^{S''}$ is unknown. For further data processing the absolute value of λ_x is used, e.g.: average of multiple power calibrations which finally yields to

$$|\lambda_x| = \sum_{i=1}^{n}\left|\frac{a_x^{S''(i)}}{a_x^{M''(i)}\overset{x}{E}_{\bar{x}x} + \frac{b_x^{M''(i)} - a_x^{M''(i)}\overset{x}{E}_{xx}}{\overset{x}{E}_{x\bar{x}}}\overset{x}{E}_{\bar{x}\bar{x}}}\right|/n. \tag{175}$$

4.1.3 Isolation

The isolation between two ports can be measured directly. Note that is is assumed that there is no drift of the isolation.

$$\overset{x}{E}_{yx} = M''^{(isol)}_{yx} \tag{176}$$

$$\overset{y}{E}_{xy} = M''^{(isol)}_{xy} \tag{177}$$

4.1.4 Transmission
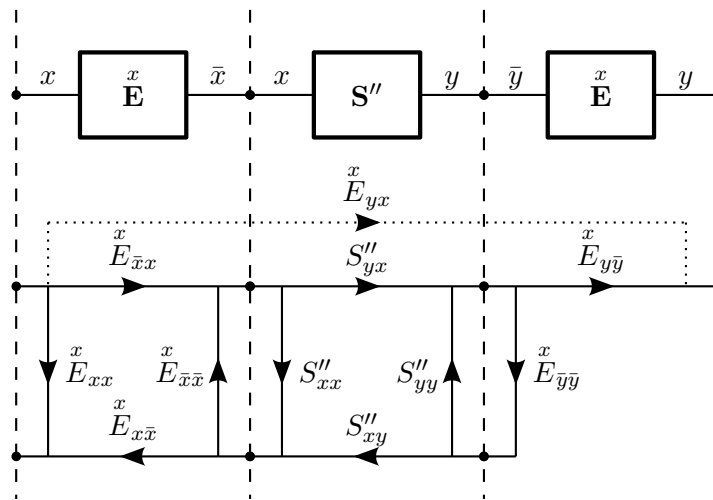
Figure 9: SOLT Forward Transmission Calibration
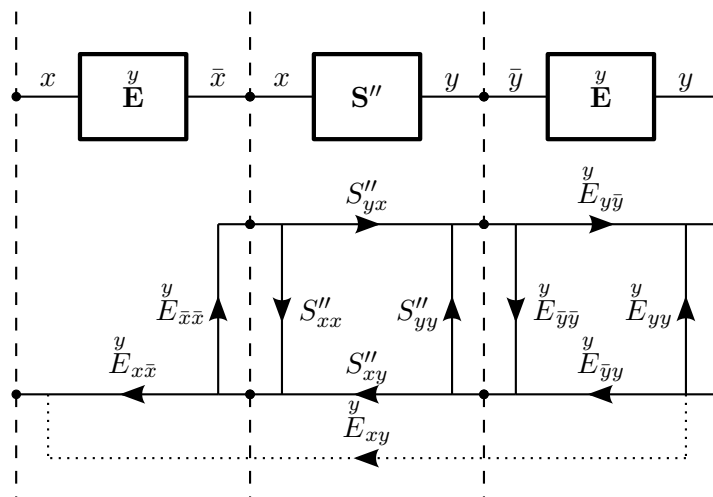
Figure 10: SOLT Reverse Transmission Calibration

The following S-parameter matrix describes the transmission standard

$$\mathbf{A}^{(i)} = \begin{pmatrix} S''^{(i)}_{xx} & S''^{(i)}_{xy} \\ S''^{(i)}_{yx} & S''^{(i)}_{yy} \end{pmatrix}. \tag{178}$$

The error box of port x is denoted as

$$\mathbf{X} = \begin{pmatrix} \overset{x}{E}_{xx} & \overset{x}{E}_{x\bar{x}} \\ \overset{x}{E}_{\bar{x}x} & \overset{x}{E}_{\bar{x}\bar{x}} \end{pmatrix} \tag{179}$$

with

$$\bar{x} = N + x \tag{180}$$

and the error box of port y is denoted as

$$\mathbf{Y} = \begin{pmatrix} \overset{y}{E}_{\bar{y}\bar{y}} & \overset{y}{E}_{\bar{y}y} \\ \overset{y}{E}_{y\bar{y}} & \overset{y}{E}_{yy} \end{pmatrix} \tag{181}$$

with

$$\bar{y} = N + y. \tag{182}$$

Cascading the error box of port x and the thru definition yields a new S-parameter matrix

$$\overset{x}{\mathbf{T}}^{(i)} = \mathbf{X} \otimes \mathbf{A}^{(i)}. \tag{183}$$

The same can be done for port y

$$\overset{y}{\mathbf{T}}^{(i)} = \mathbf{A}^{(i)} \otimes \mathbf{Y}. \tag{184}$$

The operator $\otimes$ denotes the cascading of two 2-ports, as described in appendix A.1.3.

One can introduce four new auxiliary variables, which describe the directivity and isolation corrected measurement of the transmission standard.

$$s_{xx} = M''^{(thru)}_{xx} - \overset{x}{T}^{(thru)}_{xx} \tag{185}$$

$$s_{yx} = M''^{(thru)}_{yx} - \overset{x}{E}_{yx} \tag{186}$$

$$s_{xy} = M''^{(thru)}_{xy} - \overset{y}{E}_{xy} \tag{187}$$

$$s_{yy} = M''^{(thru)}_{yy} - \overset{y}{T}^{(thru)}_{yy} \tag{188}$$

Next one can come up with equations for the transmission tracking and the load match of port

x and y.

$$\overset{x}{E}_{\bar{y}\bar{y}} \quad = \quad \frac{s_{xx}}{s_{xx}\overset{x}{T}_{yy}^{(thru)} + \overset{x}{T}_{yx}^{(thru)}\overset{x}{T}_{xy}^{(thru)}} \tag{189}$$

$$\overset{x}{E}_{y\bar{y}} \quad = \quad s_{yx}\frac{1 - \overset{x}{E}_{\bar{y}\bar{y}}\overset{x}{T}_{yy}^{(thru)}}{\overset{x}{T}_{yx}^{(thru)}} \tag{190}$$

$$\overset{y}{E}_{\bar{x}\bar{x}} \quad = \quad \frac{s_{yy}}{s_{yy}\overset{y}{T}_{xx}^{(thru)} + \overset{y}{T}_{yx}^{(thru)}\overset{y}{T}_{xy}^{(thru)}} \tag{191}$$

$$\overset{y}{E}_{x\bar{x}} \quad = \quad s_{xy}\frac{1 - \overset{y}{E}_{\bar{x}\bar{x}}\overset{y}{T}_{yy}^{(thru)}}{\overset{y}{T}_{xy}^{(thru)}} \tag{192}$$

$\overset{x}{E}_{\bar{y}\bar{y}}$ is the load match of port y,

$\overset{x}{E}_{y\bar{y}}\overset{x}{E}_{\bar{x}x}$ is the transmission tracking from port x to port y,

$\overset{y}{E}_{x\bar{x}}\overset{y}{E}_{\bar{y}y}$ is the transmission tracking from port y to port x and

$\overset{y}{E}_{\bar{x}\bar{x}}$ is the load match of port x.

4.2 Incomplete Calibrations

4.2.1 Reflection Normalization
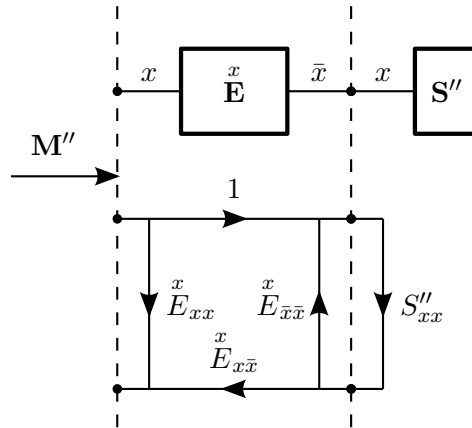
Figure 11: Reflection Normalization

The following equation describes the cascading of the error terms and the definition of the calibration standard

$$M_{xx}''^{(i)} = \overset{x}{E}_{xx} + \frac{\overset{x}{E}_{x\bar{x}} S_{xx}''^{(i)}}{1 - \overset{x}{E}_{\bar{x}\bar{x}} S_{xx}''^{(i)}} \tag{193}$$

with

$$\bar{x} = N + x. \tag{194}$$

N is the number of ports and x is the actual port where the reflection normalization is performed. Equation 193 can be rearranged as

$$\overset{x}{E}_{x\bar{x}} = \frac{\left(M_{xx}''^{(i)} - \overset{x}{E}_{xx} \right) \left(1 - \overset{x}{E}_{\bar{x}\bar{x}} S_{xx}''^{(i)} \right)}{S_{xx}''^{(i)}}. \tag{195}$$

Equation 195 is used for reflection normalization where $\overset{x}{E}_{x\bar{x}}$ denotes the reflection tracking. The unknown directivity $\overset{x}{E}_{xx}$ and the unknown source match $\overset{x}{E}_{\bar{x}\bar{x}}$ are assumed as multivariate normal distributions at the origin of the complex plane $(0 \pm \ldots) + (0 \pm \ldots)i$.

For error correction, equation 193 is rearranged as

$$S_{xx}''^{(i)} = \frac{M_{xx}''^{(i)} - \overset{x}{E}_{xx}}{\overset{x}{E}_{x\bar{x}} + \overset{x}{E}_{\bar{x}\bar{x}} \left(M_{xx}''^{(i)} - \overset{x}{E}_{xx} \right)}. \tag{196}$$

4.2.2 Transmission Normalization
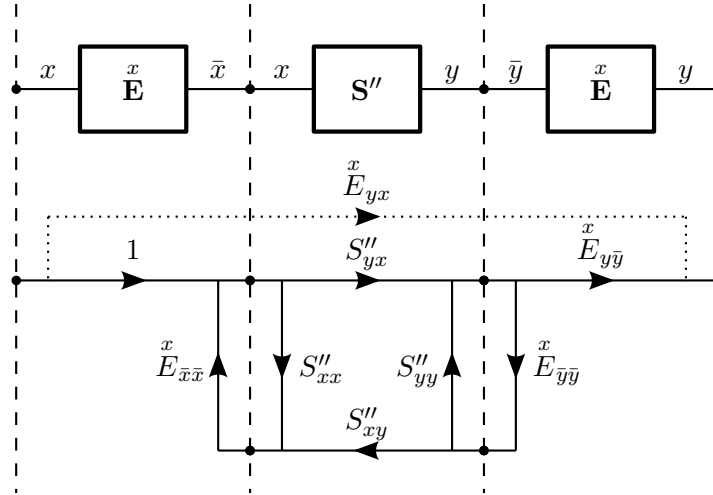
Figure 12: Transmission Normalization

The following equations describe the cascading of the transmission tracking $\overset{x}{E}_{y\bar{y}}$, the load match $\overset{x}{E}_{\bar{y}\bar{y}}$ and the definition of the transmission calibration standard

$$T''^{(i)}_{xx} = S''^{(i)}_{xx} + \frac{S''^{(i)}_{xy}\overset{x}{E}_{\bar{y}\bar{y}}S''^{(i)}_{yx}}{1 - \overset{x}{E}_{\bar{y}\bar{y}}S''^{(i)}_{yy}} \tag{197}$$

and

$$T''^{(i)}_{yx} = \frac{\overset{x}{E}_{y\bar{y}}S''^{(i)}_{yx}}{1 - \overset{x}{E}_{\bar{y}\bar{y}}S''^{(i)}_{yy}} \tag{198}$$

with

$$\bar{x} = N + x \tag{199}$$
$$\bar{y} = N + y. \tag{200}$$

N is the number of ports and x is the source port and y is the receiving port.

In a second step, the cascading of the source match $\overset{x}{E}_{\bar{x}\bar{x}}$, the crosstalk $\overset{x}{E}_{yx}$ and the results from equations 197 and 198 are used to compute the raw measured transmission

$$M''^{(i)}_{yx} = \overset{x}{E}_{yx} + \frac{T''^{(i)}_{yx}}{1 - \overset{x}{E}_{\bar{x}\bar{x}}T''^{(i)}_{xx}}. \tag{201}$$

Putting equations 197 and 198 into the above equation 201 yields into

$$M''^{(i)}_{yx} = \overset{x}{E}_{yx} + \frac{\overset{x}{E}_{y\bar{y}}S''^{(i)}_{yx}}{\left(1 - \overset{x}{E}_{\bar{y}\bar{y}}S''^{(i)}_{yy}\right)\left(1 - \overset{x}{E}_{\bar{x}\bar{x}}\left(S''^{(i)}_{xx} + \frac{S''^{(i)}_{xy}\overset{x}{E}_{\bar{y}\bar{y}}S''^{(i)}_{yx}}{1 - \overset{x}{E}_{\bar{y}\bar{y}}S''^{(i)}_{yy}}\right)\right)}. \tag{202}$$

Equation 202 can be rewritten as

$$M_{yx}''^{(i)} = \overset{x}{E}_{yx} + \frac{\overset{x}{E}_{y\bar{y}}S_{yx}''^{(i)}}{1 - \overset{x}{E}_{\bar{y}\bar{y}}S_{yy}''^{(i)} - \overset{x}{E}_{\bar{x}\bar{x}}S_{xx}''^{(i)} - \overset{x}{E}_{\bar{y}\bar{y}}\overset{x}{E}_{\bar{x}\bar{x}}S_{yx}''^{(i)}S_{xy}''^{(i)} + \overset{x}{E}_{\bar{y}\bar{y}}\overset{x}{E}_{\bar{x}\bar{x}}S_{yy}''^{(i)}S_{xx}''^{(i)}}. \quad (203)$$

Equation 203 can be rearranged as

$$\overset{x}{E}_{y\bar{y}} = \frac{M_{yx}''^{(i)} - \overset{x}{E}_{yx}}{S_{yx}''^{(i)}} \left(1 - \overset{x}{E}_{\bar{y}\bar{y}}S_{yy}''^{(i)} - \overset{x}{E}_{\bar{x}\bar{x}}S_{xx}''^{(i)} - \overset{x}{E}_{\bar{y}\bar{y}}\overset{x}{E}_{\bar{x}\bar{x}}S_{yx}''^{(i)}S_{xy}''^{(i)} + \overset{x}{E}_{\bar{y}\bar{y}}\overset{x}{E}_{\bar{x}\bar{x}}S_{yy}''^{(i)}S_{xx}''^{(i)} \right). \quad (204)$$

Equation 204 is used for transmission normalization where $\overset{x}{E}_{y\bar{y}}$ denotes the transmission tracking. The unknown crosstalk $\overset{x}{E}_{yx}$, the unknown source match $\overset{x}{E}_{\bar{x}\bar{x}}$ and the unknown load match $\overset{x}{E}_{\bar{y}\bar{y}}$ are assumed as multivariate normal distributions at the origin of the complex plane $(0 \pm \ldots) + (0 \pm \ldots)i$.

For error correction, equation 203 is rearranged as

$$S_{yx}''^{(i)} = \frac{\left(M_{yx}''^{(i)} - \overset{x}{E}_{yx}\right)\left(1 - \overset{x}{E}_{\bar{y}\bar{y}}S_{yy}''^{(i)}\right)\left(1 - \overset{x}{E}_{\bar{x}\bar{x}}S_{xx}''^{(i)}\right)}{\overset{x}{E}_{y\bar{y}} + \left(M_{yx}''^{(i)} - \overset{x}{E}_{yx}\right)\overset{x}{E}_{\bar{y}\bar{y}}\overset{x}{E}_{\bar{x}\bar{x}}S_{xy}''^{(i)}}. \quad (205)$$

The unknown S-parameters of the DUT $S_{xx}^{(i)}$, $S_{xy}^{(i)}$ and $S_{yy}^{(i)}$ in equation 205 are assumed as multivariate normal distributions at the origin of the complex plane $(0 \pm 1) + (0 \pm 1)i$ for $k = 2$.

The uncertainties are computed with linear uncertainty propagation. This leads to a well known problem for linear propagation of uncertainties. Multiplying two quantities with value zero and uncertainties larger than zero yields zero with zero uncertainty. Using Monte-Carlo uncertainty propagation yields a value of zero and an uncertainty of the product of the uncertainties of the two input quantities. This is only valid as long the input quantities are not correlated.

To overcome this problem the linear uncertainty propagation has been extended with the following function

$$
\begin{align}
(0 \pm \mathrm{u}(c)) &= \mathrm{multiply0by0}\left((0 \pm \mathrm{u}(a)), (0 \pm \mathrm{u}(b))\right) \quad (206) \\
&= (0 \pm \mathrm{u}(a * b)). \quad (207)
\end{align}
$$

The above function is used when multiplying $\overset{x}{E}_{\bar{y}\bar{y}}S_{yy}''^{(i)}$ and $\overset{x}{E}_{\bar{x}\bar{x}}S_{xx}''^{(i)}$ of equation 205. Like that, the error corrected transmission $S_{yx}''^{(i)}$ of the DUT depends as well on the unknown source match, unknown load match and the unknown S-parameters of the DUT.

The second term $\overset{x}{E}_{\bar{y}\bar{y}}\overset{x}{E}_{\bar{x}\bar{x}}S_{xy}''^{(i)}$ of the denominator of equation 205 can be neglected because it's very small. This finally yields to

$$S_{yx}''^{(i)} \approx \frac{M_{yx}''^{(i)} - \overset{x}{E}_{yx}}{\overset{x}{E}_{y\bar{y}}} \left(1 - \mathrm{multiply0by0}\left(\overset{x}{E}_{\bar{y}\bar{y}}, S_{yy}''^{(i)}\right) \right)\left(1 - \mathrm{multiply0by0}\left(\overset{x}{E}_{\bar{x}\bar{x}}, S_{xx}''^{(i)}\right) \right). \quad (208)$$

4.2.3 One Path Two Ports Calibration
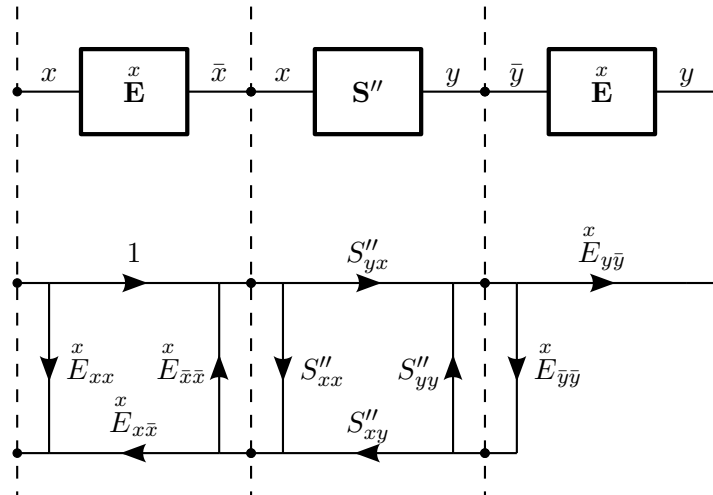
Figure 13: One Path Two Ports Calibration

In a first step, the reflection error terms $\overset{x}{E}_{xx}$, $\overset{x}{E}_{x\bar{x}}$ and $\overset{x}{E}_{\bar{x}\bar{x}}$ are computed using a reflection calibration, see section 4.1.1.

In a second step, the the transmission error terms $\overset{y}{E}_{y\bar{y}}$ and $\overset{x}{E}_{\bar{y}\bar{y}}$ are computed using a forward transmission calibration, see section 4.1.4. The S-parameters of the transmission standard definition $S''^{(i)}_{xx}$, $S''^{(i)}_{yx}$, $S''^{(i)}_{xy}$ and $S''^{(i)}_{yy}$ need to be fully known.

For error correction, see appendix B.3. The unknown reverse S-parameters of the DUT $S^{(i)}_{xy}$ and $S^{(i)}_{yy}$ are assumed as multivariate normal distributions at the origin of the complex plane $(0 \pm 1) + (0 \pm 1)i$ for $k = 2$.

5   VNA Optimization Calibration

For the optimization calibration [19] the optimizer computes the switch and calibration error terms and the unknown terms of the calibration standard definitions for an over-determined calibration. It uses an optimization algorithm for the VNA measurement model. The following equation describes the in METAS VNA Tools used N-port VNA measurement model, see section 2.

$$\mathbf{M}^{(i)} = \mathbf{R}^{(i)} + \left[\left(\mathbf{W} + \mathbf{V}^{(i)} \right) \oplus \left[\mathbf{E} \oplus \left[\mathbf{D}^{(i)} \oplus \left[\mathbf{C}^{(i)} \oplus \mathbf{S}^{(i)} \right] \right] \right] \right] \tag{209}$$

The inverse function of the above equation can be used for error correction.

$$\mathbf{S}^{(i)} = \left[\left[\left[\left(\mathbf{M}^{(i)} - \mathbf{R}^{(i)} \right) \ominus \left(\mathbf{W} + \mathbf{V}^{(i)} \right) \right] \ominus \mathbf{E} \right] \ominus \mathbf{D}^{(i)} \right] \ominus \mathbf{C}^{(i)} \tag{210}$$

The optimizer minimizes the following objective function for all measurements.

$$\left[\left[\left[\left[\left(\mathbf{M}^{(i)} - \mathbf{R}^{(i)} \right) \ominus \left(\mathbf{W} + \mathbf{V}^{(i)} \right) \right] \ominus \mathbf{E} \right] \ominus \mathbf{D}^{(i)} \right] \ominus \mathbf{C}^{(i)} \right] - \mathbf{S}^{(i)} \tag{211}$$

5.1   Weighting

The following equation describes the objective function f where $\mathbf{X}$ are the variable optimization parameters and $\mathbf{P}$ are the constant optimization parameters.

$$\mathbf{F} = f(\mathbf{X}, \mathbf{P}) \tag{212}$$

5.1.1   Covariance Weighting

For the weighting of the optimization problem the covariance of the objective function can be used.

$$\mathbf{C}_F = \mathbf{J}_{F,P} \mathbf{C}_P \mathbf{J}'_{F,P} \tag{213}$$

The optimization problem is described with the following expression.

$$\min_{\mathbf{X} \in \mathbb{R}^n} \left(\mathbf{F} \mathbf{C}_F^{-1} \mathbf{F}' \right) \tag{214}$$

One can introduce $\mathbf{G} = \mathbf{F} \mathbf{W}_F$, then the optimization problem becomes

$$\min_{\mathbf{X} \in \mathbb{R}^n} \left(\mathbf{G} \mathbf{G}' \right) \tag{215}$$

where the weights $\mathbf{W}_F$ are computed from the covariance of the objective function $\mathbf{C}_F$ using the Cholesky decomposition and the inverse of a triangular matrix.

5.1.2   User-Defined Weighting

Using user-defined weights $\mathbf{W}_U$ changes the objective function to

$$\mathbf{G} = \mathbf{F} \mathbf{W}_U. \tag{216}$$

5.2   Uncertainty Propagation

The Jacobi matrix $\mathbf{X}$ to $\mathbf{P}$ at the point of the solution is described with the following equation.

$$\mathbf{J}_{X,P} = \left(\mathbf{J}'_{G,X} \mathbf{J}_{G,X} \right)^{-1} \mathbf{J}'_{G,X} \mathbf{J}_{G,P} \tag{217}$$

It can be used for the uncertainty propagation.

6 VNA Calibration Standard

6.1 Agilent Model Standard

The Agilent model standard is described in [20].
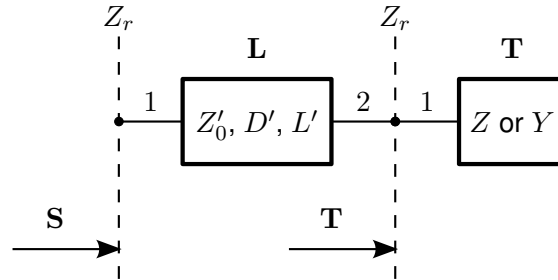
Figure 14: Agilent Model Standard

The S-parameters of an Agilent model reflection standard are defined by the following equation where $\mathbf{L}$ is the transmission line section and $\mathbf{T}$ is the reflection part.

$$\mathbf{S} = \mathbf{L} \oplus \mathbf{T} \tag{218}$$

The coaxial transmission line section is computed with the following two equations. Where Z_0' is the Offset Z0 in Ohm, D' is the Offset Delay in s and L' is the Offset Loss in Ohm/s.

$$Z_0 = Z_0' \left(1 + (1 - j) \frac{L'}{2\omega Z_0'} \sqrt{\frac{f}{1\,\mathrm{GHz}}} \right) \tag{219}$$

$$\gamma l = j\omega D' \left(1 + (1 - j) \frac{L'}{2\omega Z_0'} \sqrt{\frac{f}{1\,\mathrm{GHz}}} \right) \tag{220}$$

The waveguide transmission line section is computed with the following equation. Where μ_0 is the vacuum permeability, ϵ_0 is the vacuum permittivity, f_c is the cutoff frequency and h/w is the height to width ratio.

$$\gamma l = D' \left(L' \sqrt{\frac{\epsilon_0 \epsilon_r}{\mu_0}} \sqrt{\frac{f}{f_c}} \left(\frac{1 + \frac{2h}{w} \left(\frac{f_c}{f} \right)^2}{\sqrt{1 - \left(\frac{f_c}{f} \right)^2}} \right) + j 2\pi f \sqrt{1 - \left(\frac{f_c}{f} \right)^2} \right) \tag{221}$$

For computing the S-parameters of a transmission line section see section A.3. Where Z_r is the reference impedance, Z_0 is the characteristic impedance and γl is the propagation constant times the length.

6.1.1 Short

The reflection part of a short standard is defined by the following equations.

$$L_{eff} = L_0 + L_1 f + L_2 f^2 + L_3 f^3 \tag{222}$$

$$Z = j\omega L_{eff} \tag{223}$$

$$T_{11} = \frac{Z - Z_r}{Z + Z_r} \tag{224}$$

For an offset short the transmission line section is cascaded to the reflection part.

6.1.2 Open

The reflection part of a open standard is defined by the following equations.

$$C_{eff} = C_0 + C_1 f + C_2 f^2 + C_3 f^3 \tag{225}$$

$$Y = j\omega C_{eff} \tag{226}$$

$$T_{11} = \frac{1 - Z_r Y}{1 + Z_r Y} \tag{227}$$

For an offset open the transmission line section is cascaded to the reflection part.

6.1.3 Load

In the Agilent model a load has no reflection.

$$T_{11} = 0 \tag{228}$$

6.1.4 Delay / Thru

The S-parameters of a Delay / Thru are equal to the S-parameters of the line section.

$$\mathbf{S} = \mathbf{L} \tag{229}$$

6.2 Anritsu and Rohde Schwarz Model Standard

These model standards are similar to the Agilent model standard except the line section. The Offset Z0 Z_0' is set to the reference impedance.

The Offset Length D'' is defined in m.

$$D'' = \frac{D'c}{\sqrt{\varepsilon_r}} \tag{230}$$

Where D' is the Offset Delay in s, $c = 299792458\,\mathrm{m/s}$ is the speed of light and $\varepsilon_r = 1$ is the relative permittivity.

The Offset Loss L'' is defined in $\mathrm{dB}/\sqrt{\mathrm{GHz}}$.

$$L'' = 8.6859 \frac{D'L'}{Z_0'} \tag{231}$$

Where Z_0' is the Offset Z0 in Ohm, D' is the Offset Delay in s and L' is the Offset Loss in Ohm/s.

6.3 Databased Standard

The S-parameters of a databased standard are explicitly stated for each data point.

6.4 Ideal Standard

Table 2 shows the S-parameters for ideal standards.

Table 2: Ideal Standards

Standard	S-parameter
Ideal Short	$\mathbf{S} = \left(\ -1\ \right)$
Ideal Open	$\mathbf{S} = \left(\ 1\ \right)$
Ideal Load	$\mathbf{S} = \left(\ 0\ \right)$
Ideal Thru	$\mathbf{S} = \begin{pmatrix} 0 & 1 \\ 1 & 0 \end{pmatrix}$
Ideal Isolation	$\mathbf{S} = \begin{pmatrix} 0 & 0 \\ 0 & 0 \end{pmatrix}$

6.5 Resistance and Series Inductance

The S-parameters of a resistance R and a series inductance L are defined by the following equation

$$\mathbf{S} = \left(\ \frac{R+j\omega L-Z_r}{R+j\omega L+Z_r}\ \right). \tag{232}$$

6.6 Resistance and Parallel Capacitance

The S-parameters of a resistance R and a parallel capacitance C are defined by the following equation

$$\mathbf{S} = \left(\ \frac{1-\left(\frac{1}{R}+j\omega C\right)Z_r}{1+\left(\frac{1}{R}+j\omega C\right)Z_r}\ \right). \tag{233}$$

6.7 Unknown Standard

Table 3 shows the S-parameters for unknown standards.

Table 3: Unknown Standards

Standard	S-parameter
Unknown Reflection	$\mathbf{S} = \left(\begin{array}{c} r \end{array} \right)$
Unknown Reflection 2	$\mathbf{S} = \left(\begin{array}{c} me^{-j4\pi fl/c} \end{array} \right)$ with $|m| \leq 1$ and $l \geq 0$
Unknown Thru	$\mathbf{S} = \left(\begin{array}{cc} r_1 & t \\ t & r_2 \end{array} \right)$
Unknown Isolation	$\mathbf{S} = \left(\begin{array}{cc} r_1 & 0 \\ 0 & r_2 \end{array} \right)$
Unknown Line	$\mathbf{S} = \left(\begin{array}{cc} 0 & e^{-\gamma l} \\ e^{-\gamma l} & 0 \end{array} \right)$
Unknown Line 2	$\mathbf{S} = \left(\begin{array}{cc} r_1 & e^{-\gamma l} \\ e^{-\gamma l} & r_2 \end{array} \right)$ with $\gamma l = g_1\sqrt{\frac{f}{10^9}} + g_2\frac{f}{10^9}$
Unknown Series Inductance	$\mathbf{S} = \left(\begin{array}{c} \frac{R+j\omega L-Z_r}{R+j\omega L+Z_r} \end{array} \right)$ with $L =?$
Unknown Capacitance	$\mathbf{S} = \left(\begin{array}{c} \frac{1-j\omega CZ_r}{1+j\omega CZ_r} \end{array} \right)$ with $C =?$ and $C \geq 0$
Unknown Mixer Mag Phase	$\mathbf{S} = \left(\begin{array}{cc} r_1 & me^{jp} \\ me^{jp} & r_2 \end{array} \right)$
Unknown Mixer Phase	$\mathbf{S} = \left(\begin{array}{cc} r_1 & m_{21}e^{jp} \\ m_{12}e^{jp} & r_2 \end{array} \right)$

6.8 Primary Airline Standard

The S-parameters of a primary airline standard are defined by the following equation

$$\mathbf{S} = \mathbf{O} \oplus \mathbf{K_1} \oplus \mathbf{C_1} \oplus \mathbf{L_1} \oplus \mathbf{P} \oplus \mathbf{L_2} \oplus \mathbf{C_2} \oplus \mathbf{K_2} \oplus \mathbf{O}^{\ominus 1}. \tag{234}$$

$\mathbf{O}$ denotes the line shift, see section 6.8.1.

$\mathbf{K_1}$ denotes the kapton or adapter effect on port 1.

$\mathbf{C_1}$ denotes the half connector of the standard at port 1.

$\mathbf{L_1}$ denotes the half of the line section on port 1 side.

$\mathbf{P}$ denotes a section of ideal line, see section 6.8.2.

$\mathbf{L_2}$ denotes the half of the line section on port 2 side.

$\mathbf{C_2}$ denotes the half connector of the standard at port 2.

$\mathbf{K_2}$ denotes the kapton or adapter effect on port 2.

6.8.1 Line Shift

The S-parameters of the line shift are defined by the following equation

$$\mathbf{O} = \begin{pmatrix} 0 & e^{-j\frac{2\pi f}{c_0}l_{shift}} \\ e^{-j\frac{2\pi f}{c_0}l_{shift}} & 0 \end{pmatrix} \tag{235}$$

where f is the frequency, c_0 is the speed of light and l_{shift} is the shift length. The line shift section has to be used when the center conductor of the device of test protrudes into a test port.

If the reference plane at port 1 of the standard definition is behind the calibration reference plane (this means towards the VNA) then the value is negative. For the opposite shift it would be positive and for no shift it is zero.

6.8.2 Propagation Constant

The following equation describes the propagation constant

$$\gamma l = g_1 \sqrt{\frac{f}{1\,\text{GHz}}} + g_2 \frac{f}{1\,\text{GHz}}. \tag{236}$$

g_1, g_2 are the unknown parameters and f is the frequency. The resulting line section is defined by the following equation

$$\mathbf{P} = \begin{pmatrix} 0 & e^{-\gamma l} \\ e^{-\gamma l} & 0 \end{pmatrix}. \tag{237}$$

6.9 Primary Offset Short Standard

The S-parameters of a primary offset short standard are defined by the following equation

$$\mathbf{S} = \mathbf{K_1} \oplus \mathbf{C_1} \oplus \mathbf{L_1} \oplus \mathbf{P} \oplus \mathbf{L_2} \oplus \mathbf{T}. \tag{238}$$

$\mathbf{K_1}$ denotes the kapton or adapter effect on port 1.

$\mathbf{C_1}$ denotes the half connector of the standard.

$\mathbf{L_1}$ denotes the half of the line section on the connector side.

$\mathbf{P}$ denotes a section of ideal line, see section 6.8.2.

$\mathbf{L_2}$ denotes the half of the line section on the side of the short plane.

$\mathbf{T}$ denotes the short plane, see section 6.9.1.

6.9.1 Short Plane

The short plane is defined by the following equations

$$Z = z_1 + z_2 \sqrt{\frac{f}{1\,\text{GHz}}} + z_3 \frac{f}{1\,\text{GHz}} \tag{239}$$

$$T_{11} = \frac{Z - Z_r}{Z + Z_r} \tag{240}$$

where z_1, z_2, z_3 are the unknown parameters, f is the frequency and Z_r is the reference impedance.

6.10 Primary Flush Short Standard

The S-parameters of a primary flush short standard are defined by the following equation

$$\mathbf{S} = \mathbf{C_1} \oplus \mathbf{T}. \tag{241}$$

$\mathbf{C_1}$ denotes the half connector of the standard.

$\mathbf{T}$ denotes the short plane, see section 6.9.1.

6.11 Waveguide Shim Standard

The S-parameters of a waveguide shim standard are defined by the following equation

$$\mathbf{S} = \mathbf{O_1} \oplus \mathbf{C_1} \oplus \mathbf{D} \oplus \mathbf{C_2} \oplus \mathbf{O_2}. \tag{242}$$

$\mathbf{O_1}$ denotes the effect related to the offset (vertical and horizontal) of the waveguide connector at port 1, see section 6.11.2.

$\mathbf{C_1}$ denotes the half connector of the standard at port 1, see section 6.11.1.

$\mathbf{D}$ denotes the shim, see section 6.11.3.

$\mathbf{C_2}$ denotes the half connector of the standard at port 2, see section 6.11.1.

$\mathbf{O_2}$ denotes the effect related to the offset (vertical and horizontal) of the waveguide connector at port 2, see section 6.11.2.

6.11.1 Waveguide Connector

The S-parameters of the waveguide connector are computed using a transmission line junction, see appendix A.2. The impedances of the test port Z_1 and of the calibration standard Z_2 are defined by the following equations

$$Z_1 = j\frac{2\pi f \mu_1}{\gamma_1} \tag{243}$$

$$Z_2 = j\frac{2\pi f \mu_2}{\gamma_2} \tag{244}$$

where f is the frequency, μ the permeability and γ the propagation constant of the waveguide section, see section 6.11.4.

6.11.2 Waveguide Connector Offset

The S-parameters of the offset (width and height) of the waveguide connector are based on a look up database which has been computed using COMSOL. The following limitations exist:

- The offset in direction of the width has to be between $0\,\%$ and $3.1496\,\%$ (corresponds to $80\,\mu\mathrm{m}$ in WR10) of the nominal width.

- The offset in direction of the height has to be between $0\,\%$ and $6.2992\,\%$ (corresponds to $80\,\mu\mathrm{m}$ in WR10) of the nominal height.

- The width height ratio has to be between 2 and 2.5.

6.11.3 Shim

The shim section is defined by the following equation

$$\mathbf{D} = \begin{pmatrix} 0 & e^{-\gamma l} \\ e^{-\gamma l} & 0 \end{pmatrix}. \tag{245}$$

where l is the length of the shim section and γ is the propagation constant, see section 6.11.4. The unknown parameters in an optimization calibration are the length l and the conductivity σ_{DC}, which is used to compute the propagation constant γ.

6.11.4 Gamma

The propagation constant of a rectangular waveguide is described in [20]. The following equations are needed:

$$\sigma = \sigma_{DC} - \sigma_{HF}\sqrt{\frac{f}{1\,\text{GHz}}} \tag{246}$$

$$w_e = w - \frac{(4-\pi)\,r^2}{h} \tag{247}$$

$$x_0 = \left(\frac{c_0}{2w_e f \sqrt{\epsilon_r}}\right)^2 \tag{248}$$

$$x_1 = \frac{2\pi f \sqrt{\epsilon_r}}{c_0} \tag{249}$$

$$x_2 = \sqrt{1 - x_0} \tag{250}$$

$$x_3 = \frac{\sqrt{\frac{\pi f \mu_0}{\sigma}}}{h} \tag{251}$$

$$x_4 = \sqrt{\frac{\epsilon_0 \epsilon_r}{\mu_0}} \tag{252}$$

$$x_5 = 1 + \frac{2h}{w_e} x_0 \tag{253}$$

$$\gamma = \frac{x_3 x_4 x_5}{x_2} + j x_1 x_2. \tag{254}$$

μ and ϵ are permeability and permittivity. The waveguide section is characterized by his conductivity σ_{DC} and σ_{HF}. The frequency is f. Width w, height h and radius r describe the geometry of the waveguide section.

6.12 Waveguide Offset Short Standard

The S-parameters of a waveguide offset short standard are defined by the following equation

$$\mathbf{S} = \mathbf{O_1} \oplus \mathbf{C_1} \oplus \mathbf{D} \oplus \mathbf{T}. \tag{255}$$

$\mathbf{O_1}$ denotes the effect related to the offset (vertical and horizontal) of the waveguide connector at port 1, see section 6.11.2.

$\mathbf{C_1}$ denotes the half connector of the standard, see section 6.11.1.

$\mathbf{D}$ denotes the shim, see section 6.11.3.

$\mathbf{T}$ denotes the short plane, see section 6.12.1.

6.12.1 Short Plane

The short plane is defined by the following equations

$$Z = z_1 + z_2\sqrt{\frac{f}{1\,\text{GHz}}} + z_3\frac{f}{1\,\text{GHz}} \tag{256}$$

$$T_{11} = \frac{Z - Z_r}{Z + Z_r} \tag{257}$$

where z_1, z_2, z_3 are the unknown parameters, f is the frequency and Z_r is the reference impedance.

6.13 Waveguide Flush Short Standard

The S-parameters of a waveguide flush short standard are defined by the following equation

$$\mathbf{S} = \mathbf{T}. \tag{258}$$

$\mathbf{T}$ denotes the short plane, see section 6.12.1.

6.14 Simple Line Standard

The distributed admittance is computed with the following equation

$$Y' = G' + j\omega C' \tag{259}$$

where G' and C' are specified by the user per frequency point. The transmission line section is computed with the following two equations

$$\gamma l = \left(x_1 \sqrt{\epsilon_r} + j x_2 \frac{\omega}{c_0} \sqrt{\epsilon_r} \right) l \tag{260}$$

$$Z_0 = \frac{\gamma}{Y'} \tag{261}$$

where l is the length of the line, c_0 is the speed of light, ϵ_r is the relative permittivity and x_1, x_2 are the unknown parameters for each frequency. For computing the S-parameters of a transmission line section see section A.3.

6.15 On Wafer Line Standard

The start values for the characteristic impedance Z_0' and the propagation constant γ' are computed using the Heinrich model which is described in [21].

The equations 8, 17 and 18 from the Heinrich model [21] are modified according to the 1993 version of his FORTRAN code [22], which take into account results of his work obtained after the paper [21] went to print.

$$\omega_{c1} := \omega_{c1} \sqrt{2} \tag{262}$$

$$F_L^{(c)} := F_L^{(c)} \left(1 - 0.1 \left(\frac{a}{b} \right)^2 \right) \tag{263}$$

$$F_L^{(g)} := F_L^{(g)} \left(1 - 0.1 \left(\frac{a}{b} \right)^2 \right) \tag{264}$$

The distributed admittance is computed with the following equation.

$$Y' = \frac{\gamma'}{Z_0'} \tag{265}$$

The transmission line section is computed with the following two equations

$$\gamma l = \left(x_1 + \mathrm{Re}\left(\gamma'\right) + jx_2\,\mathrm{Im}\left(\gamma'\right)\right) l \tag{266}$$

$$Z_0 = \frac{\gamma}{Y'} \tag{267}$$

where l is the length of the line and x_1, x_2 are the unknown parameters for each frequency. For computing the S-parameters of a transmission line section see section A.3.

6.16   On Wafer Offset Short Standard

The S-parameters of an on wafer offset short standard are defined by the following equation

$$\mathbf{S} = \mathbf{L} \oplus \mathbf{T}. \tag{268}$$

$\mathbf{L}$ denotes the offset line section, see section 6.16.1.

$\mathbf{T}$ denotes the short plane, see section 6.16.2.

6.16.1   Offset Line Section

The characteristic impedance Z_0 and the propagation constant γ of the offset line section are computed using the Heinrich model which is described in [21]. The equations 8, 17 and 18 from the Heinrich model [21] are modified, see section 6.15. The length l is the unknown parameter. For computing the S-parameters of a transmission line section see section A.3.

6.16.2   Short Plane

The short plane is defined by the following equations

$$Z = z_1 + z_2\sqrt{\frac{f}{1\,\mathrm{GHz}}} + z_3\frac{f}{1\,\mathrm{GHz}} \tag{269}$$

$$T_{11} = \frac{Z - Z_r}{Z + Z_r} \tag{270}$$

where z_1, z_2, z_3 are the unknown parameters, f is the frequency and Z_r is the reference impedance.

6.17   On Wafer Flush Short Standard

The S-parameters of an on wafer flush short standard are defined by the following equation

$$\mathbf{S} = \mathbf{T}. \tag{271}$$

$\mathbf{T}$ denotes the short plane, see section 6.16.2.

6.18 Power Sensor Standard

The power sensor standard is described as a two-port using S-parameters, see figure 15
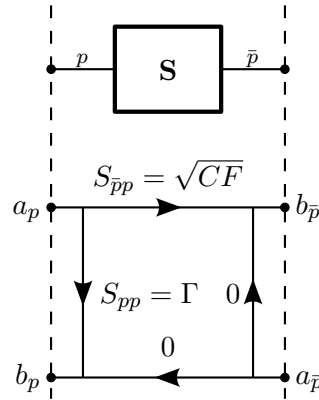
Figure 15: Power sensor standard

where

S_{pp} denotes the reflection coefficient Γ of the power sensor,

$S_{\bar{p}p}$ denotes the square root of the calibration factor $\sqrt{CF}$ of the power sensor,

a_p denotes the incident wave in $\sqrt{\text{mW}}$,

b_p denotes the reflected wave in $\sqrt{\text{mW}}$,

$|a_p|^2$ denotes the incident power in mW and

$|b_{\bar{p}}|^2$ denotes the indicated power in mW.

The following concept is proposed to map power sensor measurements with the VNA: An N-port VNA is extended by further N logical ports. As a difference to a physical port p the logical port $\bar{p}$ has no error network associated with it. For measurements, a power sensor, described as a two-port device, is inserted between a physical port and a logical port. Each physical port p has a corresponding logical port $N + p$.

7 VNA Uncertainty Contributions

Tables 4, 5, 6, 7 and 8 show the uncertainty input ids.

7.1 Noise and linearity

The noise influence is uncorrelated for each measurement because it's a random effect. The linearity influence is correlated for each measurement because it's a systematic effect.
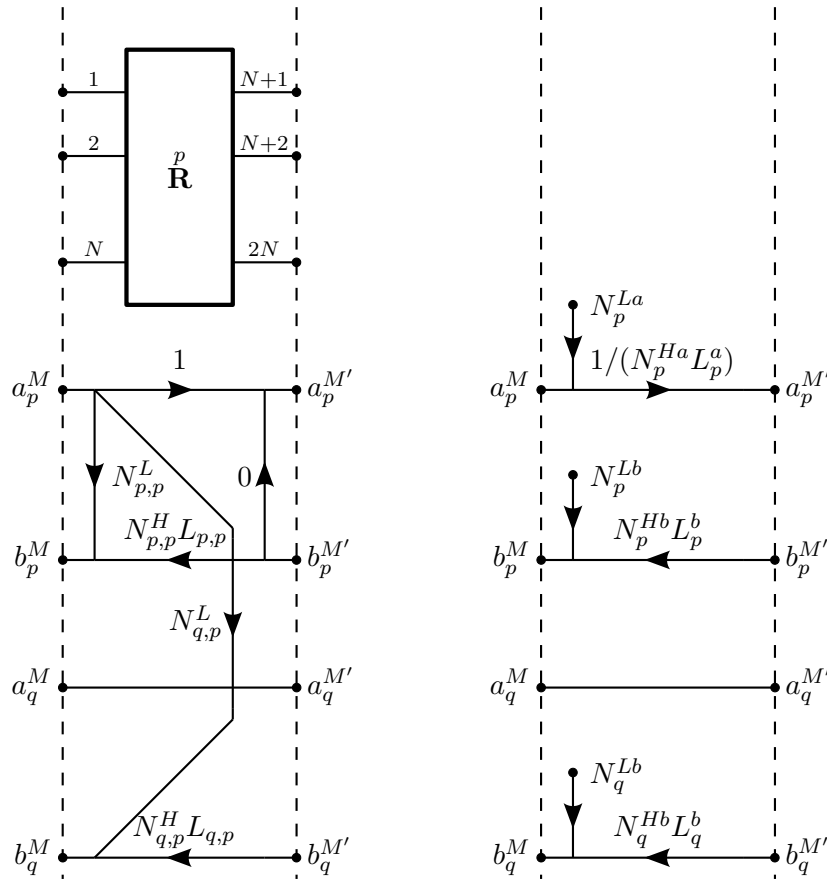
Figure 16: Noise and linearity influences (left: S-parameters, right: receivers)

Uncertainty definition:

$N_{p,p}^L = (b_p^M + N_p^{Lb})/(a_p^M + N_p^{La}) - b_p^M/a_p^M$ is the noise floor in dB (add.) of source port p.

$N_{q,p}^L = (b_q^M + N_q^{Lb})/(a_p^M + N_p^{La}) - b_q^M/a_p^M$ is the noise floor in dB (add.) from port p to q.

$N_{p,p}^H = N_p^{Hb}/N_p^{Ha}$ is the trace noise in dB and deg (multiplicative) of source port p.

$N_{q,p}^H = N_q^{Hb}/N_p^{Ha}$ is the trace noise in dB and deg (multiplicative) from port p to q.

$L_{p,p} = L_p^b/L_p^a$ is the linearity in dB and deg (multiplicative) of source port p.

$L_{q,p} = L_q^b/L_p^a$ is the linearity in dB and deg (multiplicative) from port p to q.

7.2 Drift of switch and error terms

The structure of $\mathbf{D}$ can but must not be a copy of $\mathbf{E}$. The drift influence $\mathbf{D}$ is acting on corrected S-parameters. Those the specification of $\mathbf{D}$ should be for the drift of the corrected S-parameters.

The individual drift contributions for the switch and error terms are uncorrelated for each measurement. The single drift terms are partly correlated over time. E.g.: the drift in directivity of a measurement i and $i+1$ are partly correlated whereas there is no correlation between directivity and tracking drift.
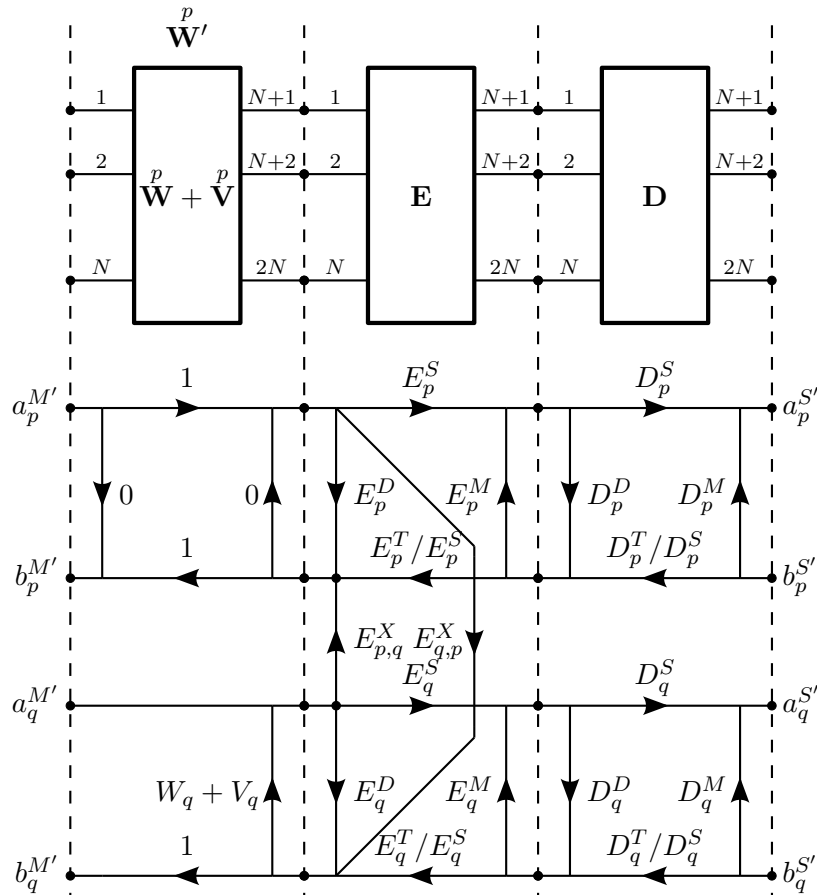
Figure 17: Drift of switch and error terms

Uncertainty definition:

V_q is the switch term drift in dB (additive) of port q when p is the source port.

D_p^D is the directivity drift in dB (additive) of port p.

D_p^T is the tracking drift in dB and deg (multiplicative) of port p.

D_p^S is the symmetry drift in dB and deg (multiplicative) of port p.

D_p^M is the match drift in dB (additive) of port p.

7.3 Cable stability, connector repeatability and DUT uncertainty

The cable influences are uncorrelated for each new cable position. The connector influences are uncorrelated for each new connection. The DUT influences are uncorrelated for each new DUT index.
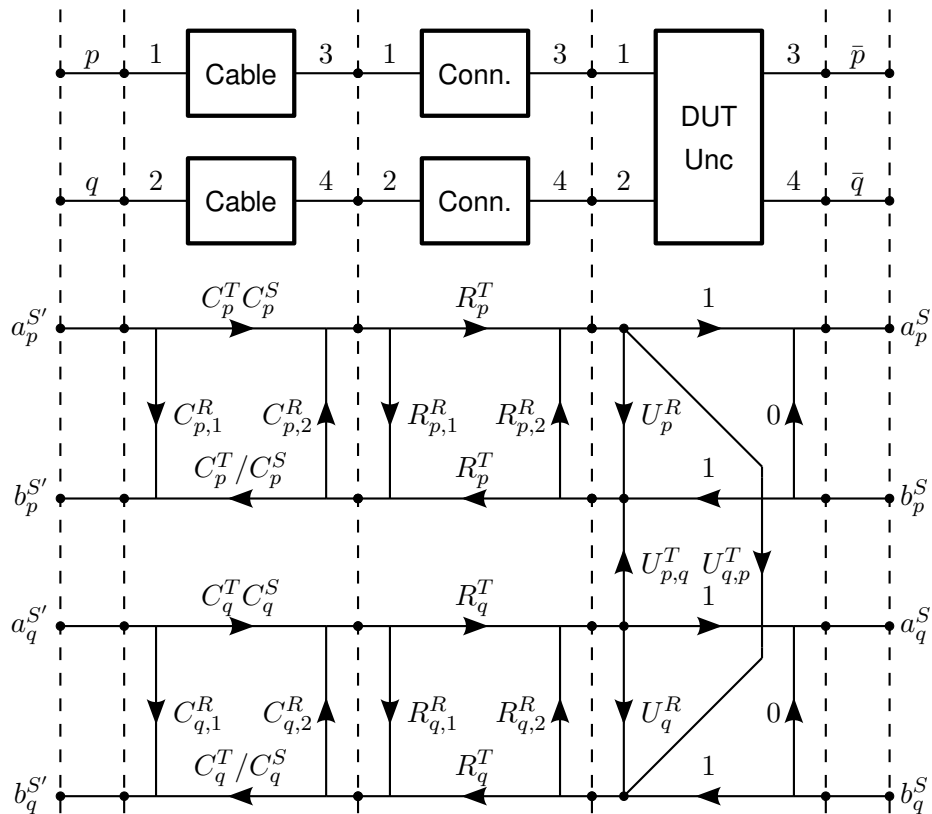
Figure 18: Cable stability, connector repeatability and DUT uncertainty

Uncertainty definition:

$C_{p,1}^R, C_{p,2}^R$ is the cable reflection stability in dB (additive) of port p.

C_p^T is the cable transmission stability in dB and deg (multiplicative) of port p.

C_p^S is the cable symmetry stability in dB and deg (multiplicative) of port p.

$R_{p,1}^R, R_{p,2}^R$ is the connector reflection repeatability in dB (additive) of port p.

R_p^T is the connector transmission repeatability in dB and deg (multiplicative).

U_p^R is the DUT reflection uncertainty (additive) of port p.

$U_{p,q}^T$ is the DUT transmission uncertainty (additive) from port q to p.

The DUT uncertainty can be used to represent the crosstalk in on-wafer measurements. In this case the DUT uncertainty is uncorrelated for every standard on the wafer and it's correlated for multiple measurements of the same standard.

Table 4: Uncertainty Input IDs

Unc Contribution	Global ID 128 bit	Influence 16 bit	Reserve 8 bit	Version 8 bit	Counter 63–48 bit	47–40 bit	39–32 bit	31–1 bit	0 bit
Unknown	Random ID	0x0000	0x00	0x00	0x0000	0x00	0x00	0x00000000	0
CMC Entry	CMC ID	0x0001	0x00	0x00	Random ID	Rcv Port	Src Port	Freq	RI
CMC Entry	CMC ID	0x0002	0x00	0x00	Random ID	Rcv Port	Src Port	Freq	MP
VNA Exp Statistical	Journal ID	0x0008	0x00	0x00	Meas Count	Rcv Port	Src Port	Freq	RI
	Journal ID	0x0008	0x00	0x01, 0x02	Meas Count	Contribution		Freq	0
	Journal ID	0x0008	0x00	0x03	Meas Count	0x00	Ref Rcv	Freq	0
VNA Exp Systematic	Journal ID	0x0009	0x00	0x00	Exp Count	Rcv Port	Src Port	Freq	RI
	Journal ID	0x0009	0x00	0x01, 0x02	Exp Count	Contribution		Freq	0
	Journal ID	0x0009	0x00	0x03	Exp Count	0x00	Ref Rcv	Freq	0
VNA Noise Floor	Journal ID	0x0011	0x00	0x00	Meas Count	Rcv Port	Src Port	Freq	RI
VNA Noise Floor	Journal ID	0x0011	0x00	0x01	Meas Count	Swt Port	0	Freq	RI
VNA Noise Floor	Journal ID	0x0011	0x00	0x02	Meas Count	0	Ref Rcv	Freq	RI
VNA Noise Trace	Journal ID	0x0012	0x00	0x00	Meas Count	Rcv Port	Src Port	Freq	MP
VNA Noise Trace	Journal ID	0x0012	0x00	0x01	Meas Count	Swt Port	0	Freq	MP
VNA Noise Trace	Journal ID	0x0012	0x00	0x02	Meas Count	0	Ref Rcv	Freq	MP
VNA Linearity	VNA ID	0x0020	0x00	0x00	$100(p+320)$	Rcv Port	0x00	0x00000000	MP
	VNA ID	0x0020	0x00	0x01, 0x02	0x0000	Rcv Port	0x00	$10^6(p+1000)$	MP
	VNA ID	0x0020	0x00	0x03	0x0000	Swt Port	0x00	$10^6(p+1000)$	MP
	VNA ID	0x0020	0x00	0x04	0x0000	Ref Rcv	0x00	$10^6(p+1000)$	MP
VNA Drift Switch Term	Journal ID	0x0031	0x00	0x00, 0x01, 0x02, 0x03	Meas Count	Port	0x00	Freq	RI
VNA Drift Directivity	Journal ID	0x0032	0x00	0x00, 0x01, 0x02, 0x03	Meas Count	Port	0x00	Freq	RI
VNA Drift Tracking	Journal ID	0x0033	0x00	0x00, 0x01, 0x02, 0x03	Meas Count	Port	0x00	Freq	MP
VNA Drift Match	Journal ID	0x0034	0x00	0x00, 0x01, 0x02, 0x03	Meas Count	Port	0x00	Freq	RI
VNA Drift Isolation	Journal ID	0x0035	0x00	0x00, 0x01, 0x02, 0x03	Meas Count	Rcv Port	Src Port	Freq	RI
VNA Drift Symmetry	Journal ID	0x0036	0x00	0x02, 0x03	Meas Count	Port	0x00	Freq	MP

Table 5: Uncertainty Input IDs cont.

Unc Contribution	Global ID 128 bit	Influence 16 bit	Reserve 8 bit	Version 8 bit	Counter 63–48 bit	47–40 bit	39–32 bit	31–1 bit	0 bit
Cable Transmission	Journal ID	0x0040	0x00	0x00	Cable Pos	Port	0x00	Freq	MP
Cable Reflection	Journal ID	0x0041	0x00	0x00	Cable Pos	Port	C_1^R, C_2^R	Freq	RI
Cable Symmetry	Journal ID	0x0042	0x00	0x00	Cable Pos	Port	0x00	Freq	MP
Connector Reflection	Journal ID	0x0050	0x00	0x00	Conn Count	Port	R_1, R_2	Freq	RI
Connector Transmission	Journal ID	0x0051	0x00	0x00	Conn Count	Port	0x00	Freq	MP
DUT Uncertainty	Journal ID	0x0058	0x00	0x00	DUT Index	Rcv Port	Src Port	Freq	RI
Cal Std Short	Cal Std ID	0x0061	0x00	0x00	0x0000	0x00	0x00	0x00000000	MP
Cal Std Open	Cal Std ID	0x0062	0x00	0x00	0x0000	0x00	0x00	0x00000000	MP
Cal Std Load	Cal Std ID	0x0063	0x00	0x00	0x0000	0x00	0x00	0x00000000	RI
Cal Std Thru / Delay Refl.	Cal Std ID	0x0064	0x00	0x00	0x0000	0x00	0x00	0x00000000	RI
Cal Std Short	Cal Std ID	0x0061	0x00	0x01	Frequency (mHz)				MP
Cal Std Open	Cal Std ID	0x0062	0x00	0x01	Frequency (mHz)				MP
Cal Std Load	Cal Std ID	0x0063	0x00	0x01	Frequency (mHz)				RI
Cal Std Thru / Delay Refl.	Cal Std ID	0x0064	0x00	0x01	Frequency (mHz)				RI
Cal Std Thru / Delay Trans.	Cal Std ID	0x0065	0x00	0x01	Frequency (mHz)				MP
Agilent Unc Calculator	Random ID	0x0071	0x00	0x00	0x0000	Rcv Port	Src Port	Freq	RI
Agilent Unc CITI File RI	Data ID	0x0072	0x00	0x00	0x0000	Rcv Port	Src Port	Freq	RI
Agilent Unc CITI File MP	Data ID	0x0073	0x00	0x00	0x0000	Rcv Port	Src Port	Freq	MP
Unknown VNA Directivity	Journal ID	0x0078	0x00	0x00	0x0000	Port	0x00	Freq	RI
Unknown VNA Refl. Tracking	Journal ID	0x0079	0x00	0x00	0x0000	Port	0x00	Freq	MP
Unknown VNA Source Match	Journal ID	0x007A	0x00	0x00	0x0000	Port	0x00	Freq	RI
Unknown VNA Isolation	Journal ID	0x007B	0x00	0x00	0x0000	Rcv Port	Src Port	Freq	RI
Unknown VNA Trans. Tracking	Journal ID	0x007C	0x00	0x00	0x0000	Rcv Port	Src Port	Freq	MP
Unknown VNA Load Match	Journal ID	0x007D	0x00	0x00	0x0000	Rcv Port	Src Port	Freq	RI
Unknown VNA Symmetry	Journal ID	0x007E	0x00	0x00	0x0000	Port	0x00	Freq	MP
	Journal ID	0x007E	0x00	0x01	0x0000	Port	0x00	0x00000000	MP
Unknown S-Parameters	Journal ID	0x0080	0x00	0x00	Meas Count	Rcv Port	Src Port	Freq	RI

Table 6: Uncertainty Input IDs cont.

Unc Contribution	Global ID 128 bit	Influence 16 bit	Reserve 8 bit	Version 8 bit	Counter 63–48 bit	47–40 bit	39–32 bit	31–1 bit	0 bit
Electrical Resistance	Random ID	0x0093	0x00	0x00	0x0000	0x00	0x00	Contribution	
Load DC Resistance	Cal Std ID	0x0094	0x00	0x00	0x0000	0x00	0x00	0x00000000	0
Load Fit Error	Cal Std ID	0x0095	0x00	0x00	0x0000	0x00	0x00	0x00000000	RI
Short DC Resistance	Cal Std ID	0x0096	0x00	0x00	0x0000	0x00	0x00	0x00000000	0
Series Inductance	Cal Std ID	0x0098	0x00	0x00	0x0000	0x00	0x00	0x00000000	0
Parallel Capacitance	Cal Std ID	0x0099	0x00	0x00	0x0000	0x00	0x00	0x00000000	0
TD Unknown DC Point	Random ID	0x0100	0x00	0x00	0x0000	0x00	0x00	0x00000000	0
TD Unknown Frequency Point	Data ID	0x0101	0x00	0x00	Frequency (mHz)				RI
Data Set	Data ID	0x0200	0x00	0x00	Freq			Contribution	
Material Parameter Length	Data ID	0x0300	0x00	0x00	0x0000	0x00	0x00	0x00000000	0
Material Relative Permittivity	Cal Std ID	0x0400	0x00	0x00	0x0000	0x00	0x00	0x00000000	0
Material Relative Permeability	Cal Std ID	0x0401	0x00	0x00	0x0000	0x00	0x00	0x00000000	0
Material Conductivity	Cal Std ID	0x0402	0x00	0x00	0x0000	0x00	0x00	0x00000000	0
Material DC Conductivity	Cal Std ID	0x0403	0x00	0x00	0x0000	0x00	0x00	0x00000000	0
Material HF Conductivity	Cal Std ID	0x0404	0x00	0x00	0x0000	0x00	0x00	0x00000000	0
Material Tan Delta	Cal Std ID	0x0405	0x00	0x00	0x0000	0x00	0x00	0x00000000	0
Conn Pin Depth	Cal Std ID	0x0410	0x00	0x00	Port	0x00	0x00	0x00000000	0
Conn Pin Gap	Cal Std ID	0x0411	0x00	0x00	Port	0x00	0x00	0x00000000	0
Conn Female Outer Chamfer	Cal Std ID	0x0412	0x00	0x00	Port	0x00	0x00	0x00000000	0
Conn Female Inner Chamfer	Cal Std ID	0x0413	0x00	0x00	Port	0x00	0x00	0x00000000	0
Conn Male Outer Chamfer	Cal Std ID	0x0414	0x00	0x00	Port	0x00	0x00	0x00000000	0
Conn Male Inner Chamfer	Cal Std ID	0x0415	0x00	0x00	Port	0x00	0x00	0x00000000	0

Table 7: Uncertainty Input IDs cont.

Unc Contribution	Global ID 128 bit	Influence 16 bit	Reserve 8 bit	Version 8 bit	Counter 63–48 bit	47–40 bit	39–32 bit	31–1 bit	0 bit
Conn Male Pin Diameter	Cal Std ID	0x0416	0x00	0x00	Port	0x00	0x00	0x00000000	0
Conn Female Hole Diameter	Cal Std ID	0x0417	0x00	0x00	Port	0x00	0x00	0x00000000	0
Conn Outer Conductor Diameter	Cal Std ID	0x0418	0x00	0x00	Port	0x00	0x00	0x00000000	0
Conn Male Center Conductor Diameter	Cal Std ID	0x0419	0x00	0x00	Port	0x00	0x00	0x00000000	0
Conn Female Hole Length	Cal Std ID	0x0420	0x00	0x00	Port	0x00	0x00	0x00000000	0
Conn Female Center Conductor Diameter	Cal Std ID	0x0421	0x00	0x00	Port	0x00	0x00	0x00000000	0
Conn Female Slot Length	Cal Std ID	0x0430	0x00	0x00	Port	0x00	0x00	0x00000000	0
Conn Female Slot Width	Cal Std ID	0x0431	0x00	0x00	Port	0x00	0x00	0x00000000	0
Conn Female Slot Chamfer	Cal Std ID	0x0432	0x00	0x00	Port	0x00	0x00	0x00000000	0
Conn Uncompressed Mid Finger Diameter	Cal Std ID	0x0441	0x00	0x00	Port	0x00	0x00	Pos Index	0
Conn Compresseed Mid Finger Diameter	Cal Std ID	0x0442	0x00	0x00	Port	0x00	0x00	Pos Index	0
Conn Outer Diameterin Finger Sections	Cal Std ID	0x0443	0x00	0x00	Port	0x00	0x00	Pos Index	0
Connector FDTD Real	Cal Std ID	0x0450	0x00	0x00	Port	0x00	0x00	0x00000000	0
Connector FDTD Imag	Cal Std ID	0x0451	0x00	0x00	Port	0x00	0x00	0x00000000	0
Pin Gap FDTD Real	Cal Std ID	0x0452	0x00	0x00	Port	0x00	0x00	0x00000000	0
Pin Gap FDTD Imag	Cal Std ID	0x0453	0x00	0x00	Port	0x00	0x00	0x00000000	0
Standard Length	Cal Std ID	0x0460	0x00	0x00	0x0000	0x00	0x00	0x00000000	0
Line Length	Cal Std ID	0x0461	0x00	0x00	0x0000	0x00	0x00	0x00000000	0
Line z Position	Cal Std ID	0x0462	0x00	0x00	0x0000	0x00	0x00	0x00000000	0
Line ICOD	Cal Std ID	0x0463	0x00	0x00	0x0000	0x00	0x00	0x00000000	0
Line OCID	Cal Std ID	0x0464	0x00	0x00	0x0000	0x00	0x00	0x00000000	0
Line Attenuation Constant	Cal Std ID	0x0470	0x00	0x00	0x0000	0x00	0x00	0x00000000	0
Line Phase Constant	Cal Std ID	0x0471	0x00	0x00	0x0000	0x00	0x00	0x00000000	0

Table 8: Uncertainty Input IDs cont.

Unc Contribution	Global ID 128 bit	Influence 16 bit	Reserve 8 bit	Version 8 bit	Counter 63–48 bit	47–40 bit	39–32 bit	31–1 bit	0 bit
Short Plane ICOD	Cal Std ID	0x0480	0x00	0x00	0x0000	0x00	0x00	0x00000000	0
Short Plane OCID	Cal Std ID	0x0481	0x00	0x00	0x0000	0x00	0x00	0x00000000	0
Misc Line Shift	Cal Std ID	0x0490	0x00	0x00	0x0000	0x00	0x00	0x00000000	0
Waveguide Length	Cal Std ID	0x0500	0x00	0x00	0x0000	0x00	0x00	0x00000000	0
Waveguide Width	Cal Std ID	0x0501	0x00	0x00	0x0000	0x00	0x00	0x00000000	0
Waveguide Height	Cal Std ID	0x0502	0x00	0x00	0x0000	0x00	0x00	0x00000000	0
Waveguide Radius	Cal Std ID	0x0503	0x00	0x00	0x0000	0x00	0x00	0x00000000	0
Waveguide Width Offset	Cal Std ID	0x0504	0x00	0x00	0x0000	0x00	0x00	0x00000000	0
Waveguide Height Offset	Cal Std ID	0x0505	0x00	0x00	0x0000	0x00	0x00	0x00000000	0
Waveguide Connector FEM	Cal Std ID	0x0506	0x00	0x00	0x0000	0x00	0x00	0x00000000	0
Simple Line Length	Cal Std ID	0x0600	0x00	0x00	0x0000	0x00	0x00	0x00000000	0
Simple Line G	Cal Std ID	0x0601	0x00	0x00	0x0000	0x00	0x00	0x00000000	0
Simple Line C	Cal Std ID	0x0602	0x00	0x00	0x0000	0x00	0x00	0x00000000	0
On Wafer Length	Cal Std ID	0x0610	0x00	0x00	0x0000	0x00	0x00	0x00000000	0
On Wafer Width of Ground Conductor	Cal Std ID	0x0611	0x00	0x00	0x0000	0x00	0x00	0x00000000	0
On Wafer Width of Signal Conductor	Cal Std ID	0x0612	0x00	0x00	0x0000	0x00	0x00	0x00000000	0
On Wafer Gap Width	Cal Std ID	0x0613	0x00	0x00	0x0000	0x00	0x00	0x00000000	0
On Wafer Conductor Thickness	Cal Std ID	0x0614	0x00	0x00	0x0000	0x00	0x00	0x00000000	0

Table 9: Uncertainty Input IDs cont.

Unc Contribution	Global ID 128 bit	Influence 16 bit	Reserve 8 bit	Version 8 bit	Counter 63–48 bit	47–40 bit	39–32 bit	31–1 bit	0 bit
Power Sensor Reflection Coefficient	Cal Std ID	0x0700	0x00	0x01	Frequency (mHz)				RI
Power Sensor Calibration Factor	Cal Std ID	0x0701	0x00	0x01	Frequency (mHz)				0
Power Sensor Exp Statistical	Journal ID	0x0708	0x00	0x00	Meas Count	0x00	0x00	Freq	0
Power Sensor Exp Systematic	Journal ID	0x0709	0x00	0x00	Exp Count	0x00	0x00	Freq	0
Power Sensor Measurement Noise	Journal ID	0x0710	0x00	0x00	Meas Count	0x00	0x00	Freq	0
Power Sensor Zero Offset	Journal ID	0x0711	0x00	0x00	Zero Count	0x00	0x00	0x00000000	0
Power Sensor Zero Drift	Journal ID	0x0712	0x00	0x00	Meas Count	0x00	0x00	Freq	0
Power Sensor Aging Freq Correlated	Cal Std ID	0x0720	0x00	0x00	0x0000	0x00	0x00	0x00000000	0
Power Sensor Aging Freq Uncorrelated	Cal Std ID	0x0721	0x00	0x01	Frequency (mHz)				0
Power Sensor Drift Freq Correlated	Journal ID	0x0722	0x00	0x00	0x0000	0x00	0x00	0x00000000	0
Power Sensor Drift Freq Uncorrelated	Journal ID	0x0723	0x00	0x00	0x0000	0x00	0x00	Freq	0
Power Sensor Linearity	Cal Std ID	0x0724	0x00	0x00	0x0000	0x00	0x00	$10^6(p + 1000)$	0
Power Sensor Power Meter	Cal Std ID	0x0725	0x00	0x00	0x0000	0x00	0x00	$10^6(p + 1000)$	0
Power Sensor Repeatability	Journal ID	0x0726	0x00	0x00	Conn Count	Port	0x00	Freq	0
Power Sensor Temperature	Journal ID	0x0727	0x00	0x00	Meas Count	0x00	0x00	Freq	0
Unknown Mixer	Cal Std ID	0x0780	0x00	0x00	Frequency (mHz)				MP

A S-Parameter Tools

A.1 Cascading

Cascading of two S-parameter sets is described in [23] and [24].
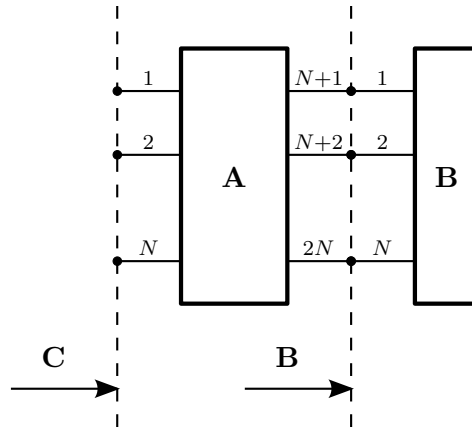
A.1.1 Cascading of a 2N-Port and a N-Port

Figure 19: Cascading of a $2N$-port ($\mathbf{A}$) and a N-port ($\mathbf{B}$)

One can use the following equation to cascade a $2N$-port and a N-port. The result will be the N-port $\mathbf{C}$

$$\mathbf{C} = \mathbf{A}_{00} + \mathbf{A}_{01} \left(\mathbf{I} - \mathbf{B}\mathbf{A}_{11}\right)^{-1} \mathbf{B}\mathbf{A}_{10} \tag{272}$$

with

$$\mathbf{A} = \left(\begin{array}{cc} \mathbf{A}_{00} & \mathbf{A}_{01} \\ \mathbf{A}_{10} & \mathbf{A}_{11} \end{array} \right). \tag{273}$$

The variables $\mathbf{A}$, $\mathbf{B}$ and $\mathbf{C}$ are S-parameter matrices. $\mathbf{A}$ is a $2N$-port and $\mathbf{B}$ is a N-port. A simplified notation can be achieved by introducing a new operator

$$\mathbf{C} = \mathbf{A} \oplus \mathbf{B}. \tag{274}$$

To find the reverse function, equation 272 can be rewritten as

$$\mathbf{A}_{01}^{-1} \left(\mathbf{C} - \mathbf{A}_{00}\right) \mathbf{A}_{10}^{-1} = \left(\mathbf{I} - \mathbf{B}\mathbf{A}_{11}\right)^{-1} \mathbf{B}. \tag{275}$$

Setting

$$\mathbf{X} = \mathbf{A}_{01}^{-1} \left(\mathbf{C} - \mathbf{A}_{00}\right) \mathbf{A}_{10}^{-1} \tag{276}$$

and rearranging equation 275 yields

$$\mathbf{B} = \mathbf{X} \left(\mathbf{I} + \mathbf{A}_{11}\mathbf{X}\right)^{-1}. \tag{277}$$

Equations 276 and 277 can be used to de-cascade the $2N$-port $\mathbf{A}$ from N-port $\mathbf{C}$ and to obtain the N-port $\mathbf{B}$. Similar to the notation in equation 274 a new operator can be introduced

$$\mathbf{B} = \mathbf{C} \ominus \mathbf{A}. \tag{278}$$
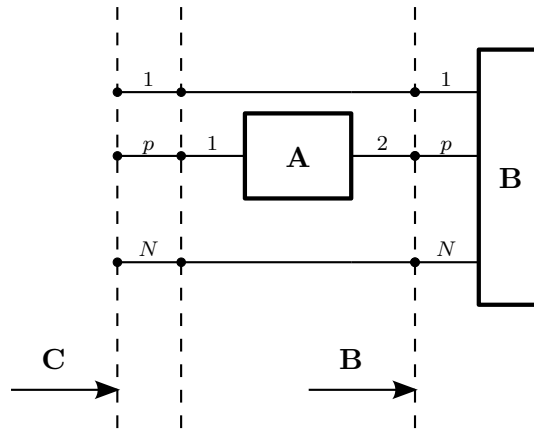
A.1.2 Cascading of a 2-Port and a N-Port

Figure 20: Cascading a of 2-port ($\mathbf{A}$) and a N-port ($\mathbf{B}$)

Cascading of a 2-port and a N-port can be computed with

$$
C_{ij} = \begin{cases} A_{11} + \frac{A_{21} B_{ij} A_{12}}{1 - A_{22} B_{pp}} & , i = j = p \\ \frac{A_{21} B_{ij}}{1 - A_{22} B_{pp}} & , i \neq p \land j = p \\ \frac{B_{ij} A_{12}}{1 - A_{22} B_{pp}} & , i = p \land j \neq p \\ B_{ij} + \frac{B_{pj} A_{22} B_{ip}}{1 - A_{22} B_{pp}} & , i \neq p \land j \neq p \land i \neq j \end{cases} .
\tag{279}
$$

Here the variables $\mathbf{A}$, $\mathbf{B}$ and $\mathbf{C}$ denote S-parameter matrices. The result $\mathbf{C}$ is a N-port with a 2-port cascaded to port p of the original N-port $\mathbf{B}$.

A.1.3 Cascading of a 2-Port and a 2-Port
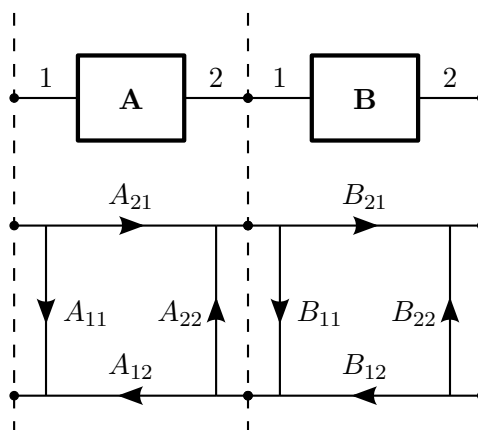
Figure 21: Cascading of a 2-port ($\mathbf{A}$) and a 2-port ($\mathbf{B}$)

A special case of cascading is a 2-port and a 2-port. Equation 279 can be rewritten as

$$C_{11} = A_{11} + \frac{A_{21}B_{11}A_{12}}{1 - A_{22}B_{11}} \tag{280}$$

$$C_{21} = \frac{A_{21}B_{21}}{1 - A_{22}B_{11}} \tag{281}$$

$$C_{12} = \frac{B_{12}A_{12}}{1 - A_{22}B_{11}} \tag{282}$$

$$C_{22} = B_{22} + \frac{B_{12}A_{22}B_{21}}{1 - A_{22}B_{11}} \tag{283}$$

and a new operator can be introduced

$$\mathbf{C} = \mathbf{A} \otimes \mathbf{B}. \tag{284}$$

To invert a 2-port, equations 280 to 283 can be rewritten as

$$B_{11} = \frac{A_{11}}{A_{11}A_{22} - A_{21}A_{12}} \tag{285}$$

$$B_{21} = \frac{1 - A_{22}B_{11}}{A_{21}} \tag{286}$$

$$B_{12} = \frac{1 - A_{22}B_{11}}{A_{12}} \tag{287}$$

$$B_{22} = -\frac{B_{12}A_{22}B_{21}}{1 - A_{22}B_{11}} \tag{288}$$

with $C_{11} = C_{22} = 0$ and $C_{21} = C_{12} = 1$. And a new operator for inverting a 2-port can be introduced.

$$\mathbf{B} = \mathbf{A}^{\ominus 1}. \tag{289}$$

A.1.4 Cascading of a 2-Port and a 1-Port

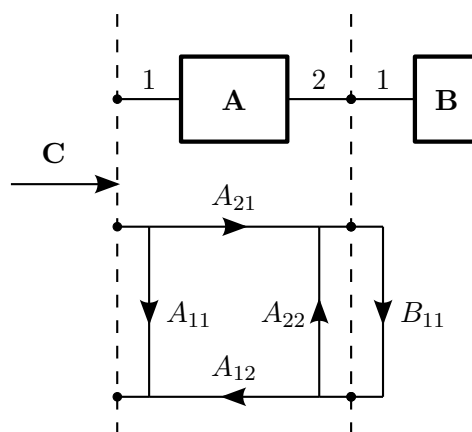Figure 22: Cascading a 2-port ($\mathbf{A}$) and a 1-port ($\mathbf{B}$)

Another special case of cascading is a 2-port and a 1-port. Then equation 279 can be rewritten as

$$C_{11} = A_{11} + \frac{A_{21}B_{11}A_{12}}{1 - A_{22}B_{11}}. \tag{290}$$

A.2 Transmission Line Junction

A transmission line junction 2-port can be used to change the reference impedance. The transformation of the reference impedance is described in [25]. VNA Tools is using pseudo waves for changing the reference impedance, see section A.2.2.
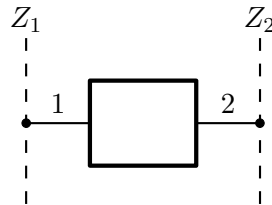

Figure 23: Transmission line junction

A.2.1 Power Waves

The S-parameters of a transmission line junction using power waves are given by the following equations

$$S_{11} = \frac{(Z_2 - Z_1)}{(Z_1 + Z_2)} \tag{291}$$

$$S_{21} = \frac{2\sqrt{Z_1 Z_2}}{(Z_1 + Z_2)} \tag{292}$$

$$S_{12} = \frac{2\sqrt{Z_1 Z_2}}{(Z_1 + Z_2)} \tag{293}$$

$$S_{22} = \frac{(Z_1 - Z_2)}{(Z_1 + Z_2)}. \tag{294}$$

The reference impedances of these S-parameters are Z_1 for port one and Z_2 for port two.

A.2.2 Pseudo Waves

The S-parameters of a transmission line junction using pseudo waves are given by the following equations

$$S_{11} = \frac{(Z_2 - Z_1)}{(Z_1 + Z_2)} \tag{295}$$

$$S_{21} = \frac{2Z_2 \left|\frac{Z_1}{Z_2}\right| \sqrt{\frac{\mathrm{Re}(Z_2)}{\mathrm{Re}(Z_1)}}}{(Z_1 + Z_2)} \tag{296}$$

$$S_{12} = \frac{2Z_1 \left|\frac{Z_2}{Z_1}\right| \sqrt{\frac{\mathrm{Re}(Z_1)}{\mathrm{Re}(Z_2)}}}{(Z_1 + Z_2)} \tag{297}$$

$$S_{22} = \frac{(Z_1 - Z_2)}{(Z_1 + Z_2)}. \tag{298}$$

The reference impedances of these S-parameters are Z_1 for port one and Z_2 for port two.

A.3 Transmission Line Section

The S-parameters of a transmission line section are given by the following equations
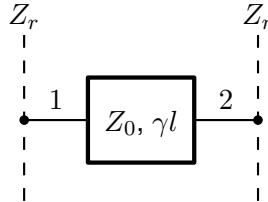
Figure 24: Transmission line section

$$
S_{11} = \frac{\left(Z_0{}^2 - Z_r{}^2\right) \sinh \gamma l}{2Z_0 Z_r \cosh \gamma l + \left(Z_0{}^2 + Z_r{}^2\right) \sinh \gamma l} \tag{299}
$$

$$
S_{21} = \frac{2Z_0 Z_r}{2Z_0 Z_r \cosh \gamma l + \left(Z_0{}^2 + Z_r{}^2\right) \sinh \gamma l} \tag{300}
$$

$$
S_{12} = \frac{2Z_0 Z_r}{2Z_0 Z_r \cosh \gamma l + \left(Z_0{}^2 + Z_r{}^2\right) \sinh \gamma l} \tag{301}
$$

$$
S_{22} = \frac{\left(Z_0{}^2 - Z_r{}^2\right) \sinh \gamma l}{2Z_0 Z_r \cosh \gamma l + \left(Z_0{}^2 + Z_r{}^2\right) \sinh \gamma l}. \tag{302}
$$

Where Z_0 is the characteristic impedance and γl is the propagation constant times the length. The reference impedance at both ports is Z_r.

A.3.1 Lossy Coaxial Transmission Line Section

A lossy coaxial transmission line section is described in [26].

$$\sigma = \sigma_{DC} - \sigma_{HF}\sqrt{\frac{f}{1\,\text{GHz}}} \tag{303}$$

$$k = \omega\sqrt{\mu\epsilon} \tag{304}$$

$$d_0 = \frac{\sqrt{\frac{2}{\sigma\omega\mu}}\left(1+\frac{b}{a}\right)}{4b\ln\left(\frac{b}{a}\right)} \tag{305}$$

$$F_0 = \frac{\frac{b^2}{a^2}-1}{2\ln\left(\frac{b}{a}\right)} - \frac{\frac{b}{a}\ln\left(\frac{b}{a}\right)}{\frac{b}{a}+1} - \frac{1}{2}\left(\frac{b}{a}+1\right) \tag{306}$$

$$C_0' = \frac{2\pi\epsilon}{\ln\left(\frac{b}{a}\right)} \tag{307}$$

$$L_0' = \frac{\mu\ln\left(\frac{b}{a}\right)}{2\pi} \tag{308}$$

$$R' = 2\omega L_0' d_0\left(1-\frac{k^2a^2F_0}{2}\right) \tag{309}$$

$$L' = L_0'\left(1+2d_0\left(1-\frac{k^2a^2F_0}{2}\right)\right) \tag{310}$$

$$G' = \omega C_0' d_0 k^2 a^2 F_0 \tag{311}$$

$$C' = C_0'\left(1+d_0 k^2 a^2 F_0\right) \tag{312}$$

$$Z' = R' + j\omega L' \tag{313}$$

$$Y' = G' + j\omega C' \tag{314}$$

$$\gamma = \sqrt{Z'Y'} \tag{315}$$

$$Z_0 = \sqrt{\frac{Z'}{Y'}} \tag{316}$$

Where μ and ϵ are permeability and permittivity of the dielectric. The conductors are characterized by their conductivity σ_{DC} and σ_{HF}. The frequency is f and the angular frequency is ω. Outer conductor inner radius b and inner conductor outer radius a describe the geometry of the line.

B   Wave Parameter Tools

The S-parameter matrix $\mathbf{S}$ is defined with the following equation

$$\mathbf{b} = \mathbf{S}\mathbf{a} \tag{317}$$

or using explicit components

$$\begin{pmatrix} b_1 \\ \vdots \\ b_N \end{pmatrix} = \begin{pmatrix} S_{1,1} & \dots & S_{1,N} \\ \vdots & \ddots & \vdots \\ S_{N,1} & \dots & S_{N,N} \end{pmatrix} \begin{pmatrix} a_1 \\ \vdots \\ a_N \end{pmatrix} \tag{318}$$

where $\mathbf{b}$ is a column vector for the test receiver wave quantities and $\mathbf{a}$ is a column vector for the reference receiver wave quantities. N is the number of ports.

The above equation can be generalized by adding additional columns to $\mathbf{b}$, $\mathbf{a}$. This yields into the following equation

$$\mathbf{B} = \mathbf{S}\mathbf{A} \tag{319}$$

or using explicit components

$$\begin{pmatrix} b_{1,1} & \dots & b_{1,N} \\ \vdots & \ddots & \vdots \\ b_{N,1} & \dots & b_{N,N} \end{pmatrix} = \begin{pmatrix} S_{1,1} & \dots & S_{1,N} \\ \vdots & \ddots & \vdots \\ S_{N,1} & \dots & S_{N,N} \end{pmatrix} \begin{pmatrix} a_{1,1} & \dots & a_{1,N} \\ \vdots & \ddots & \vdots \\ a_{N,1} & \dots & a_{N,N} \end{pmatrix} \tag{320}$$

where $\mathbf{A}$ and $\mathbf{B}$ are wave parameter matrices. The row index indicates the port and the column index indicates the stimulus port.

B.1   Cascading

Figure 25 describes cascading of an S-parameter matrix $\mathbf{Y}$, which consist of a product of wave parameter matrices, with a conventional S-parameter matrix $\mathbf{X}$. The variables $\mathbf{X}$, $\mathbf{Y}$ and $\mathbf{Z}$ are S-parameter matrices. The variables $\mathbf{B}_Y$, $\mathbf{A}_Y$ and $\mathbf{B}_Z$, $\mathbf{A}_Z$ are wave parameter matrices. $\mathbf{X}$ is a $2N$-port and $\mathbf{Y}$ is a N-port. $\mathbf{Z}$ will be a N-port. According to [23] and [24] the S-parameter matrix $\mathbf{X}$ can be split up into

$$\mathbf{X} = \begin{pmatrix} \mathbf{X}_{00} & \mathbf{X}_{01} \\ \mathbf{X}_{10} & \mathbf{X}_{11} \end{pmatrix} \tag{321}$$

and the following set of equations holds

$$\mathbf{B}_Z = \mathbf{X}_{00}\mathbf{A}_Z + \mathbf{X}_{01}\mathbf{B}_Y \tag{322}$$
$$\mathbf{A}_Y = \mathbf{X}_{10}\mathbf{A}_Z + \mathbf{X}_{11}\mathbf{B}_Y. \tag{323}$$

One can solve equation 323 for $\mathbf{A}_Z$

$$\mathbf{A}_Z = \mathbf{X}_{10}^{-1}\mathbf{A}_Y - \mathbf{X}_{10}^{-1}\mathbf{X}_{11}\mathbf{B}_Y \tag{324}$$

and plug the result into 322

$$\mathbf{B}_Z = \mathbf{X}_{00}\mathbf{X}_{10}^{-1}\mathbf{A}_Y - \left(\mathbf{X}_{00}\mathbf{X}_{10}^{-1}\mathbf{X}_{11} - \mathbf{X}_{01}\right)\mathbf{B}_Y. \tag{325}$$
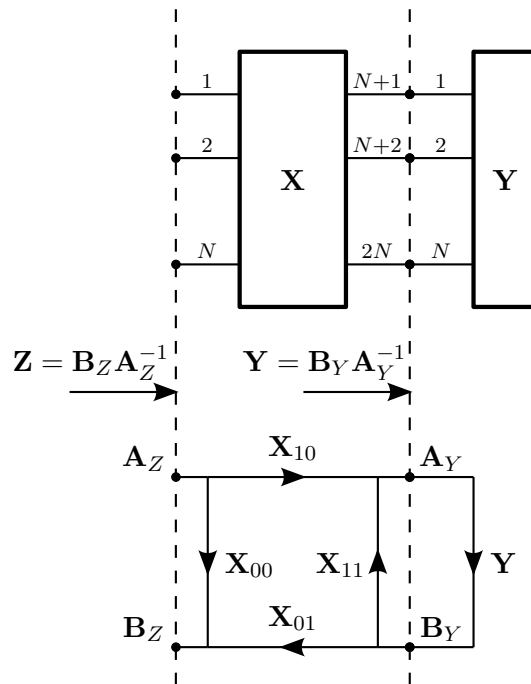
Figure 25: Cascading of a $2N$-port S-parameter ($\mathbf{X}$) and the N-port wave parameter matrices $(\mathbf{B}_Y, \mathbf{A}_Y)$

The above two equations 324 and 325 can be used to cascade a $2N$-port S-parameter and the N-port wave parameter matrices. The result will be the N-port wave parameter matrices $\mathbf{B}_Z, \mathbf{A}_Z$.

A simplified notation can be achieved by introducing a new operator

$$(\mathbf{B}_Z, \mathbf{A}_Z) = \mathbf{X} \odot (\mathbf{B}_Y, \mathbf{A}_Y). \tag{326}$$

B.2 De-cascading

One can solve equation 322 for $\mathbf{B}_Y$

$$\mathbf{B}_Y = \mathbf{X}_{01}^{-1}\mathbf{B}_Z - \mathbf{X}_{01}^{-1}\mathbf{X}_{00}\mathbf{A}_Z \tag{327}$$

and plug the result into 323

$$\mathbf{A}_Y = \mathbf{X}_{11}\mathbf{X}_{01}^{-1}\mathbf{B}_Z - \left(\mathbf{X}_{11}\mathbf{X}_{01}^{-1}\mathbf{X}_{00} - \mathbf{X}_{10}\right)\mathbf{A}_Z. \tag{328}$$

The above two equations 327 and 328 can be used to de-cascade a $2N$-port S-parameter $\mathbf{X}$ from the N-port wave parameter matrices $\mathbf{B}_Z, \mathbf{A}_Z$. The result will be the N-port wave parameter matrices $\mathbf{B}_Y, \mathbf{A}_Y$.

A simplified notation can be achieved by introducing a new operator

$$(\mathbf{B}_Y, \mathbf{A}_Y) = (\mathbf{B}_Z, \mathbf{A}_Z) \oslash \mathbf{X}. \tag{329}$$

B.3 SOLT Error Correction

Figure 26 describes the SOLT error correction of a 2-port using error terms for each switch position x of the source.
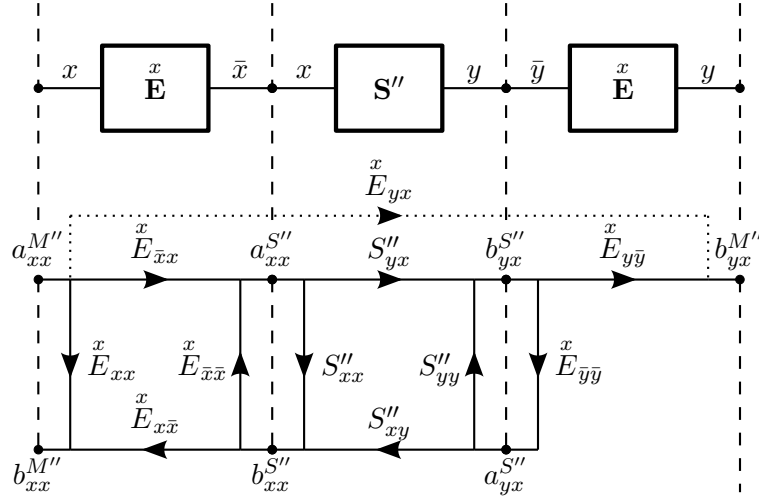
Figure 26: SOLT Error Correction

The following set of equations holds for the VNA test receivers wave quantities

$$b_{xx}^{M''} = a_{xx}^{M''}\overset{x}{E}_{xx} + b_{xx}^{S''}\overset{x}{E}_{x\bar{x}} \tag{330}$$

$$b_{yx}^{M''} = a_{xx}^{M''}\overset{x}{E}_{yx} + b_{yx}^{S''}\overset{x}{E}_{y\bar{y}} \tag{331}$$

where $\bar{x} = N + x$, $\bar{y} = N + y$ and N is the number of ports. The above equations can be solved for the reflected and transmitted wave quantities of the device under test

$$b_{xx}^{S''} = (b_{xx}^{M''} - a_{xx}^{M''}\overset{x}{E}_{xx})/\overset{x}{E}_{x\bar{x}} \tag{332}$$

$$b_{yx}^{S''} = (b_{yx}^{M''} - a_{xx}^{M''}\overset{x}{E}_{yx})/\overset{x}{E}_{y\bar{y}}. \tag{333}$$

The following set of equations holds for the incident wave quantities of the device under test

$$a_{xx}^{S''} = b_{xx}^{S''}\overset{x}{E}_{\bar{x}\bar{x}} + a_{xx}^{M''}\overset{x}{E}_{\bar{x}x} \tag{334}$$

$$a_{yx}^{S''} = b_{yx}^{S''}\overset{x}{E}_{\bar{y}\bar{y}}. \tag{335}$$

This concept can be generalized to N-ports by adding additional receiving ports.

B.4 Switch Terms

The S-parameter matrix $\mathbf{S}$ is defined with the following equation

$$\mathbf{B} = \mathbf{S}\mathbf{A} \tag{336}$$

or using explicit components

$$
\begin{pmatrix}
b_{1,1} & \dots & b_{1,N} \\
\vdots & \ddots & \vdots \\
b_{N,1} & \dots & b_{N,N}
\end{pmatrix}
=
\begin{pmatrix}
S_{1,1} & \dots & S_{1,N} \\
\vdots & \ddots & \vdots \\
S_{N,1} & \dots & S_{N,N}
\end{pmatrix}
\begin{pmatrix}
a_{1,1} & \dots & a_{1,N} \\
\vdots & \ddots & \vdots \\
a_{N,1} & \dots & a_{N,N}
\end{pmatrix}
\tag{337}
$$

where $\mathbf{A}$ and $\mathbf{B}$ are wave parameter matrices. The row index indicates the port and the column index indicates the stimulus port. N is the number of ports.

In most of the cases only the diagonal of the wave parameter matrix $\mathbf{A}$ is measured, because some VNA manufactures can not collect all test and reference receivers in the same sweep. Another reason is that measuring the complete matrix $\mathbf{A}$ will introduce more noise to the S-parameters $\mathbf{S}$ because the measured signal at the passive reference receivers is closer to the noise floor. This yields into the following equation

$$\mathbf{B} = \mathbf{S}\underbrace{\mathbf{C}\mathbf{A}_{diag}}_{\mathbf{A}}. \tag{338}$$

The off-diagonal of the matrix $\mathbf{A}$ can be reconstructed with the correction matrix $\mathbf{C}$

$$\mathbf{C} = \mathbf{A}\mathbf{A}_{diag}^{-1} \tag{339}$$

or using explicit components

$$
\mathbf{C} =
\begin{pmatrix}
1 & \frac{a_{1,2}}{a_{2,2}} & \frac{a_{1,3}}{a_{3,3}} & \dots & \frac{a_{1,N}}{a_{N,N}} \\
\frac{a_{2,1}}{a_{1,1}} & 1 & \frac{a_{2,3}}{a_{3,3}} & \dots & \frac{a_{2,N}}{a_{N,N}} \\
\frac{a_{3,1}}{a_{1,1}} & \frac{a_{3,2}}{a_{2,2}} & 1 & & \frac{a_{3,N}}{a_{N,N}} \\
\vdots & \vdots & & \ddots & \vdots \\
\frac{a_{N,1}}{a_{1,1}} & \frac{a_{N,2}}{a_{2,2}} & \frac{a_{N,3}}{a_{3,3}} & \dots & 1
\end{pmatrix}. \tag{340}
$$

One can expand the off-diagonal elements of the matrix $\mathbf{C}$ with $\frac{b_{i,j}}{b_{i,j}}$

$$
\mathbf{C} =
\begin{pmatrix}
1 & \frac{b_{1,2}}{a_{2,2}}\frac{a_{1,2}}{b_{1,2}} & \frac{b_{1,3}}{a_{3,3}}\frac{a_{1,3}}{b_{1,3}} & \dots & \frac{b_{1,N}}{a_{N,N}}\frac{a_{1,N}}{b_{1,N}} \\
\frac{b_{2,1}}{a_{1,1}}\frac{a_{2,1}}{b_{2,1}} & 1 & \frac{b_{2,3}}{a_{3,3}}\frac{a_{2,3}}{b_{2,3}} & \dots & \frac{b_{2,N}}{a_{N,N}}\frac{a_{2,N}}{b_{2,N}} \\
\frac{b_{3,1}}{a_{1,1}}\frac{a_{3,1}}{b_{3,1}} & \frac{b_{3,2}}{a_{2,2}}\frac{a_{3,2}}{b_{3,2}} & 1 & & \frac{b_{3,N}}{a_{N,N}}\frac{a_{3,N}}{b_{3,N}} \\
\vdots & \vdots & & \ddots & \vdots \\
\frac{b_{N,1}}{a_{1,1}}\frac{a_{N,1}}{b_{N,1}} & \frac{b_{N,2}}{a_{2,2}}\frac{a_{N,2}}{b_{N,2}} & \frac{b_{N,3}}{a_{3,3}}\frac{a_{N,3}}{b_{N,3}} & \dots & 1
\end{pmatrix}. \tag{341}
$$

It can be shown that the ratio $\frac{a_{i,j}}{b_{i,j}}$ is independent of the switch position j of the source. This ratio is called switch term of port i. The switch terms can be measured once. Afterwards they can be used to reconstruct the full matrix $\mathbf{A}$.

B.5   Absorbed Power

The absorbed power by a device under test is described in [25]. VNA Tools is using pseudo waves to compute the absorbed power, see section B.5.4.

B.5.1   Power Waves 1-Port

The following equation describes the absorbed power of a 1-port using power waves

$$P = |a|^2 - |b|^2 \tag{342}$$

where a is incident wave and b is the reflected wave. The above equations can be rewritten as

$$P = |a|^2 \left(1 - |S|^2\right) \tag{343}$$

where S is the reflection coefficient of the 1-port.

B.5.2   Pseudo Waves 1-Port

The following equation describes the absorbed power of a 1-port using pseudo waves

$$P = |a|^2 - |b|^2 + 2\operatorname{Im}(ab^*)\frac{\operatorname{Im}(Z_r)}{\operatorname{Re}(Z_r)} \tag{344}$$

where a is incident wave and b is the reflected wave. The operator * denotes the conjugate transpose and Z_r is the complex reference impedance. The above equation can be rewritten as

$$P = |a|^2 - |b|^2 - 2\operatorname{Im}\left(aa^*\frac{b}{a}\right)\frac{\operatorname{Im}(Z_r)}{\operatorname{Re}(Z_r)} \tag{345}$$

which yields to

$$P = |a|^2 \left(1 - |S|^2 - 2\operatorname{Im}(S)\frac{\operatorname{Im}(Z_r)}{\operatorname{Re}(Z_r)}\right) \tag{346}$$

where S is the reflection coefficient of the 1-port.

In the case where the imaginary part of Z_r is zero, the absorbed power using power waves and the absorbed power using pseudo waves are the same.

B.5.3   Power Waves N-Port

The following equation describes the absorbed power of a N-port using power waves

$$P_k = \sum_{j=1}^{N} |a_{j,k}|^2 \left(1 - \sum_{i=1}^{N} |S_{i,j}|^2\right). \tag{347}$$

The absorbed power can be computed for each source position k.

B.5.4   Pseudo Waves N-Port

In a first step the complex reference impedance of N-port is changed to a real reference impedance by cascading a transmission line junction to each port, see sections A.2.2 and B.1. In a second step the absorbed power is computed by using equation 347.

C   Mixed-Mode S-Parameters

The mixed-mode S-parameters are described in [27] and [28].

C.1   Single-Ended S-Parameters to Mixed-Mode S-Parameters

The single-ended S-parameter matrix

$$\mathbf{S} = \begin{pmatrix} S_{1,1} & S_{1,2} & S_{1,3} & S_{1,4} \\ S_{2,1} & S_{2,2} & S_{2,3} & S_{2,4} \\ S_{3,1} & S_{2,3} & S_{3,3} & S_{3,4} \\ S_{4,1} & S_{2,4} & S_{4,3} & S_{4,4} \end{pmatrix} \tag{348}$$

and the mode conversion matrix

$$\mathbf{M} = \frac{1}{\sqrt{2}} \begin{pmatrix} 1 & -1 & 0 & 0 \\ 1 & 1 & 0 & 0 \\ 0 & 0 & 1 & -1 \\ 0 & 0 & 1 & 1 \end{pmatrix} \tag{349}$$

and the relation for the mixed-mode matrix

$$\mathbf{S}_M = \mathbf{M}\mathbf{S}\mathbf{M}^{-1} \tag{350}$$

yield

$$\mathbf{S}_M = \begin{pmatrix} \frac{S_{1,1}-S_{1,2}-S_{2,1}+S_{2,2}}{2} & \frac{S_{1,1}+S_{1,2}-S_{2,1}-S_{2,2}}{2} & \frac{S_{1,3}-S_{1,4}-S_{2,3}+S_{2,4}}{2} & \frac{S_{1,3}+S_{1,4}-S_{2,3}-S_{2,4}}{2} \\ \frac{S_{1,1}-S_{1,2}+S_{2,1}-S_{2,2}}{2} & \frac{S_{1,1}+S_{1,2}+S_{2,1}+S_{2,2}}{2} & \frac{S_{1,3}-S_{1,4}+S_{2,3}-S_{2,4}}{2} & \frac{S_{1,3}+S_{1,4}+S_{2,3}+S_{2,4}}{2} \\ \frac{S_{3,1}-S_{3,2}-S_{4,1}+S_{4,2}}{2} & \frac{S_{3,1}+S_{3,2}-S_{4,1}-S_{4,2}}{2} & \frac{S_{3,3}-S_{3,4}-S_{4,3}+S_{4,4}}{2} & \frac{S_{3,3}+S_{3,4}-S_{4,3}-S_{4,4}}{2} \\ \frac{S_{3,1}-S_{3,2}+S_{4,1}-S_{4,2}}{2} & \frac{S_{3,1}+S_{3,2}+S_{4,1}+S_{4,2}}{2} & \frac{S_{3,3}-S_{3,4}+S_{4,3}-S_{4,4}}{2} & \frac{S_{3,3}+S_{3,4}+S_{4,3}+S_{4,4}}{2} \end{pmatrix}. \tag{351}$$

The mode conversion matrix $\mathbf{M}$ delivers the mixed-mode in the order 1d, 1c, 2d, 2c. The numbers refer to the logical port number where d is differential and c is common mode. The following matrix describes the mixed-mode S-parameters

$$\mathbf{S}_M = \begin{pmatrix} S_{1d,1d} & S_{1d,1c} & S_{1d,2d} & S_{1d,2c} \\ S_{1c,1d} & S_{1c,1c} & S_{1c,2d} & S_{1c,2c} \\ S_{2d,1d} & S_{2d,1c} & S_{2d,2d} & S_{2d,2c} \\ S_{2c,1d} & S_{2c,1c} & S_{2c,2d} & S_{2c,2c} \end{pmatrix}. \tag{352}$$

C.2   Mixed-Mode S-Parameters to Single-Ended S-Parameters

One can solve equation 350 for the single-ended matrix $\mathbf{S}$

$$\mathbf{S} = \mathbf{M}^{-1}\mathbf{S}_M\mathbf{M}. \tag{353}$$

D Time Domain

The here used transformation of frequency domain S-parameters to time domain and time gating is described in [29].

D.1 Frequency Domain to Time Domain

The transformation from frequency to time domain is shown in figure 27.
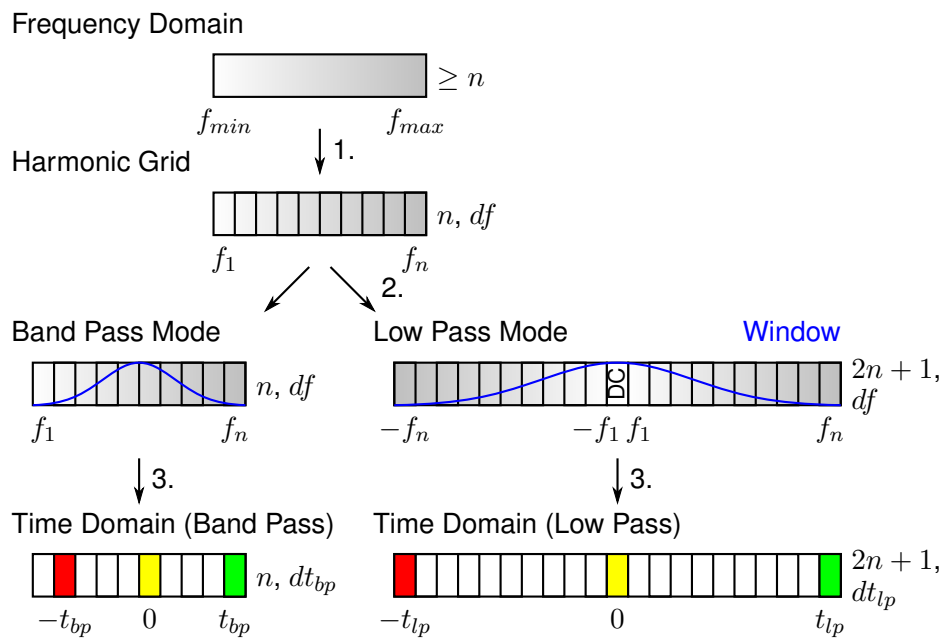
Figure 27: Illustration of the transformation from frequency domain to time domain using the band pass mode or the low pass mode.

1. The original data in frequency domain is interpolated on a harmonic grid. A harmonic grid is formed by a set of equidistant frequency points f_i $(i = 1 \ldots n)$ with spacing df. The frequency step df of the harmonic grid is equal to the largest frequency step of the original data in frequency domain. The first frequency f_1 of the harmonic grid has to be a multiple of df and $f_{min} \le f_1$. The last frequency $f_n = f_{max}$ of the harmonic grid has to be a multiple of df.

2. In the low pass mode, the data of the harmonic grid is mirrored (conjugate complex) to the negative frequencies and the DC point is added.

3. The data on the harmonic grid is multiplied with the window function and then transformed to time domain using the inverse DFT (discrete fourier transform).

D.1.1 Band Pass Mode

The band pass mode simulates a narrow-band TDR (Time Domain Reflectometer). It allows the user to identify locations of mismatches but does not indicate whether the mismatches are capacitive, inductive or resistive. However, it's suitable for displaying a magnitude proportional to the response of a TDR. Since the band pass mode does not include a DC value and low frequency values, only the impulse excitation is supported.

The time resolution is computed with the following equation.

$$dt_{bp} = \frac{1}{n \cdot df} \tag{354}$$

Note that the time resolution gets finer with a larger frequency span $f_n - f_1$.

The maximum time is computed with the following equation.

$$t_{bp} = \left\lfloor \frac{n-1}{2} \right\rfloor \cdot dt_{bp} \tag{355}$$

The operation $\lfloor\ \rfloor$ denotes rounding to the lower integer number. Note that the maximum time gets larger with a smaller frequency step df.

The minimum time is computed with the following equation.

$$-t'_{bp} = -\left\lfloor \frac{n}{2} \right\rfloor \cdot dt_{bp} \tag{356}$$

Note that for an odd number of points n, it is $t'_{bp} = t_{bp}$.

D.1.2 Low Pass Mode

The low pass mode is used to simulate a traditional TDR measurement. This mode gives the user information to determine the type of discontinuity (R, L, or C) that is present. Low pass mode provides the best resolution (fastest rise time), and it my be used to either compute the step or impulse response of a device.

The low pass mode is less general than the band pass mode in that it places strict limitations on the frequency range of the measurement. The first frequency f_1 must be equal to the frequency step df. The DC frequency response is either measured or extrapolated from the two lowest frequency points in frequency domain. The requirement for a DC point is the same limitation that exists for traditional TDR measurements.

The time resolution of the low pass mode is computed with the following equation.

$$dt_{lp} = \frac{1}{(2n+1) \cdot df} \tag{357}$$

Note that the time resolution of the low pass mode is about twice as fine as the time resolution of the band pass mode.

The maximum and minimum time is computed with the following equation.

$$t_{lp} = n \cdot dt_{lp} \tag{358}$$

D.1.3 Frequency and Time Uncertainty

In the following example the band pass mode is used. Let's assume a frequency uncertainty of

$$\mathrm{u}\left(f_{stab}\right) = 10^{-6}\, \frac{\mathrm{Hz}}{\mathrm{Hz}} \tag{359}$$

and a frequency step $df = 100\,\mathrm{MHz}$ and $n = 500$ measurement points. The time resolution would be computed with

$$dt_{bp} = \frac{1}{n \cdot df} = 20\,\mathrm{ps} \pm 20\,\mathrm{as}. \tag{360}$$

The maximum time would be

$$t_{bp} = \left\lfloor \frac{n-1}{2} \right\rfloor \cdot dt_{bp} = 4.98\,\mathrm{ns} \pm 4.98\,\mathrm{fs} \tag{361}$$

and the minimum time would be

$$-t'_{bp} = -\left\lfloor \frac{n}{2} \right\rfloor \cdot dt_{bp} = -5.00\,\mathrm{ns} \pm 5.00\,\mathrm{fs}. \tag{362}$$

The ratio of the worst case time uncertainty to the time resolution is

$$\frac{\mathrm{u}\left(t_{bp} + t'_{bp}\right)}{dt_{bp}} = \frac{9.98\,\mathrm{fs}}{20\,\mathrm{ps}} = (n-1)\,\mathrm{u}\left(f_{stab}\right) = (500-1)\,10^{-6}\,\frac{\mathrm{Hz}}{\mathrm{Hz}} = 4.99 \cdot 10^{-4}. \tag{363}$$

Note that the maximum and minimum time get larger the more measurement points n are used. Therefore the above ratio gets as well larger (worse) when more points n are used. The uncertainty of frequency and time is not taken into account by VNA Tools.

D.2   Time Gating

This section describes the transformation from frequency to time domain, gating the data in time domain and transforming back to frequency domain.

D.2.1   Band Pass Mode

For time gating, using the band pass mode, see figure 28.

Figure 28: Illustration of time gating using the band pass mode. The steps 2 and 3 on the left side are used for time domain representation and to choose the gating parameters of the gate shape. The steps 4, 5 and 6 on the right side are used for the time gating process.

1. The original data in frequency domain is interpolated on a harmonic grid, see as well section D.1.

2. The data on the harmonic grid is multiplied with the window function and then transformed to time domain using the inverse DFT (discrete fourier transform).

---

3. The gating parameters t_{center}, t_{span} and t_{delta} are chosen. See section D.2.3 for computing the gate shape.

4. The data on the harmonic grid is extrapolated at the lower and higher frequency ranges. The extrapolated points are a mirrored version of the harmonic grid and have large standard uncertainties of $\pm(1+|v_{re}|)/\sqrt{3}$ in real part and $\pm(1+|v_{im}|)/\sqrt{3}$ in imaginary part where $|v_p|$ is the absolute value of the part p. They are used to regularize the value and compute the uncertainty at the boundaries of the time gated data in frequency domain.

5. The extrapolated data in frequency domain is transformed to time domain without applying any window function.

6. The complex data in time domain from step 5 is multiplied with the gate shape and then transformed back to frequency domain. A subset of the frequencies is the result (time gated data in frequency domain).

D.2.2 Low Pass Mode

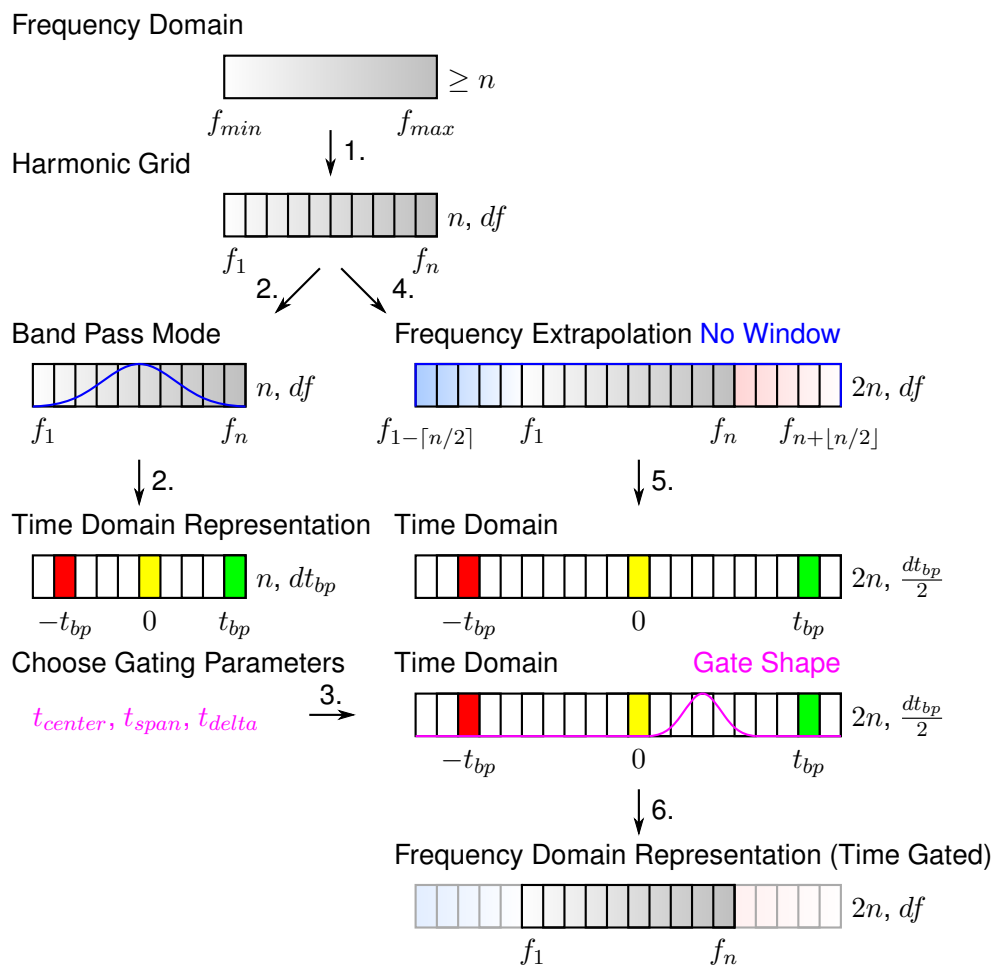For time gating, using the low pass mode, see figure 29.
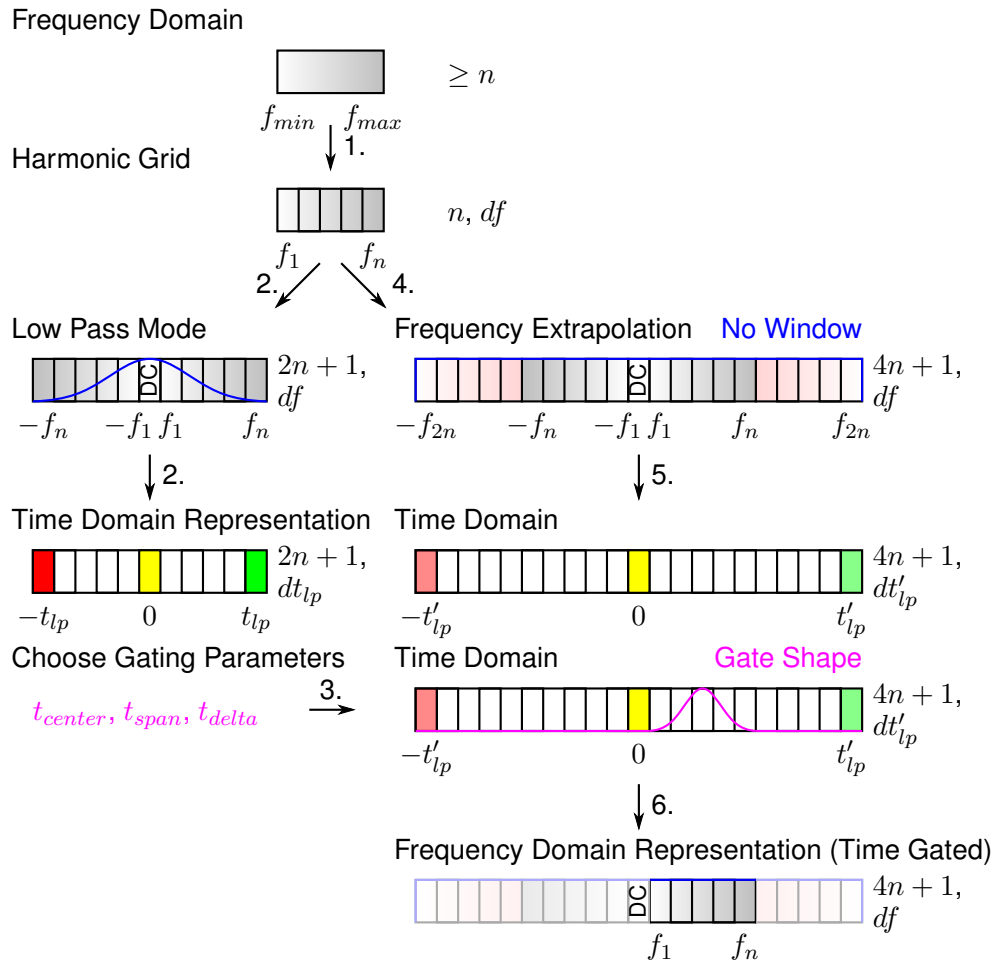
Figure 29: Illustration of time gating using the low pass mode. The steps 2 and 3 on the left side are used for time domain representation and to choose the gating parameters of the gate shape. The steps 4, 5 and 6 on the right side are used for the time gating process.

1. The original data in frequency domain is interpolated on a harmonic grid, see as well section D.1.

2. In the low pass mode, the data of the harmonic grid is mirrored (conjugate complex) to the negative frequencies and the DC point is added if required. The data on the harmonic grid is multiplied with the window function and then transformed to time domain using the inverse DFT (discrete fourier transform).

3. The gating parameters t_{center}, t_{span} and t_{delta} are chosen. See section D.2.3 for computing the gate shape.

4. The data on the harmonic grid is extrapolated at the higher negative and positive frequency ranges. The extrapolated points are a mirrored version of the harmonic grid and have large standard uncertainties of $\pm(1+|v_{re}|)/\sqrt{3}$ in real part and $\pm(1+|v_{im}|)/\sqrt{3}$ in imaginary part where $|v_p|$ is the absolute value of the part p. They are used to regularize the value and compute the uncertainty at the boundaries of the time gated data in frequency domain.

5. The extrapolated data in frequency domain is transformed to time domain without applying any window function.
   Note that the time resolution is $dt'_{lp} = \frac{2n+1}{4n+1}dt_{lp} \approx 0.5dt_{lp}$.

6. The complex data in time domain from step 5 is multiplied with the gate shape and then transformed back to frequency domain. A subset of the frequencies is the result (time gated data in frequency domain).

D.2.3 Gate Shape

The gate shape with the parameters center time t_{center}, time span t_{span} and delta time t_{delta} is shown in figure 30.
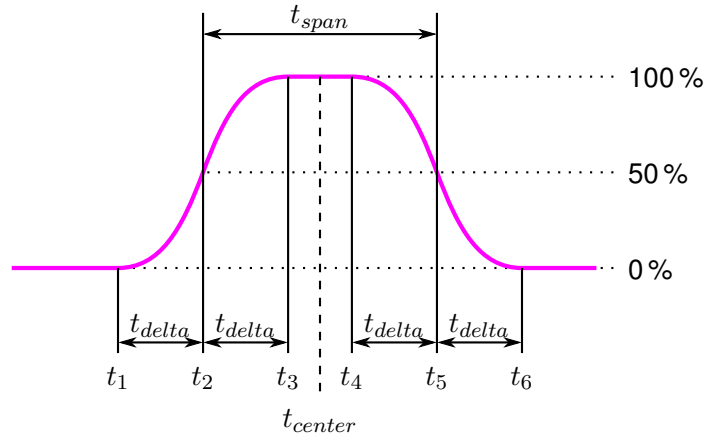
Figure 30: Gate shape

The gate shape $GS_{bandpass}$ is computed with the following function

$$
GS_{bandpass} = \begin{cases}
0 & , t \leq t_1 \\
\text{HannFilter}\,(t, t_1, t_3 + 2t_{delta}) & , t_1 < t < t_3 \\
1 & , t_3 \leq t \leq t_4 \\
\text{HannFilter}\,(t, t_4 - 2t_{delta}, t_6) & , t_4 < t < t_6 \\
0 & , t_6 \leq t
\end{cases}
\tag{364}
$$

and for a notch gate type

$$
GS_{notch} = 1 - GS_{bandpass}
\tag{365}
$$

where the Hann filter is defined as

$$
\text{HannFilter}\,(t, t_{start}, t_{stop}) = 1 + \frac{\cos\left(2\pi \frac{t - (t_{start} + t_{stop})/2}{t_{stop} - t_{start}}\right)}{2}
\tag{366}
$$

between $t_{start} < t < t_{stop}$. Otherwise it returns 0.

E METAS UncLib

METAS UncLib [8], [9] is a generic measurement uncertainty calculator that supports the multivariate propagation of measurement uncertainty [7], taking correlations between quantities fully into account, see figure 31.
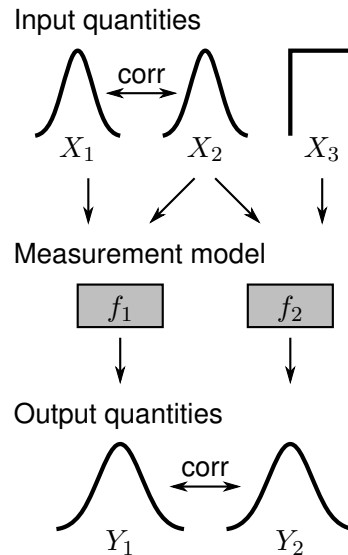
Figure 31: Illustration of multivariate uncertainty propagation: The uncertainties and correlations of basic input quantities X_1, X_2, X_3 are propagated through a measurement model resulting in uncertainties and correlations of multiple output quantities Y_1, Y_2, see [7].

The user only needs to specifies the input quantities $\mathbf{X}$ with uncertainties, or, more general with an input covariance matrix $\mathbf{V}_X$, and the measurement model $\mathbf{f}$. The actual propagation of uncertainty is done in the background in an automated way. METAS UncLib keeps automatically track of the derivatives with respect to the input quantities. Formally this means that METAS UncLib computes the output quantities $\mathbf{Y} = \mathbf{f}(\mathbf{X})$ and the Jacobi matrix $\mathbf{J}_{YX}$ of $\mathbf{f}$ that contains the drivatives of the components of $\mathbf{Y}$ with respect to the components of $\mathbf{X}$. On demand METAS UncLib can compute the output covariance matrix $\mathbf{V}_Y = \mathbf{J}_{YX}\mathbf{V}_X\mathbf{J}_{YX}'$. Further information about the technique behind METAS UncLib can be found in [9].

F Small Sample Statistics

The standard uncertainty associated with the final result is multiplied with the coverage factor to obtain an expanded uncertainty with a desired coverage probability (usually 95 %). The calculation of the coverage factor is not straightforward anymore, if the uncertainty contribution due to small sample statistics is significant. The GUM documents [6, 7] are not very consistent in how to treat such a situation, in particular for the multivariate case. We find neither the solution in GUM Supplement 2 with the multivariate t-distribution [7] nor the multivariate generalization of the Welch-Satterthwaite approach [30, 31] satisfactory. The following solution is a self-developed, pragmatic and safe approach to the problem. It will generally overestimate the uncertainty contribution due to small sample statistics.

A series of n measurements $(x_1,\ x_2,\ x_3, \dots , x_n)$ of a vector quantity with length N leads to a sample covariance matrix of of the mean

$$\mathbf{S} = \frac{1}{n\,(n-1)} \left[(x_1 - \overline{x})\,(x_1 - \overline{x})' + \dots + (x_n - \overline{x})\,(x_n - \overline{x})' \right]. \tag{367}$$

with $\overline{x}$ being the sample mean vector.

It is assumed that the n drawings are from a N-dimensional normal distribution. To obtain a $p{\cdot}100$ % confidence region the covariance matrix needs to be expanded with the following factor squared

$$k_{n,N,p} = \begin{cases} \text{NormalDistCDF}^{-1}\left(\frac{p+1}{2}\right) & , N = 1 \wedge n = \infty \\[2ex] \text{StudentTDistCDF}^{-1}\left(n-1, \frac{p+1}{2}\right) & , N = 1 \wedge n < \infty \\[2ex] \sqrt{\text{Chi}^2\text{DistCDF}^{-1}\left(N, p\right)} & , N > 1 \wedge n = \infty \\[2ex] \sqrt{\frac{(n-1)N}{n-N}\,\text{FDistCDF}^{-1}\left(n-N, N, p\right)} & , N > 1 \wedge n < \infty \end{cases} \tag{368}$$

Direct application of this factor can be done, if the covariance matrix is associated with the final result. If it is just an uncertainty contribution among others, which needs to be propagated to the end result, the following practical solution is applied. The sample covariance matrix of the mean $\mathbf{S}$ is extended using the factor

$$(f_{n,N,p})^2 = \left(\frac{k_{n,N,p}}{k_{\infty,N,p}}\right)^2, \tag{369}$$

leading to

$$\mathbf{T} = (f_{n,N,p})^2\,\mathbf{S}. \tag{370}$$

$\mathbf{T}$ is then used for subsequent uncertainty propagation to the end result. Finally, the covariance matrix associated with the end result is multiplied with $(k_{\infty,N,p})^2$.

Table 10 shows selected k- and f-factors for different numbers of measurement repetitions n and dimensions N.

Table 10: Coverage Factors

n	$k_{n,1,0.95}$	$k_{n,2,0.95}$	$k_{n,8,0.95}$	$f_{n,1,0.95}$	$f_{n,2,0.95}$	$f_{n,8,0.95}$
1						
2	12.7062			6.4829		
3	4.3027	28.2489		2.1953	11.5408	
4	3.1824	7.5498		1.6237	3.0844	
5	2.7764	5.0470		1.4166	2.0619	
6	2.5706	4.1666		1.3115	1.7022	
7	2.4469	3.7265		1.2484	1.5224	
8	2.3646	3.4642		1.2065	1.4153	
9	2.3060	3.2906	123.6466	1.1766	1.3444	31.3989
10	2.2622	3.1674	26.4075	1.1542	1.2940	6.7059
11	2.2281	3.0755	15.3582	1.1368	1.2565	3.9001
12	2.2010	3.0044	11.5284	1.1230	1.2274	2.9275
13	2.1788	2.9477	9.6183	1.1117	1.2042	2.4425
14	2.1604	2.9014	8.4781	1.1022	1.1853	2.1529
15	2.1448	2.8630	7.7209	1.0943	1.1696	1.9606
16	2.1314	2.8305	7.1813	1.0875	1.1564	1.8236
17	2.1199	2.8028	6.7773	1.0816	1.1450	1.7210
18	2.1098	2.7788	6.4633	1.0765	1.1352	1.6413
19	2.1009	2.7578	6.2122	1.0719	1.1267	1.5775
20	2.0930	2.7394	6.0068	1.0679	1.1191	1.5254
50	2.0096	2.5523	4.4984	1.0253	1.0427	1.1423
100	1.9842	2.4983	4.1914	1.0124	1.0206	1.0644
∞	1.9600	2.4477	3.9379	1.0000	1.0000	1.0000

The table helps to determine the improvements in accuracy that can be achieved by increasing the number of measurements. E.g. for $N = 2$ increasing the measurement repetitions from 4 to 5 leads to a reduction of the uncertainty contribution by approximately 2/3. The selected dimensions are based on the most often used cases:

$N = 1$: Scalar quantity

$N = 2$: Complex reflection factor of a 1-port DUT

$N = 8$: Complex S-matrix of a 2-port DUT

G   Normalized Error

The normalized error is described in [32].

G.1   Scalar Case

A suitable quantitative verification criteria for a scalar parameter is based on the normalized difference ϵ, also referred to as normalized error, between measurement and reference data. The pass condition is $\epsilon \leq 1$. The normalized error is expressed as

$$\epsilon = \frac{|d|}{k\,\mathrm{u}\,(d)}. \tag{371}$$

The quantity d is the difference between measurement and reference of a scalar quantity. $\mathrm{u}\,(d)$ is the standard uncertainty of d.

k is the coverage factor used to expand the uncertainty in denominator in above equation. A value that is often used is $k = 1.96$. It expands the uncertainty associated with d to a 95 % coverage interval. $k = 1$ corresponds to a 68 % coverage interval. This verification procedure assumes that the underlying PDF associated with d is Gaussian.

Remark: tiny differences d smaller than 10^{-15} are set to zero which yields to a normalized error of 0.

G.2   Multivariate Case

A straightforward generalization of the scalar criterion is expressed by the matrix equation

$$\epsilon = \frac{1}{k}\sqrt{\mathbf{d}\,(\mathbf{u}\,(\mathbf{d}))^{-1}\,\mathbf{d}'} \tag{372}$$

with prime denoting the transposed. The pass criteria is as well $\epsilon \leq 1$.

$\mathbf{d}$ is a row vector, which contains the components of the difference between measurement and reference data. $\mathbf{u}\,(\mathbf{d})$ is the covariance matrix associated with $\mathbf{d}$.

The coverage factor k plays the same role as in the scalar case, but the coverage factor k in the multivariate case is larger than in the scalar case. E.g.: for 95 % coverage probability in the two-dimensional case the value $k = 2,45$ should be used and for $k = 1$ the coverage probability would be 39 %. Again, this assumes that the probability density function associated with the measurement uncertainty of $\mathbf{d}$ is a multivariate Gaussian one.

The inverse of the covariance matrix is computed using the eigenvalue decomposition

$$(\mathbf{u}\,(\mathbf{d}))^{-1} = \mathbf{V}\mathbf{D}^{-1}\mathbf{V}' \tag{373}$$

where $\mathbf{V}$ are the eigenvectors and $\mathbf{D}^{-1}$ is a diagonal matrix. The elements of the diagonal matrix $\mathbf{D}^{-1}$ are the inverse of the eigenvalues. The elements of the diagonal matrix $\mathbf{D}$, which are smaller in value than 10^{-15} times the largest eigenvalue, are not inverted but set to zero. This is done to avoid numerical problems which may arise from rank deficient covariance matrix $\mathbf{u}\,(\mathbf{d})$.

Remark: tiny differences in the row vector $\mathbf{d}$ smaller than 10^{-15} are set to zero.

H Circle Fitting

For circle fitting see figure 32. The algorithm is described in [33].
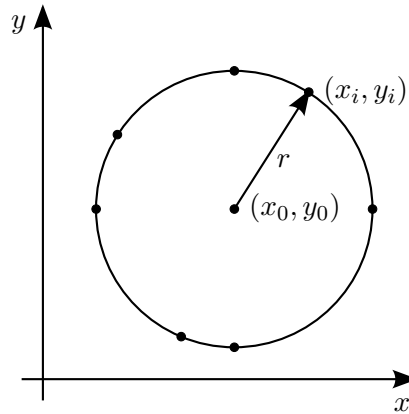
Figure 32: Circle Fitting

The following equation describes a circle

$$r = \sqrt{(x_i - x_0)^2 + (y_i - y_0)^2} \tag{374}$$

where r is the radius, x_0, y_0 are the coordinates of the center of the circle and x_i, y_i are the coordinates of a point i on the circle.

One can square the above equation

$$r^2 = (x_i - x_0)^2 + (y_i - y_0)^2 \tag{375}$$

and multiply out the brackets

$$r^2 = x_i^2 - 2x_i x_0 + x_0^2 + y_i^2 - 2y_i y_0 + y_0^2. \tag{376}$$

The above equation can be rearranged as

$$2x_i x_0 + 2y_i y_0 + \underbrace{r^2 - x_0^2 - y_0^2}_{r_0} = x_i^2 + y_i^2. \tag{377}$$

Finally one can setup an over-determined equation system for the unknown coordinates of the center of the circle x_0, y_0 and the unknown intermediate quantity r_0

$$\begin{bmatrix} 2x_1 & 2y_1 & 1 \\ 2x_2 & 2y_2 & 1 \\ \vdots & \vdots & \vdots \\ 2x_n & 2y_n & 1 \end{bmatrix} \begin{bmatrix} x_0 \\ y_0 \\ r_0 \end{bmatrix} = \begin{bmatrix} x_1^2 + y_1^2 \\ x_2^2 + y_2^2 \\ \vdots \\ x_n^2 + y_n^2 \end{bmatrix} \tag{378}$$

where n is the number of points on the circle. The radius r is described with the following equation

$$r = \sqrt{r_0^2 + x_0^2 + y_0^2}. \tag{379}$$

I Eigenvalue Problem

The most general problem is an over-determined non-linear eigenvalue problem

$$\mathbf{A_0}\mathbf{v} + \lambda\mathbf{A_1}\mathbf{v} + \lambda^2\mathbf{A_2}\mathbf{v} + \ldots + \lambda^n\mathbf{A_n}\mathbf{v} = 0. \tag{380}$$

The over-determined non-linear eigenvalue problem can be transformed to a balanced non-linear eigenvalue problem with order $m = 2n$ by squaring the over-determined non-linear problem

$$\underbrace{\mathbf{A_0^*}\mathbf{A_0}}_{\mathbf{B_0}}\mathbf{v} + \lambda\underbrace{(\mathbf{A_0^*}\mathbf{A_1} + \mathbf{A_1^*}\mathbf{A_0})}_{\mathbf{B_1}}\mathbf{v} + \lambda^2\underbrace{(\mathbf{A_0^*}\mathbf{A_2} + \mathbf{A_1^*}\mathbf{A_1} + \mathbf{A_2^*}\mathbf{A_0})}_{\mathbf{B_2}}\mathbf{v} + \ldots + \lambda^m\underbrace{\mathbf{A_n^*}\mathbf{A_n}}_{\mathbf{B_m}}\mathbf{v} = 0. \tag{381}$$

The operator $*$ denotes the conjugate transpose.

This non-linear eigenvalue problem can then be rewritten as a linear eigenvalue problem by substitution

$$\underbrace{\begin{bmatrix} \mathbf{B_0} & \mathbf{0} & \mathbf{0} & \cdots & \mathbf{0} \\ \mathbf{0} & -\mathbf{I} & \mathbf{0} & \cdots & \mathbf{0} \\ \mathbf{0} & \mathbf{0} & -\mathbf{I} & & \mathbf{0} \\ \vdots & \vdots & & \ddots & \\ \mathbf{0} & \mathbf{0} & \mathbf{0} & & -\mathbf{I} \end{bmatrix}}_{\mathbf{C_0}}\underbrace{\begin{bmatrix} \mathbf{v} \\ \lambda\mathbf{v} \\ \lambda^2\mathbf{v} \\ \vdots \\ \lambda^m\mathbf{v} \end{bmatrix}}_{\mathbf{w}} + \lambda\underbrace{\begin{bmatrix} \mathbf{B_1} & \mathbf{B_2} & \mathbf{B_3} & \cdots & \mathbf{B_m} \\ \mathbf{I} & \mathbf{0} & \mathbf{0} & \cdots & \mathbf{0} \\ \mathbf{0} & \mathbf{I} & \mathbf{0} & \cdots & \mathbf{0} \\ \vdots & \ddots & \ddots & \ddots & \vdots \\ \mathbf{0} & \mathbf{0} & \mathbf{0} & & \mathbf{0} \end{bmatrix}}_{\mathbf{C_1}}\underbrace{\begin{bmatrix} \mathbf{v} \\ \lambda\mathbf{v} \\ \lambda^2\mathbf{v} \\ \vdots \\ \lambda^m\mathbf{v} \end{bmatrix}}_{\mathbf{w}} = 0 \tag{382}$$

where $\mathbf{I}$ is the identity matrix.

This linear eigenvalue problem can finally be transformed to a standard eigenvalue problem

$$\underbrace{\mathbf{C_0}^{-1}\mathbf{C_1}}_{\mathbf{D}}\,\mathbf{w} = \underbrace{-\frac{1}{\lambda}}_{\lambda'}\,\mathbf{w}. \tag{383}$$

Note that $\mathbf{C_0}$ is only invertible if $\mathbf{B_0}$ is invertible. Otherwise the inverse of $\mathbf{C_1}$ is needed. This yields to the following standard eigenvalue problem

$$\underbrace{\mathbf{C_1}^{-1}\mathbf{C_0}}_{\mathbf{E}}\,\mathbf{w} = \underbrace{-\lambda}_{\lambda''}\,\mathbf{w}. \tag{384}$$

The eigenvalue computation with linear uncertainty propagation is described in [34] and it is fully implemented in METAS UncLib [8, 9].

J   VNA Calibration Model Details

The following figures show the details of the VNA calibration models:

Figure 33 describes the one-port model.

Figure 34 describes an one-port calibration.

Figure 35 describes the difference between the generic and switched two-port model.

Figure 36 describes generic multi-port calibration model.

Figure 37 describes switched multi-port calibration model.

Raw Data | Noise, Linearity | Error Terms | Drift of Error Terms | Cable Stability, Connector Repeatability, DUT Uncertainty | Error Corrected Data

a ref. receiver
b test receiver

N^L noise floor
N^H trace noise
L linearity

E^D directivity
E^T tracking
E^M match

D^D directivity drift
D^T tracking drift
D^M match drift

C^R reflection stability
C^T transmission stability

R^R reflection repeatability
R^T transmission repeatability

U^R reflection uncertainty

S S-parameter

Michael Wollensack METAS - 22.08.2017

Figure 33: VNA 1-Port Calibration Model

1. Calibration: $\mathbf{E} = f_1 \left(\mathbf{M_{Open}}, \mathbf{R_{Open}}, \mathbf{D_{Open}}, \mathbf{C_{Open}}, \mathbf{S_{Open}}, \mathbf{M_{Short}}, \mathbf{R_{Short}}, \mathbf{D_{Short}}, \mathbf{C_{Short}}, \mathbf{S_{Short}}, \mathbf{M_{Load}}, \mathbf{R_{Load}}, \mathbf{D_{Load}}, \mathbf{C_{Load}}, \mathbf{S_{Load}} \right)$

| Raw Data | Noise, Linearity | | Error Terms? | Drift of Error Terms | Cable Stability, Connector Repeatability, DUT Uncertainty | Cal. Standard Definitions |

$\mathbf{C_{Open}}$

$\mathbf{M_{Open}}$ — 1 | $\mathbf{R_{Open}}$ | 2 — 1 | E | 2 — 1 | $\mathbf{D_{Open}}$ | 2 — 1 | Cable — Connector — DUT U. | 2 — 1 | $\mathbf{S_{Open}}$

$\mathbf{C_{Short}}$

$\mathbf{M_{Short}}$ — 1 | $\mathbf{R_{Short}}$ | 2 — 1 | E | 2 — 1 | $\mathbf{D_{Short}}$ | 2 — 1 | Cable — Connector — DUT U. | 2 — 1 | $\mathbf{S_{Short}}$

$\mathbf{C_{Load}}$

$\mathbf{M_{Load}}$ — 1 | $\mathbf{R_{Load}}$ | 2 — 1 | E | 2 — 1 | $\mathbf{D_{Load}}$ | 2 — 1 | Cable — Connector — DUT U. | 2 — 1 | $\mathbf{S_{Load}}$

2. Error Correction: $\mathbf{S_{DUT}} = f_2 \left(\mathbf{M_{DUT}}, \mathbf{R_{DUT}}, \mathbf{D_{DUT}}, \mathbf{C_{DUT}}, \mathbf{E} \right)$

| Raw Data | Noise, Linearity | | Error Terms | Drift of Error Terms | Cable Stability, Connector Repeatability, DUT Uncertainty | Error Corrected Data? |

$\mathbf{C_{DUT}}$

$\mathbf{M_{DUT}}$ — 1 | $\mathbf{R_{DUT}}$ | 2 — 1 | E | 2 — 1 | $\mathbf{D_{DUT}}$ | 2 — 1 | Cable — Connector — DUT U. | 2 — 1 | $\mathbf{S_{DUT}}$

a_1 1 1 1 1 C_1^T R_1^T 1

$N_{1,1}^L$ 0 E_1^D E_1^M D_1^D D_1^M $C_{1,1}^R$ $C_{1,2}^R$ $R_{1,1}^R$ $R_{1,2}^R$ $U_{1,1}^R$ 0 $S_{1,1}$

$N_{1,1}^H L_1$ E_1^T D_1^T C_1^T R_1^T

b_1 1 1 1 1 1

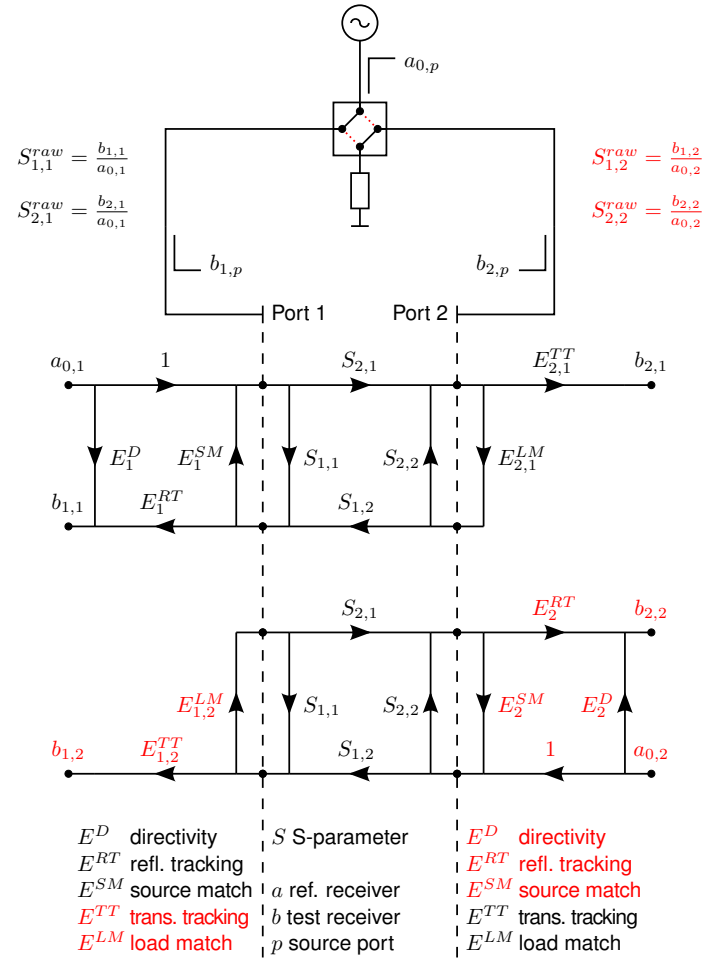| a ref. receiver | N^L noise floor | | E^D directivity | D^D directivity drift | C^R reflection stability | R^R reflection repeatability | U^R reflection uncertainty | S S-parameter |
| b test receiver | N^H trace noise | | E^T tracking | D^T tracking drift | C^T transmission stability | R^T transmission repeatability | | |
| | L linearity | | E^M match | D^M match drift | | | | |

Michael Wollensack METAS - 25.10.2017

Figure 34: VNA 1-Port Calibration Model cont.

VNA Generic Calibration Model
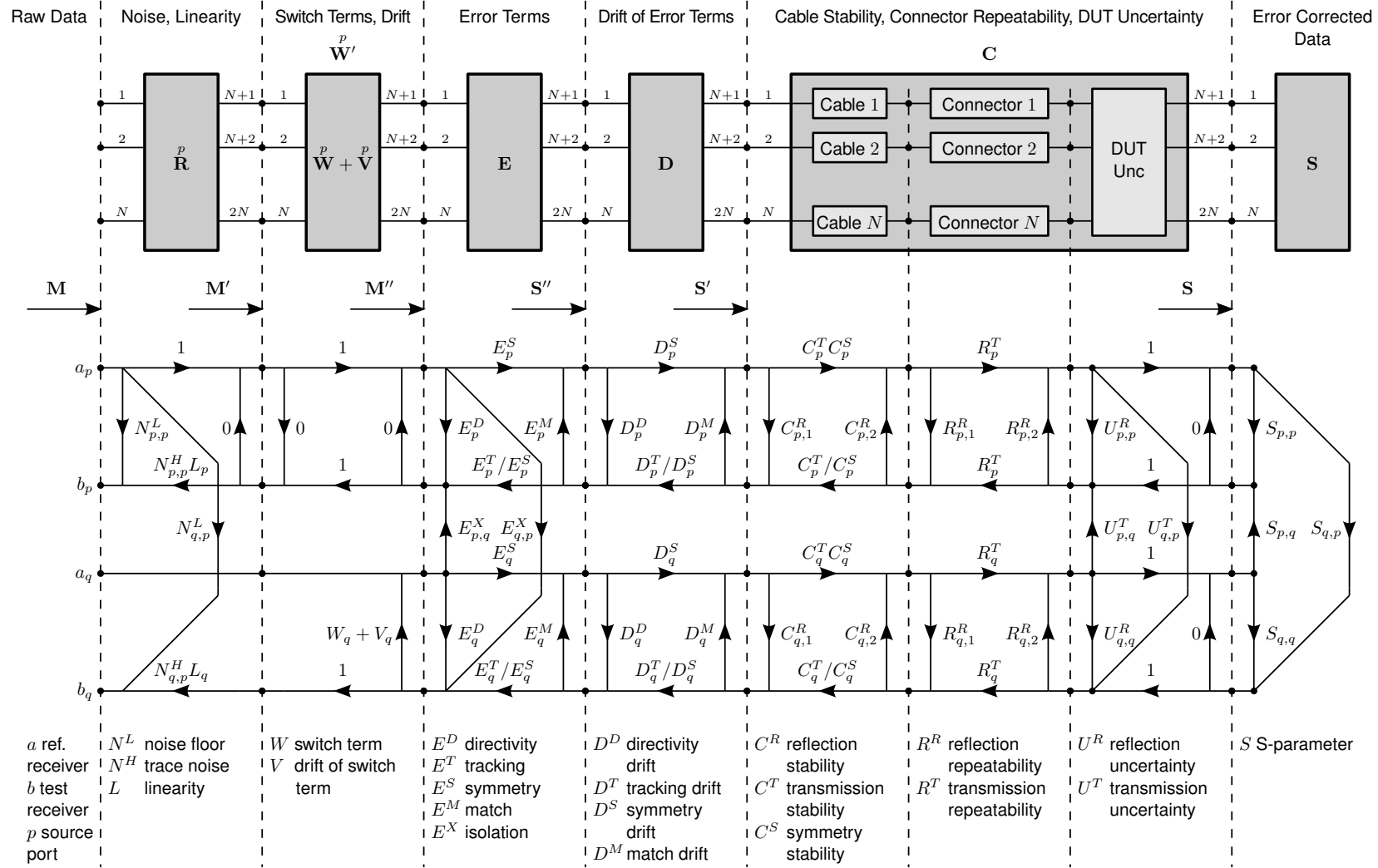QSOLT, Unknown Thru, TRL (4 Receiver, 7 Error and 2 Switch Terms)
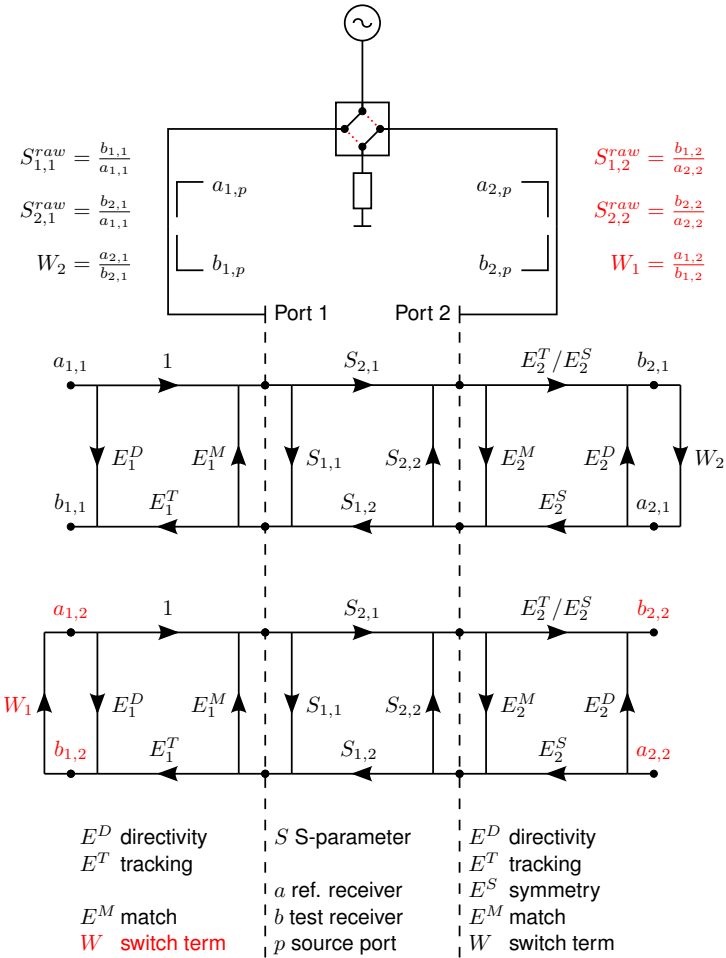
VNA Switched Calibration Model
SOLT (3 Receiver, 10 Error Terms)

$S_{1,1}^{raw} = \frac{b_{1,1}}{a_{1,1}}$ $S_{1,2}^{raw} = \frac{b_{1,2}}{a_{2,2}}$

$S_{2,1}^{raw} = \frac{b_{2,1}}{a_{1,1}}$ $S_{2,2}^{raw} = \frac{b_{2,2}}{a_{2,2}}$

$W_2 = \frac{a_{2,1}}{b_{2,1}}$ $W_1 = \frac{a_{1,2}}{b_{1,2}}$

$a_{1,p}$ $a_{2,p}$

$b_{1,p}$ $b_{2,p}$

Port 1   Port 2

$S_{1,1}^{raw} = \frac{b_{1,1}}{a_{0,1}}$ $S_{1,2}^{raw} = \frac{b_{1,2}}{a_{0,2}}$

$S_{2,1}^{raw} = \frac{b_{2,1}}{a_{0,1}}$ $S_{2,2}^{raw} = \frac{b_{2,2}}{a_{0,2}}$

$a_{0,p}$

$b_{1,p}$ $b_{2,p}$

Port 1   Port 2

$a_{1,1}$ 1 $S_{2,1}$ E_2^T/E_2^S $b_{2,1}$

E_1^D E_1^M $S_{1,1}$ $S_{2,2}$ E_2^M E_2^D W_2

$b_{1,1}$ E_1^T $S_{1,2}$ E_2^S $a_{2,1}$

$a_{1,2}$ 1 $S_{2,1}$ E_2^T/E_2^S $b_{2,2}$

W_1 E_1^D E_1^M $S_{1,1}$ $S_{2,2}$ E_2^M E_2^D

$b_{1,2}$ E_1^T $S_{1,2}$ E_2^S $a_{2,2}$

$a_{0,1}$ 1 $S_{2,1}$ $E_{2,1}^{TT}$ $b_{2,1}$

E_1^D E_1^{SM} $S_{1,1}$ $S_{2,2}$ $E_{2,1}^{LM}$

$b_{1,1}$ E_1^{RT} $S_{1,2}$

$S_{2,1}$ E_2^{RT} $b_{2,2}$

$E_{1,2}^{LM}$ $S_{1,1}$ $S_{2,2}$ E_2^{SM} E_2^D

$b_{1,2}$ $E_{1,2}^{TT}$ $S_{1,2}$ 1 $a_{0,2}$

E^D directivity	S S-parameter	E^D directivity
E^T tracking		E^T tracking
	a ref. receiver	E^S symmetry
E^M match	b test receiver	E^M match
W switch term	p source port	W switch term

E^D directivity	S S-parameter	E^D directivity
E^{RT} refl. tracking		E^{RT} refl. tracking
E^{SM} source match	a ref. receiver	E^{SM} source match
E^{TT} trans. tracking	b test receiver	E^{TT} trans. tracking
E^{LM} load match	p source port	E^{LM} load match

Figure 35: VNA 2-Port Calibration Model

Figure 36: VNA Generic Calibration Model
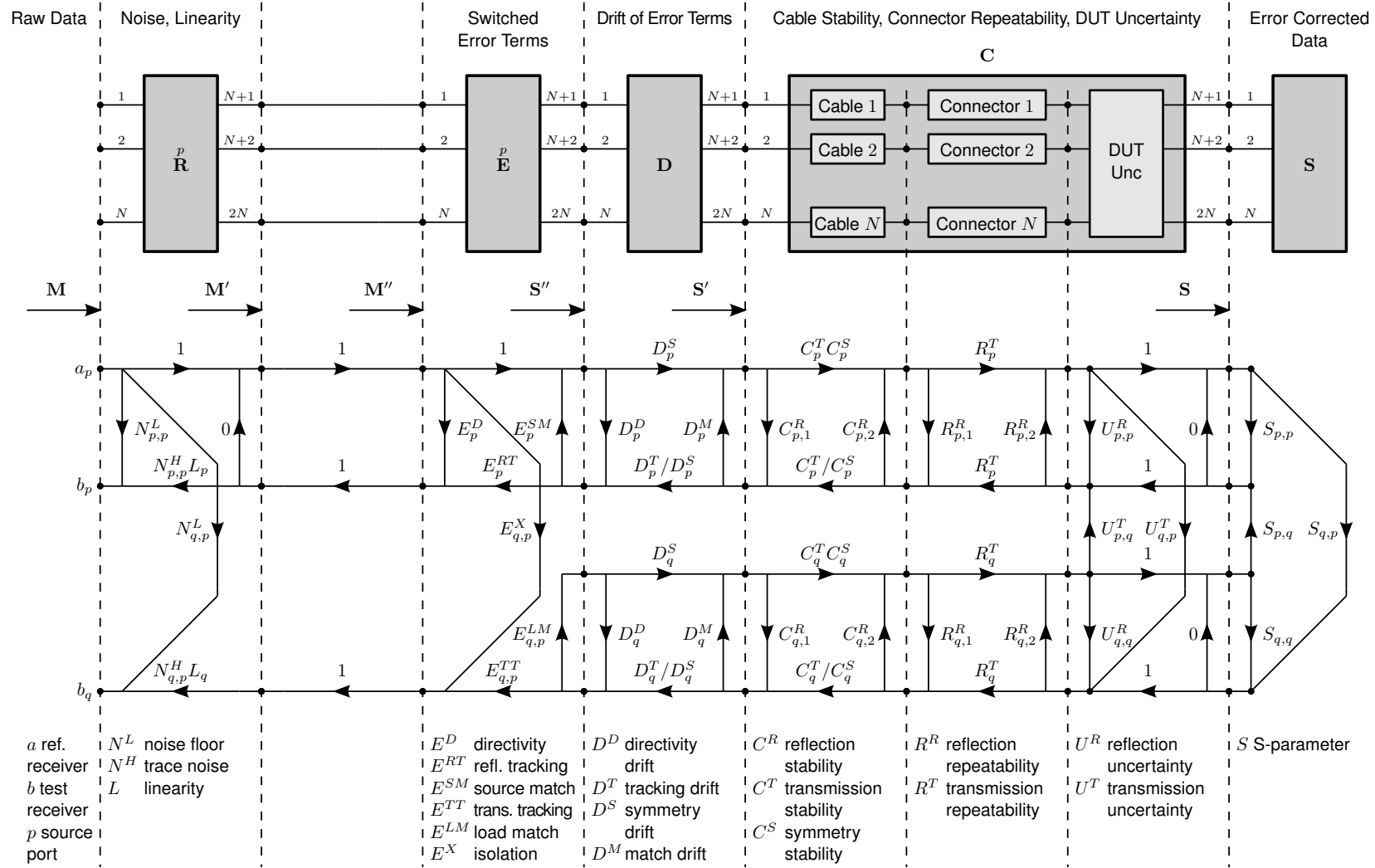
Figure 37: VNA Switched Calibration Model

K Material Parameters

K.1 Nicholson-Ross-Weir

The algorithm called 'Nicholson-Ross-Weir' is described in [35] and [36]. The algorithm is applied to calculate the relative permittivity ε_r and the relative permeability μ_r from transmission S_{21} and reflection S_{11} parameters. The results can have poles for low loss samples with thickness of $> \frac{1}{2}$ wavelength.

The procedure prescribed by the 'Nicholson-Ross-Weir' method starts with

$$S_{11} = \frac{\Gamma \left(1 - T^2\right)}{1 - \Gamma^2 T^2} \tag{385}$$

and

$$S_{21} = \frac{T \left(1 - \Gamma^2\right)}{1 - \Gamma^2 T^2}. \tag{386}$$

The reflection coefficient can be deduced with

$$\Gamma = X \pm \sqrt{X^2 - 1} \tag{387}$$

where $|\Gamma| < 1$ is the criterion for finding the correct root. In terms of S-parameters X can be written as

$$X = \frac{S_{11}^2 - S_{21}^2 + 1}{2 S_{11}}. \tag{388}$$

Knowing Γ the transmission coefficient is

$$T = \frac{S_{11} + S_{21} - \Gamma}{1 - (S_{11} + S_{21})\,\Gamma}. \tag{389}$$

The wavelength Λ in the sample can be deduced with

$$\frac{1}{\Lambda^2} = \left(\frac{\varepsilon_\mathrm{r} \mu_\mathrm{r}}{\lambda_0^2} - \frac{1}{\lambda_c^2}\right) = -\left(\frac{1}{2\pi L}\left(\ln\left(\frac{1}{T}\right) + j 2\pi n\right)\right)^2. \tag{390}$$

Here λ_0 is the free space wavelength, λ_c is the cut off wavelength and L is the sample length or thickness. The integer n is chosen such that the difference between the 'New Non-Iterative' (NNI) method and the 'Direct' method gets minimized

$$\min_{n \in \mathbb{Z}} \left((\Re(d))^2 + (\Im(d))^2\right) \tag{391}$$

with

$$d = \underbrace{\varepsilon_\mathrm{eff} \mu_\mathrm{eff}}_{\text{NNI}} - \underbrace{\frac{\varepsilon_\mathrm{eff}}{\mu_\mathrm{eff}}}_{\text{Direct}} \mu_\mathrm{guess}^2 = \frac{\lambda_{og}^2}{\Lambda^2} - \frac{(S_{11} - 1)^2 - S_{21}^2}{(S_{11} + 1)^2 - S_{21}^2} \mu_\mathrm{guess}^2 \tag{392}$$

where μ_guess is the guess for the relative permeability. The wavelength in an empty cell λ_{og} is

$$\lambda_{og}^2 = \frac{1}{\frac{1}{\lambda_0^2} - \frac{1}{\lambda_c^2}} = \frac{c_0^2}{f_0^2 - f_c^2}. \tag{393}$$

Here f_0 is the frequency, f_c is the waveguide cut off frequency and c_0 is the speed of light in vacuum. The effective material parameters are defined as

$$\mu_{\text{eff}} = \frac{\lambda_{og}}{\Lambda}\left(\frac{1+\Gamma}{1-\Gamma}\right) \tag{394}$$

and

$$\varepsilon_{\text{eff}} = \frac{\lambda_{og}}{\Lambda}\left(\frac{1-\Gamma}{1+\Gamma}\right). \tag{395}$$

The relative permeability is defined as

$$\mu_{\text{r}} = \mu_{\text{eff}}. \tag{396}$$

The relative permittivity is defined as

$$\varepsilon_{\text{r}} = \left(1 - \frac{f_c^2}{f_0^2}\right)\varepsilon_{\text{eff}} + \frac{f_c^2}{f_0^2}\frac{1}{\mu_{\text{eff}}}. \tag{397}$$

K.2   NIST Iterative

The algorithm called 'NIST Iterative' is described in [37]. The algorithm is used to calculate the relative permittivity ε_{r} from transmission S_{21}, S_{12} and reflection S_{11}, S_{22} parameters. The relative permeability is assumed as $\mu_{\text{r}} = 1$.

The procedure prescribed by the 'NIST Iterative' method starts with the following equations

$$S_{11} = R_1^2\frac{\Gamma\left(1 - T^2\right)}{1 - \Gamma^2 T^2} \tag{398}$$

$$S_{21} = S_{12} = R_1 R_2\frac{T\left(1 - \Gamma^2\right)}{1 - \Gamma^2 T^2} \tag{399}$$

$$S_{22} = R_2^2\frac{\Gamma\left(1 - T^2\right)}{1 - \Gamma^2 T^2} \tag{400}$$

$$R_1 = e^{-\gamma_0 L_1} \tag{401}$$

$$R_2 = e^{-\gamma_0 L_2}. \tag{402}$$

Here L_1 and L_2 are the distances from the calibration reference planes to the sample ends, and R_1 and R_2 are the expressions for reference plane transformation.

The propagation constant in a with material filled sample holder can be written as

$$\gamma = j\sqrt{\frac{\left(2\pi f_0\right)^2\mu_{\text{r}}\varepsilon_{\text{r}} - \left(2\pi f_c\right)^2}{c_0^2}} \tag{403}$$

where f_0 is the frequency, f_c is the waveguide cut off frequency and c_0 is the speed of light in vacuum. The propagation constant in an empty sample holder can be written as

$$\gamma_0 = j\sqrt{\frac{\left(2\pi f_0\right)^2\varepsilon_{\text{air}} - \left(2\pi f_c\right)^2}{c_0^2}}. \tag{404}$$

The reflection coefficient is defined as

$$\Gamma = \frac{\frac{\gamma_0}{\mu_0} - \frac{\gamma}{\mu_0 \mu_{\mathrm{r}}}}{\frac{\gamma_0}{\mu_0} + \frac{\gamma}{\mu_0 \mu_{\mathrm{r}}}} \tag{405}$$

and for DC

$$\Gamma = \frac{\sqrt{\varepsilon_{\mathrm{air}} \frac{\mu_{\mathrm{r}}}{\varepsilon_{\mathrm{r}}}} - 1}{\sqrt{\varepsilon_{\mathrm{air}} \frac{\mu_{\mathrm{r}}}{\varepsilon_{\mathrm{r}}}} + 1}. \tag{406}$$

The transmission coefficient can be written as

$$T = e^{-\gamma L} \tag{407}$$

where L is the sample length or thickness. The transmission S-parameter of an empty sample holder is

$$S_{21}^0 = R_1 R_2 e^{-\gamma_0 L}. \tag{408}$$

The optimizer minimizes the following two objective functions

$$f_1 = S_{21} S_{12} - S_{11} S_{22} - e^{-2\gamma_0 (L_1 + L_2)} \left(\frac{T^2 - \Gamma^2}{1 - \Gamma^2 T^2} \right) \tag{409}$$

and

$$f_2 = \frac{S_{21}}{S_{21}^0} - e^{\gamma_0 L} \left(\frac{T \left(1 - \Gamma^2\right)}{1 - \Gamma^2 T^2} \right) \tag{410}$$

by adjusting ε_{r}.

K.3 New Non-Iterative

The algorithm called 'New Non-Iterative' is based on the 'Nicholson-Ross-Weir' algorithm, see appendix K.1. The algorithm is used to calculate the relative permittivity ε_{r} from transmission S_{21} and reflection S_{11} parameters. The relative permeability is assumed as $\mu_{\mathrm{r}} = \mu_{\mathrm{eff}} = 1$.

Multiplying equations 394 and 395 from the 'New Non-Iterative' algorithm yields the following effective material parameter

$$\varepsilon_{\mathrm{eff}} \mu_{\mathrm{eff}} = \frac{\lambda_{og}^2}{\Lambda^2}. \tag{411}$$

Note that this solution has no poles. The relative permittivity is defined as

$$\varepsilon_{\mathrm{r}} = \left(1 - \frac{f_c^2}{f_0^2}\right) \frac{\varepsilon_{\mathrm{eff}} \mu_{\mathrm{eff}}}{\mu_{\mathrm{eff}}} + \frac{f_c^2}{f_0^2} \frac{1}{\mu_{\mathrm{eff}}}. \tag{412}$$

Here f_0 is the frequency and f_c is the waveguide cut off frequency.

K.4 Direct

The algorithm called 'Direct' is based on the 'Nicholson-Ross-Weir' algorithm, see appendix K.1. The algorithm is used to calculate the relative permittivity ε_{r}

$$\varepsilon_{\mathrm{r}} = \left(1 - \frac{f_c^2}{f_0^2}\right) \frac{\varepsilon_{\mathrm{eff}}}{\mu_{\mathrm{eff}}} \mu_{\mathrm{eff}} + \frac{f_c^2}{f_0^2} \frac{1}{\mu_{\mathrm{eff}}} \tag{413}$$

with

$$\frac{\varepsilon_{\mathrm{eff}}}{\mu_{\mathrm{eff}}} = \frac{(S_{11} - 1)^2 - S_{21}^2}{(S_{11} + 1)^2 - S_{21}^2} \tag{414}$$

from transmission S_{21} and reflection S_{11} parameters. f_0 is the frequency and f_c is the waveguide cut off frequency. The relative permeability is assumed as $\mu_{\mathrm{r}} = \mu_{\mathrm{eff}} = 1$. The result can have poles for low loss samples with thickness of $> \frac{1}{2}$ wavelength.

K.5 Transmission Only

The algorithm called 'Transmission Only' is described in [38]. This method utilizes the S_{21} parameter to derive the transmission coefficient T and to extract the permittivity $\varepsilon_{\mathrm{r}} = \varepsilon_{\mathrm{r}}' - j\varepsilon_{\mathrm{r}}''$. Here T is a function of the sample length or thickness L and its permittivity and permeability. In this method the relative permeability is assumed as $\mu_r = 1$. For the materials which are not very lossy $\varepsilon_{\mathrm{r}}''/\varepsilon_{\mathrm{r}}' = \tan\delta < 0.1$, T can be separated directly to phase and magnitude parts

$$T \approx e^{\left(-j\frac{2\pi f_0 L}{v}\sqrt{\varepsilon_{\mathrm{eff}}'}\right)} e^{\left(-\frac{2\pi f_0 L}{2v\sqrt{\varepsilon_{\mathrm{eff}}'}}\varepsilon_{\mathrm{eff}}''\right)} \tag{415}$$

with the phase velocity

$$v = \frac{c_0}{\sqrt{1 - \frac{f_c^2}{f_0^2}}} \tag{416}$$

where $\varepsilon_{\mathrm{eff}}$ is the effective permittivity, f_0 is the frequency, f_c is the waveguide cut off frequency and c_0 is the speed of light in vacuum. From equation 415 one can compute the real part of the effective permittivity

$$\varepsilon_{\mathrm{eff}}' = \left(-\frac{v}{2\pi f_0 L}\arg(T)\right)^2 \tag{417}$$

where $\arg(T)$ is the unwrapped phase of T. The imaginary part of the effective permittivity is

$$\varepsilon_{\mathrm{eff}}'' = -\frac{2v\sqrt{\varepsilon_{\mathrm{eff}}'}}{2\pi f_0 L}\ln(|T|). \tag{418}$$

From the effective permittivity $\varepsilon_{\mathrm{eff}} = \varepsilon_{\mathrm{eff}}' - j\varepsilon_{\mathrm{eff}}''$ one can compute the relative permittivity using the following equation

$$\varepsilon_{\mathrm{r}} = \left(1 - \frac{f_c^2}{f_0^2}\right)\varepsilon_{\mathrm{eff}} + \frac{f_c^2}{f_0^2}\frac{1}{\mu_{\mathrm{eff}}} \tag{419}$$

where the relative permeability is assumed as $\mu_{\mathrm{r}} = \mu_{\mathrm{eff}} = 1$.

Using an unknown reflection coefficient Γ the following steps are needed to compute the relative permittivity:

1. One computes a guess of the real part of the relative permittivity ε_r' using the above equations 417 and 419 at frequency points where the phase of S_{21} is a multiple of π. At these points the unwrapped phase of T is equal to the unwrapped phase of S_{21}. The guess of the imaginary part of the relative permittivity is assumed as $\varepsilon_r'' = 0$. This guess for the relative permittivity is assumed to be constant for all frequency points.

2. The guess of the relative permittivity is used to compute the reflection coefficient, which is defined as

$$\Gamma = \frac{\sqrt{f_0^2 - f_c^2} - \sqrt{f_0^2 \varepsilon_r - f_c^2}}{\sqrt{f_0^2 - f_c^2} + \sqrt{f_0^2 \varepsilon_r - f_c^2}}. \tag{420}$$

3. One solves the following equation for T

$$S_{21} = \frac{T \left(1 - \Gamma^2\right)}{1 - \Gamma^2 T^2} \tag{421}$$

using the reflection coefficient Γ from the step before and the S_{21} parameter. This yields into a quadratic equation

$$S_{21} \Gamma^2 \, T^2 + \left(1 - \Gamma^2\right) T - S_{21} = 0. \tag{422}$$

The solution of T which has the smaller magnitude is chosen.

4. One computes the relative permittivity ε_r for each frequency point using T from step three and equations 417, 418 and 419.

The unwrapped phase of S_{21} has an unknown offset of $2\pi n$. The integer n is chosen such that the standard deviation of the different frequency points of ε_r' of the above steps gets minimized.

References

[1] K. Wong, "Traceability of vector network analyzer measurements", in *72th ARFTG Conf. Dig.*, pp. 157-167, December 2008

[2] *Guidelines on the Evaluation of Vector Network Analysers (VNA)*, European Association of National Metrology Institutes (EURAMET), cg-12, Version 2.0, March 2011.

[3] J. Hoffmann, P. Leuchtmann, J. Ruefenacht, and K. Wong, "S-parameters of Slotted and Slotless Coaxial Connectors", in *74th ARFTG Conf. Dig.*, pp. 1-5, December 2009

[4] D. F. Williams, J. C. M. Wang, and U. Arz, "An optimal vector-network-analyzer calibration algorithm", *IEEE Trans. Microwave Theory & Tech.*, vol. 51, no. 12, pp. 987-993, December 2003.

[5] D. K. Rytting, "Network Analyzer Accuracy Overview ", in *58th ARFTG Conf. Dig.*, pp. 1-13, November 2001

[6] BIPM, IEC, IFCC, ILAC, ISO, IUPAC, IUPAP and OIML, *Evaluation of measurement data - Guide to the expression of uncertainty in measurement*, International Organization for Standardization (ISO), Online: https://www.bipm.org/en/publications/guides/gum.html, September 2008

[7] BIPM, IEC, IFCC, ILAC, ISO, IUPAC, IUPAP and OIML, *Evaluation of measurement data - Supplement 2 to the "Guide to the expression of uncertainty in measurement" - Extension to any number of output quantities*, International Organization for Standardization (ISO), Online: https://www.bipm.org/en/publications/guides/gum.html, October 2011

[8] M. Zeier, J. Hoffmann, and M. Wollensack, "Metas.UncLib - a measurement uncertainty calculator for advanced problems", *Metrologia*, vol. 49, no. 6, pp. 809-815, Online: https://stacks.iop.org/0026-1394/49/i=6/a=809, November 2012.

[9] M. Wollensack, *METAS UncLib*, Online: https://www.metas.ch/unclib, 2009.

[10] M. Wollensack, J. Hoffmann, J. Ruefenacht, and M. Zeier, "VNA Tools II: S-parameter uncertainty calculation", in *79th ARFTG Conf. Dig.*, pp. 1-5, June 2012

[11] A. Ferrero, and U. Pisani, "QSOLT: a new fast calibration algorithm for two port S-parameter measurements", in *38th ARFTG Conf. Dig.*, pp. 15-24, December 1991.

[12] A. Ferrero, and U. Pisani, "Two-port network analyzer calibration using an unknown thru", *IEEE Microwave & Guided Wave Letters*, vol. 2, no. 12, pp. 505-507, December 1992.

[13] G. F. Engen, and C. A. Hoer, "Thru-reflect-line: An improved technique for calibrating the dual six-port automatic network analyzer", *IEEE Trans. Microwave Theory & Tech.*, vol. 27, no. 12, pp. 987-993, December 1979.

[14] F. Purroy and L. Pradell, "New theoretical analysis for the LRRM calibration technique for vector network analyzers", *IEEE Trans. Microwave Theory & Tech.*, vol. 50, no. 5, pp. 1307-1314, October 2001.

[15] J. R. Juroshek, "A direct calibration method for measuring equivalent source mismatch", *Microwave Journal*, vol. 40, no. 10, pp. 106-118, October 1997

[16] A. Ferrero, V. Teppati, M. Garelli and A. Neri, "A Novel Calibration Algorithm for a Special Class of Multiport Vector Network Analyzers", *IEEE Trans. Microwave Theory & Tech.*, vol. 56, no. 3, pp. 693-699, March 2008.

[17] M. Wollensack, J. Hoffmann, J. Ruefenacht, and M. Zeier, "VNA Tools II: Calibrations Involving Eigenvalue Problems", in *89th ARFTG Conf. Dig.*, pp. 1-4, June 2017

[18] R. B. Marks, "Formulations of the basic vector network analyzer error model including switch-terms", in *50th ARFTG Conf. Dig.*, pp. 115-126, December 1997

[19] J. Hoffmann, P. Leuchtmann, J. Ruefenacht, and R. Vahldieck, "A stable bayesian vector network analyzer calibration algorithm", *IEEE Trans. Microwave Theory & Tech.*, vol. 57, no. 4, pp. 869-880, April 2009.

[20] Keysight Technologies, *Specifying Calibration Standards and Kits for Keysight Vector Network Analyzers*, Application Note 1287-11, Online: https://www.keysight.com/us/en/assets/7018-01375/application-notes/5989-4840.pdf, June 2021.

[21] W. Heinrich, "Quasi-TEM Description of MMIC Coplanar Lines Including Conductor-Loss Effects", *IEEE Trans. Microwave Theory & Tech.*, vol. 41, no. 1, pp. 45-52, January 1993.

[22] W. Heinrich, private communication.

[23] A. Ferrero, U. Pisani, and K. J. Kerwin, "A new implementation of a multiport automatic network analyzer", *IEEE Trans. Microwave Theory & Tech.*, vol. 40, no. 11, pp. 2078-2085, November 1992.

[24] A. Ferrero, and F. Sanpietro, "A simplified algorithm for leaky network analyzer calibration", *IEEE Microwave and Guided Wave Letters*, vol. 5, no. 4, pp. 119-121, April 1995.

[25] R. B. Marks, and D. F. Williams, "A general waveguide circuit theory", *Journal of Research of the National Institute of Standards and Technology*, vol. 97, no. 5, pp. 533-562, October 1992.

[26] W. C. Daywitt, "First-order symmetric modes for a slightly lossy coaxial transmission line", *IEEE Trans. Microwave Theory & Tech.*, vol. 38, no. 11, pp. 1644-1650, November 1990.

[27] Rohde & Schwarz, *Calculate the mixed-mode S-parameter from an S4P file*, FAQ, Online: https://www.rohde-schwarz.com/us/faq/calculate-the-mixed-mode-s-parameter-from-an-s4p-file-faq_78704-30300.html, March 2021.

[28] A. Ferrero, and M. Pirola, "Generalized mixed-mode S-parameters", *IEEE Trans. Microwave Theory & Tech.*, vol. 54, no. 1, pp. 458-463, January 2006.

[29] Keysight Technologies, *Time Domain Analysis using a Network Analyzer*, Application Note 1287-12, Online: https://literature.cdn.keysight.com/litweb/pdf/5989-5723EN.pdf, August 2014.

[30] R. Willink, and B. D. Hall, "A classical method for uncertainty analysis with multidimensional data", *Metrologia*, vol. 39, no. 4, pp. 361-369, 2002.

[31] R. Willink, and B. D. Hall, "An extension to GUM methodology: degrees-of-freedom calculations for correlated multidimensional estimates", Online: https://arxiv.org/abs/1311.0343, 2013.

[32] *Guidelines on the Evaluation of Vector Network Analysers (VNA)*, European Association of National Metrology Institutes (EURAMET), cg-12, Version 3.0, March 2018.

[33] I. Kåsa, "A circle fitting procedure and its error analysis", *IEEE Trans. Microwave Theory & Tech.*, vol. 25, no. 1, pp. 8-14, March 1976.

[34] J. R. Magnus, "On Differentiating Eigenvalues and Eigenvectors", *Econometric Theory*, vol. 1, no. 2, pp. 179-191, Online: https://janmagnus.nl/papers/JRM011.pdf, August 1985

[35] A. M. Nicolson, "Measurement of intrinsic properties of materials by time-domain techniques", *IEEE Trans. Microwave Theory & Tech.*, vol. 19, no. 4, pp. 377-382, November 1970.

[36] W. B. Weir, "Automatic measurement of complex dielectric constant and permeability at microwave frequencies", *Proc. IEEE*, vol. 62, no. 1, pp. 33-36, January 1974.

[37] J. Baker-Jarvis, E. J. Vanzura, and W. A. Kissick, "Improved technique for determining complex permittivity with transmission/reflection method", *IEEE Trans. Microwave Theory & Tech.*, vol. 38, no. 8, pp. 1096-1103, August 1990.

[38] A. Kazemipour, M. Wollensack, J. Hoffmann, et al., "Analytical uncertainty evaluation of material parameter measurements at THz frequencies", *Journal of Infrared, Millimeter, and Terahertz Waves*, vol. 41, no. 10, pp. 1199-1217, 2020.